

# Strong seasonality in arctic estuarine microbial food webs

Colleen T. Kellogg<sup>1</sup>, James W. McClelland<sup>2</sup>, Kenneth H. Dunton<sup>2</sup>, Byron C. Crump<sup>3\*</sup>

<sup>1</sup>Hakai Institute, Canada, <sup>2</sup>Marine Science Institute, University of Texas at Austin, United States,

<sup>3</sup>College of Earth, Ocean, and Atmospheric Sciences, Oregon State University, United States

**Submitted to Journal:**  
Frontiers in Microbiology

**Specialty Section:**  
Aquatic Microbiology

**Article type:**  
Original Research Article

**Manuscript ID:**  
479205

**Received on:**  
18 Jun 2019

**Revised on:**  
09 Oct 2019

**Frontiers website link:**  
[www.frontiersin.org](http://www.frontiersin.org)

### ***Conflict of interest statement***

The authors declare that the research was conducted in the absence of any commercial or financial relationships that could be construed as a potential conflict of interest

### ***Author contribution statement***

CTEK collected and processed samples, performed sequence and data analysis, and lead writing. BCC contributed to writing and interpretation. BCC, JWM, and KHD conceptualized project. JWM and KHD lead field efforts and collected samples. All authors contributed to manuscript revision, read and approved the submitted version.

### ***Keywords***

Arctic, Beaufort Sea, Bacteria, Protists, seasonal dynamics, Coastal lagoons, co-occurrence network, 16S rRNA gene, 18S rRNA gene

### ***Abstract***

Word count: 347

Microbial communities in the coastal Arctic Ocean experience extreme variability in organic matter and inorganic nutrients driven by seasonal shifts in sea ice extent and freshwater inputs. Lagoons border more than half of the Beaufort Sea coast and provide important habitats for migratory fish and seabirds yet little is known about the planktonic food webs supporting these higher trophic levels. To investigate seasonal changes in bacterial and protistan planktonic communities, amplicon sequences of 16S and 18S rRNA genes were generated from samples collected during periods of ice-cover (April), ice break-up (June), and open water (August) from shallow lagoons along the eastern Alaska Beaufort Sea coast from 2011 through 2013. Protist communities shifted from heterotrophic to photosynthetic taxa (mainly diatoms) during the winter-spring transition, and then back to a heterotroph-dominated summer community that included dinoflagellates and mixotrophic picophytoplankton such as *Micromonas* and *Bathycoccus*. Planktonic parasites belonging to *Syndiniales* were abundant under ice in winter at a time when allochthonous carbon inputs were low. Bacterial communities shifted from coastal marine taxa (*Oceanospirillaceae*, *Altermomonadales*) to estuarine taxa (*Polaromonas*, *Bacteroidetes*) during the winter-spring transition, and then to oligotrophic marine taxa (*SAR86*, *SAR92*) in summer. Chemolithoautotrophic taxa were abundant under ice, including iron-oxidizing *Zetaproteobacteria*. These results suggest that wintertime Arctic bacterial communities capitalize on the unique biogeochemical gradients that develop below ice near shore, potentially using chemoautotrophic metabolisms at a time when carbon inputs to the system are low. Co-occurrence networks constructed for each season showed that under ice networks were dominated by relationships between parasitic protists and other microbial taxa, while spring networks were by far the largest and dominated by bacteria-bacteria co-occurrences. Summer networks were the smallest and least connected, suggesting a more detritus-based food web less reliant on interactions among microbial taxa. Eukaryotic and bacterial community compositions were significantly related to trends in concentrations of stable isotopes of particulate organic carbon and nitrogen, among other physiochemical variables such as dissolved oxygen, salinity, and temperature. This suggests the importance of sea ice cover and terrestrial carbon subsidies in contributing to seasonal trends in microbial communities in the coastal Beaufort Sea.

### ***Contribution to the field***

Microbial communities in the coastal Arctic Ocean experience extreme variability in organic matter and inorganic nutrients driven by seasonal shifts in sea ice extent and freshwater inputs. Lagoons border more than half of the Beaufort Sea coast and provide important habitat for migratory fish and seabirds yet little is known about the planktonic food webs supporting these higher trophic levels. In order to understand how seasonal changes in environmental conditions influence bacterial and protistan community composition, we sequenced the 16S and 18S rRNA genes from samples collected during periods of ice-cover, ice break-up, and open water from shallow lagoons along the eastern Alaska Beaufort Sea coast from 2011-2013. Eukaryotic and bacterial community compositions were significantly related to trends in concentrations of stable isotopes of particulate organic carbon and nitrogen, among other physiochemical variables, suggesting the importance of sea ice cover and terrestrial carbon subsidies in contributing to seasonal trends in microbial communities in the coastal Beaufort Sea. These results help to inform our understanding about which microbial populations may thrive in a warming and freshening Arctic Ocean and how these changes may influence the productivity of this important coastal ecosystem.

### ***Funding statement***

This research was funded by grants from the National Science Foundation to BCC, KHD and JWM, awards OPP-1023465, OPP-1023582, and OPP-1656026.

### ***Ethics statements***

#### ***Studies involving animal subjects***

Generated Statement: No animal studies are presented in this manuscript.

#### ***Studies involving human subjects***

Generated Statement: No human studies are presented in this manuscript.

#### ***Inclusion of identifiable human data***

Generated Statement: No potentially identifiable human images or data is presented in this study.

#### ***Data availability statement***

Generated Statement: The datasets generated for this study can be found in the NCBI Short Read Archive BioProject # PRJNA530074 (SRR8832739-SRR8833063 for 16S rRNA and SRR8837972-SRR8838296 for 18S rRNA): <https://www.ncbi.nlm.nih.gov/sra/PRJNA530074> .

1    **Title**

2    Strong seasonality in arctic estuarine microbial food webs

3    **Authors**

4    Colleen T. E. Kellogg<sup>1</sup>, James W. McClelland<sup>2</sup>, Kenneth H. Dunton<sup>2</sup>, Byron C. Crump<sup>3</sup>

5    **Affiliations**

6    <sup>1</sup> Hakai Institute, Heriot Bay, BC, Canada,

7    <sup>2</sup> The University of Texas at Austin Marine Science Institute, Port Aransas, TX 78373, USA

8    <sup>3</sup> College of Earth, Ocean, and Atmospheric Sciences, Oregon State University, Corvallis, OR,  
9    97331, USA

10    **Abstract**

11    Microbial communities in the coastal Arctic Ocean experience extreme variability in organic  
12    matter and inorganic nutrients driven by seasonal shifts in sea ice extent and freshwater inputs.  
13    Lagoons border more than half of the Beaufort Sea coast and provide important habitats for  
14    migratory fish and seabirds yet little is known about the planktonic food webs supporting these  
15    higher trophic levels. To investigate seasonal changes in bacterial and protistan planktonic  
16    communities, amplicon sequences of 16S and 18S rRNA genes were generated from samples  
17    collected during periods of ice-cover (April), ice break-up (June), and open water (August) from  
18    shallow lagoons along the eastern Alaska Beaufort Sea coast from 2011 through 2013. Protist  
19    communities shifted from heterotrophic to photosynthetic taxa (mainly diatoms) during the  
20    winter-spring transition, and then back to a heterotroph-dominated summer community that  
21    included dinoflagellates and mixotrophic picophytoplankton such as *Micromonas* and  
22    *Bathycoccus*. Planktonic parasites belonging to Syndiniales were abundant under ice in winter at  
23    a time when allochthonous carbon inputs were low. Bacterial communities shifted from coastal  
24    marine taxa (Oceanospirillaceae, Alteromonadales) to estuarine taxa (*Polaromonas*,  
25    Bacteroidetes) during the winter-spring transition, and then to oligotrophic marine taxa (SAR86,  
26    SAR92) in summer. Chemolithoautotrophic taxa were abundant under ice, including iron-  
27    oxidizing Zetaproteobacteria. These results suggest that wintertime Arctic bacterial communities  
28    capitalize on the unique biogeochemical gradients that develop below ice near shore, potentially  
29    using chemoautotrophic metabolisms at a time when carbon inputs to the system are low. Co-  
30    occurrence networks constructed for each season showed that under ice networks were  
31    dominated by relationships between parasitic protists and other microbial taxa, while spring  
32    networks were by far the largest and dominated by bacteria-bacteria co-occurrences. Summer  
33    networks were the smallest and least connected, suggesting a more detritus-based food web less  
34    reliant on interactions among microbial taxa. Eukaryotic and bacterial community compositions  
35    were significantly related to trends in concentrations of stable isotopes of particulate organic  
36    carbon and nitrogen, among other physiochemical variables such as dissolved oxygen, salinity,  
37    and temperature. This suggests the importance of sea ice cover and terrestrial carbon subsidies in  
38    contributing to seasonal trends in microbial communities in the coastal Beaufort Sea.

39  
40  
41  
42

43 **Introduction**

44 Aquatic microorganisms drive global cycling of carbon, nitrogen, and many other elements by  
45 carrying out key ecosystem functions including primary production, organic matter  
46 remineralization, and transformations of inorganic compounds (Falkowski et al., 2008; Ferrera et  
47 al., 2015; Worden et al., 2015). The efficiency with which microbes perform these functions is  
48 undoubtedly influenced by their physical and chemical environment (Gilbert et al., 2012), but  
49 also by interactions with each other within microbial communities (Azam and Malfatti, 2007;  
50 Fuhrman et al., 2015; Guidi et al., 2016). The composition and function of microbial  
51 communities varies strongly with seasonal changes in coastal ecosystems including day length,  
52 solar radiation, temperature, and salinity (Bunse and Pinhassi, 2017; Cram et al., 2015; Gilbert et  
53 al., 2012), and in polar regions these seasonal changes are particularly extreme, with additional  
54 complexities including ice cover and wide variations in river runoff (Holmes et al., 2012).  
55 Climate change is warming the Arctic approximately two times faster than lower latitudes  
56 (Serreze and Barry, 2011), and is amplifying seasonal variations in temperature (Serreze and  
57 Barry, 2011), ice extent (Stroeve et al., 2012), and river flow (McClelland et al., 2006; Morison  
58 et al., 2012). Moreover, increased river runoff in spring is accelerating coastal ice melt  
59 (Whitefield et al., 2015), particularly along the extensive Arctic continental shelf, where the  
60 interplay between these variables influences the timing and magnitude of biological production  
61 (Arrigo and van Dijken, 2015; Marchese et al., 2017), the species composition of primary  
62 producers (Ardyna et al., 2014; Li et al., 2009), and, in turn, higher and lower trophic levels  
63 (Vernet et al., 2017; Wassmann et al., 2011). Establishing the baseline relationship between  
64 microbial communities in Arctic coastal waters and their physical and chemical environment is  
65 key to understanding and predicting how they will respond to continued climate-induced changes  
66 to the Arctic system.

67 Most investigations of seasonality in microbial community composition and function in  
68 the Arctic Ocean have focused on offshore regions in the Chukchi and Canadian Beaufort Seas,  
69 the Norwegian Coast, and the plumes of very large Arctic rivers (Alonso-Sáez et al., 2008;  
70 Garneau et al., 2008; Ghiglione et al., 2012; Marquardt et al., 2016; Onda et al., 2017). Less is  
71 known about shallow estuarine environments on Arctic coastlines, despite their importance to  
72 coastal fisheries (von Biela et al., 2013) and as breeding habitat for over 157 species of migrating  
73 birds (Brown et al., 2006). Nearly one-half the Alaskan Beaufort Sea coast and one-third of the  
74 Chukchi Sea coast is skirted by an irregular and discontinuous chain of barrier islands that  
75 enclose shallow (< 6 m deep) lagoons (Dunton et al., 2006; Schreiner et al., 2013). Seasonal  
76 changes in these lagoons are different than in the open Arctic Ocean. For example, the  
77 magnitude of seasonal temperature fluctuations is larger in the lagoons, ranging from as low as -  
78 2.1°C in the winter to over 10°C in the summer, while much of the rest of the Arctic Ocean does  
79 not exceed 0-4°C (Timmermans and Ladd, 2018). Salinity fluctuations are also larger in the  
80 lagoons, in some cases ranging from hypersaline in winter due to sea ice brine rejection to nearly  
81 fresh conditions in spring due to river inputs (Harris et al., 2017). The organisms inhabiting these  
82 lagoon systems must be capable of surviving rapid changes in physical and chemical conditions.

83 Several studies have demonstrated that organic carbon from terrestrial runoff subsidizes  
84 lagoon food webs in the Arctic (Bell et al., 2016; Dunton et al., 2006, 2012; Harris et al., 2018;  
85 Mohan et al., 2016). These subsidies likely enter food webs via heterotrophic bacterial and  
86 protistan communities; however, the extent to which terrestrial subsidies influence the  
87 composition of microbial communities in these lagoons remains unknown. One study in a lagoon  
88 near Barrow, Alaska, used experimental incubations to show a change in Arctic marine bacterial

89 community composition and an increase in production in response to tundra-derived organic  
90 matter amendments (Sipler et al., 2017). Understanding how coastal microbial populations  
91 incorporate terrestrial organic matter and use terrestrially-derived nutrients is paramount to  
92 refining our understanding of pathways for the integration of terrestrial carbon into coastal Arctic  
93 marine systems. A first step in achieving this is to characterize how microbial populations in  
94 terrestrially-influenced Arctic waters change seasonally and in response to inputs of riverine  
95 material.

96 In this study, we describe seasonal variation in prokaryotic and protistan community  
97 composition in coastal lagoons of the Alaskan Arctic Ocean, and identify potential controls on  
98 microbial population dynamics, including organic matter source and prokaryotic-eukaryotic  
99 associations. This work was carried out in the context of a larger interdisciplinary study aimed at  
100 understanding how terrestrial inputs control physical (Harris et al., 2017), biogeochemical  
101 (Connelly et al., 2015; Mohan et al., 2016), and ecological (Dunton et al., 2012; Harris et al.,  
102 2018; Nolan et al., 2011) properties of lagoon ecosystems along the Alaskan Beaufort Sea coast.  
103

## 104 **Materials and Methods**

### 105 *Sample Collection*

106 Water samples (2-4 L) for microbial community analyses were collected from several sites  
107 within lagoons and outside barrier islands along the Alaskan Beaufort Sea coast in August 2011,  
108 and April, June, and August 2012 and 2013. Four lagoons, Kaktovik (KA), Jago (JA), Angun  
109 (AN), and Nuvagapak (NU), and one site outside the barrier islands near Barter Island (BP) were  
110 sampled in all three seasons (Fig. 1, BP was not sampled in August 2011). Two more lagoons,  
111 Tapkaurak (TA) and Demarcation Bay (DE), and 3 additional sites outside the barrier islands,  
112 near the Hulahula River (HU), Bernard Spit (BE) and Demarcation Point (DP), were also  
113 sampled in August (Fig. 1). Severe weather limited sample collection to KA, JA, AN, BP and  
114 BE in August 2013. Samples were collected from 1-2 stations per site in April and June, and 2-3  
115 stations per site in August of each year. BP had only one station in all seasons. Most sites were  
116 less than 4 m deep, with the exception of BE and DP, which were ~9-10 m deep. Samples were  
117 collected approximately 10 cm below the bottom off the ice cover in April (ice thickness 1.3 –  
118 1.7 m) and from the top 2m of the water column in June using a peristaltic pump, and by  
119 submerging hand-held sample bottles to ~0.5 m below the water surface in August. River  
120 endmembers were collected from the Canning, Jago and HulaHula rivers in August 2011 and  
121 from Canning and Jago rivers in August 2012.

122 Samples were also collected for a suite of environmental measurements including  
123 particulate organic carbon (POC) and nitrogen (PON) concentrations and stable isotope ratios  
124 (POC  $\delta^{13}\text{C}$  and PN  $\delta^{15}\text{N}$ ), chlorophyll *a* (Chl *a*) concentration, dissolved organic carbon and  
125 nitrogen concentrations, dissolved inorganic nitrogen (DIN= $\text{NO}_3 + \text{NH}_4$ ) concentrations, and  
126 oxygen stable isotope ratios of water ( $\text{H}_2\text{O-}\delta^{18}\text{O}$ ). Sample processing methods and  
127 measurements of particulate parameters (POC, PON, Chl *a*) are discussed in Connelly et al.  
128 (2015). Methods for dissolved parameters follow procedures described in McClelland et al.  
129 (2014). A YSI Sonde was used for temperature, salinity and dissolved oxygen from depths  
130 sampled (in addition to other depths throughout the water column) See Harris et al. (2017) for  
131 details of physical measurements and oxygen stable isotope ratios.

### 132 133 *Microbial sample processing, DNA extraction and PCR amplification*

134 After collection, samples were kept under shade during transit back to the Arctic National  
135 Wildlife Refuge field station in Kaktovik, Alaska. Within hours of collection, 2 L of water was  
136 filtered onto a 0.22- $\mu$ m Sterivex filter (Millipore) using a peristaltic pump and preserved with 1  
137 mL of DNA extraction buffer (100 mM Tris, 100 mM NaEDTA, 100 mM phosphate buffer, 1.5  
138 M NaCl, 1% CTAB) and kept frozen until extraction. Prior to filtration, duplicate 14 mL  
139 samples were collected from the sample bottles, fixed with glutaraldehyde (2% final  
140 concentration), and frozen for estimation of bacterial abundance using flow cytometry.

141 Prior to extraction, Sterivex filter cartridges were cracked open with pliers and filters  
142 were removed using an ethanol-flamed scalpel. The DNA extraction buffer from the cartridge  
143 was decanted into a sterile 2-mL microcentrifuge tube and the filter was subsequently cut into  
144 multiple pieces on a sterile cutting board and placed in the same tube. Samples were then  
145 subjected to 3 freeze-thaw cycles, followed by enzymatic lysis with Lysozyme (0.2 mg/ml final  
146 concentration) and Proteinase K (2 mg/ml final concentration) at 37°C for 30 minutes and  
147 continued digestion and lysis with the addition of SDS (1% final concentration) at 65°C for up to  
148 2 hours. Samples were then extracted 2 times with an equal volume of  
149 Phenol:Chloroform:Isoamyl alcohol (25:24:1) and nucleic acids were precipitated using 100%  
150 isopropanol (0.6 x volumes of the resulting supernatant) for two hours up to overnight. Samples  
151 were then pelleted at 18,000 RCF for 30 minutes, rinsed and re-pelleted two times with 70%  
152 ethanol, and dried down in a roto-evaporator. Once dry, samples were resuspended in 250 mL of  
153 nuclease-free water.

154 For community composition analysis, we amplified the V4 region (515F,  
155 GTGCCAGCMGCCGCGTAA and 806R, GGACTACHVGGGTWTCTAAT) of the 16S  
156 rRNA gene for prokaryotic composition, and the V9 region (1391F, GTACACACCGCCCCGTC  
157 and EukBr, TGATCCTCTGCAGGTTCACCTAC) of the 18S rRNA gene for eukaryotic  
158 composition for sequencing on the Illumina MiSeq platform using Earth Microbiome Project  
159 protocols (<http://www.earthmicrobiome.org/emp-standard-protocols>, but with only 30 PCR  
160 cycles). However, a known mismatch in the 16S primers with Thaumarchaeota, a dominant  
161 phylum of the marine Archaeal community, precluded us from drawing conclusions about  
162 Archaeal community composition. Each sample was amplified 3 times, pooled, quantified using  
163 Picogreen, and then, for each amplicon, pooled at equimolar concentrations (100  $\mu$ mol each).  
164 The 16S sample pool and 18S sample pool were each cleaned using a MoBio Ultraclean PCR  
165 Clean-Up Kit and quantified using Picogreen. Amplicon pools were sequenced at Argonne  
166 National Lab (the 16S sample library composed of August 2011, and April and June 2012  
167 samples) or the Oregon State University Center for Genome Research and Biocomputing (all  
168 18S sample libraries and an additional 16S library from August 2012 and all 2013 samples)  
169 2x150 bp paired-end reads. Gene amplicon sequences have been deposited in NCBI Sequence  
170 Read Archive (SRA) bioproject accession number PRJNA530074, under run accessions  
171 SRR8832739-SRR8833063 (16S rRNA gene) and SRR8837972-SRR8838296 (18S rRNA gene)  
172 (<https://www.ncbi.nlm.nih.gov>).

#### 173 *Bacterial abundance measurements*

174 Cell counts were performed using a BD Biosciences FACSCalibur Flow Cytometer at UM CES  
175 Horn Point Laboratory (2011 and 2012 samples) and Oregon State University (2013 samples).  
176 Single samples were counted for 2011 sites, while duplicate samples were counted and averaged  
177 for all sites after 2011. In the field, 14 mL of seawater was preserved with glutaraldehyde (2%  
178 final concentration) and frozen. In the lab, samples were thawed and 1.5 mL aliquots were

180 stained overnight in the case of 2011 and 2012 samples with 20  $\mu$ l of 1:200 SYBR Green I. The  
181 next day, samples were spiked with 15  $\mu$ l (25  $\mu$ l in 2013) of a sonicated beadstock created from  
182 PeakFlow Flow Cytometry Reference Beads (Life Technologies, Inc.) for internal reference.  
183 2013 samples were stained and counted on the same day. Data was collected using the program  
184 CellQuest Pro (BD Biosciences) in logarithmic mode based on side scatter (SSC) and green  
185 fluorescence (FL1) with a target rate of 100-1000 events sec<sup>-1</sup> for a total of 20,000 events for  
186 2011-2012 samples and for a set period of time for 2013 samples (average 78,000 events). See  
187 Meyer et al. (2014) for additional methodological details, including how cell concentration was  
188 calculated from counted events.

189

#### 190 *Sequence analysis*

191 Reads that were successfully paired using fastq-join (Aronesty, 2011) were quality filtered with  
192 an expected error rate of 0.5, dereplicated (derep\_fulllength), and abundance sorted (sortbysize)  
193 using UPARSE (fastq\_filter; Edgar, 2013). Singleton sequences were removed in the latter step  
194 to prevent them from seeding clusters when clustering sequences into operational taxonomic  
195 units (OTUs). Reads were then clustered into OTUs (cluster\_ottus in UPARSE pipeline) at 97%  
196 similarity. A de novo chimera check is inherent in the cluster\_ottus algorithm and chimeric  
197 sequences were removed during OTU clustering. Reference-based chimera filtering was  
198 performed using UPARSE (uchime\_ref) with the Gold Database  
199 (<http://www.genomesonline.org/>) as reference. Reads (including singletons) were subsequently  
200 mapped back to OTUs using UPARSE (usearch\_global) and an OTU table created. Taxonomy  
201 of the representative sequences was assigned in QIIME v. 1.9 (assign\_taxonomy.py; Caporaso et  
202 al., 2010) using the RDP classifier trained to the Greengenes database (v. 13.8,  
203 <http://greengenes.secondgenome.com/>) for 16S amplicons or the Silva database (v. 119; Quast et  
204 al., 2013; Yilmaz et al., 2014) for 18S amplicons. Any remaining singletons and OTUs occurring  
205 in only one sample were removed in QIIME (filter\_ottus\_from\_ottu\_table.py). Sequences  
206 identified as Archaeal, chloroplast and mitochondrial were also removed from 16S reads. For the  
207 18S rRNA gene library, we removed clades known to have multicellularity, as well as  
208 unclassified reads, in order to focus on protists. After these quality control steps, the average  
209 number of reads per sample were 22,326 for 16S amplicons (range 3651–73,169 sequences per  
210 sample) and 43,093 sequences for 18S amplicons (range 6720–103,750 sequences per sample).

211

#### 212 *Statistical analyses*

213 Given recent insights that rarefying microbiome datasets may not be the best method for  
214 comparing samples (McMurdie and Holmes, 2014), we chose not to randomly subsample OTU  
215 tables for the bulk of our analyses, with the exception of alpha diversity estimates. For alpha  
216 diversity measurements, the 18S rRNA gene OTU table was rarefied to 6700 sequences per  
217 sample, and the 16S rRNA gene OTU table to 3650 sequences per sample. Alpha diversity was  
218 calculated as Chao1 Diversity Index to measure species richness (Chao, 1984), Simpson's  
219 Evenness Measure (Smith and Wilson, 1996) to measure evenness, and Phylogenetic Diversity,  
220 which incorporates phylogenetic differences among species in the calculation of diversity  
221 (Caporaso et al., 2011; Faith, 1992). For beta diversity analyses, comparisons with  
222 environmental data, and indicator species analysis, OTU tables were normalized using  
223 proportional abundance of each OTU within each sample. To verify that using proportional  
224 abundance did not substantially change our conclusions compared to using OTU tables that were

225 subsampled, we ran a subset of the analyses described in this paper using rarefied OTU tables  
226 and found no significant difference in results or conclusions.

227 Microbial community structure was assessed using nonmetric multidimensional scaling  
228 (NMDS) calculated using the metaMDS function in the Vegan package for R (Oksanen et al.,  
229 2019). Variability in bacterial and eukaryotic community composition among samples was  
230 calculated using Bray-Curtis dissimilarity. Permutational multivariate analysis of variance  
231 (PERMANOVA; Anderson, 2017) and Analysis of Similarity (ANOSIM; Clarke, 1993)  
232 calculated using the adonis and anosim functions in the Vegan package for R (Oksanen et al.,  
233 2019), were used to test for differences among sample groupings determined *a priori* (e.g., by  
234 season, inside versus outside of barrier islands). PERMANOVA provides a pseudo-F-ratio, a p-  
235 value for the group-wise tests for differences (as you would get from a standard ANOVA), and  
236 the percent of variation in the community dataset explained by the grouping. ANOSIM provides  
237 an R value ranging from 0 to 1 with higher values indicator stronger differences between or  
238 among groups, and a significance value for the ANOSIM R value based on 999 permutations.

239 The degree to which physico-chemical data explained the variation in bacterial and  
240 eukaryotic communities was assessed using three methods. First, a Procrustes analysis was used  
241 to compare ordinations of community and physico-chemical data (Peres-Neto and Jackson, 2001)  
242 yielding correlation and significance values. Second, envfit in the Vegan package of R was used  
243 to decipher which variables were contributing to the structure of community nonmetric  
244 multidimensional scaling ordinations by fitting vectors of significant physico-chemical variables  
245 onto community NMDS ordinations. Finally, redundancy analysis (RDA) was used to quantify  
246 the percent of variation in bacterial or eukaryotic community composition explained by the  
247 physico-chemical environmental characteristics. Bacterial and Eukaryotic OTU tables were  
248 Hellinger-transformed prior to use in the RDA. Before running the RDA, physico-chemical  
249 variables for the model were selected to reduce multicollinearity using correlation matrices. The  
250 absence of substantial multicollinearity in this subset of variables was verified using the vif.cca  
251 function available in the Vegan package for R. RDA was run using the Vegan package for R.

252 Indicator species analysis (Dufrêne and Legendre, 1997) was used to identify bacterial  
253 and eukaryotic taxa that significantly contributed to seasonal differences in the coastal Beaufort  
254 Sea microbial community. In order to distinguish between river indicator species and lagoon  
255 indicator species in June samples, four samples groups were used for this analysis: River, April,  
256 June, and August. The indval program in the labdsv package for R was used to run the Dufrêne-  
257 Legendre Indicator Species Analysis, and OTUs having an indicator value (IV) > 0.7 and p <  
258 0.005 were considered significant indicators. Monthly indicators were then further broken down  
259 into two groups, high abundance indicators, having an average relative abundance of greater than  
260 0.5% of the total average population for that month, and low abundance indicators, which were  
261 significant but had an average relative abundance of less than 0.5%. The taxonomic composition  
262 of only high abundance indicators was further scrutinized. The relationship between the  
263 distribution of high abundance indicators and the Beaufort Sea environment was examined using  
264 Spearman correlations, with p-values adjusted using the Benjamini & Hochberg correction  
265 (Benjamini and Hochberg, 1995) Correlations were calculated using the Hmisc package for R,  
266 while the calculated p-values were adjusted base R stats package.

267  
268 *Co-occurrence network analysis*

269 Microbial association networks were generated for each month, across all years, using CoNet  
270 (Faust et al., 2012). In order for an OTU to be included in the network it had to be present in

271 25-33% of the samples (April = 4 samples, June = 5 samples, and August = 14 samples). In  
272 April and June, a percentage slightly higher than 25% was used because the number of  
273 correlations was very large and compute time was too great, preventing the network  
274 calculations from completing otherwise. Pairwise scores were computed for both Bray-Curtis  
275 similarity and Spearman correlation. Associations with a Spearman Correlation above 0.7 or  
276 below -0.7 and a Bray-Curtis similarity of above 0.6 or below 0.4 were retained. For each  
277 measure and edge, 1000 permutations (with renormalization for correlation measures) and  
278 bootstrap scores were generated, following the ReBoot routine. P-values were calculated as  
279 described in Weiss et al. (Weiss et al., 2016) and measure-specific P-values were merged  
280 using Brown's method. Associations were corrected using the Benjamini-Hochberg's false  
281 discovery rate (Benjamini and Hochberg, 1995) and edges with merged P-values below 0.05  
282 were retained. Edges had to be significant using both similarity measures to be kept.  
283 Network Statistics were calculated in Cytoscape 3.6.1 (Smoot et al., 2011). Chord diagrams,  
284 created using the R package *circlize*, were used to display significant associations among the 15  
285 most abundant taxa groups across all three network (Gu et al., 2014).

## 287 Results

### 289 Environmental conditions

290 April waters were ice-covered and cold (average of -2°C; Harris et al., 2017), with high salinity  
291 and inorganic nutrients, and low Chl *a*, dissolved oxygen, pH, organic matter and bacteria  
292 abundance (Fig. 2A). June waters, sampled during ice-breakup, were also cold but had the  
293 highest organic matter concentrations, the highest SUVA<sub>254</sub> (a measure of DOC aromaticity), and  
294 the lowest salinity because of freshwater input from rivers (Table 1). August waters were  
295 warmer (average of 8.9°C), with lower concentrations of inorganic nutrients and organic matter,  
296 and higher values of H<sub>2</sub>O- $\delta^{18}\text{O}$ , POC  $\delta^{13}\text{C}$  and PN  $\delta^{15}\text{N}$ . Ranges of these variables fluctuated  
297 interannually, but seasonal patterns of change in coastal Beaufort Sea waters were the same from  
298 year to year.

### 300 Bacterial diversity and community composition

#### 302 Alpha Diversity

303 We identified 17,340 bacterial OTUs and 9,583 protistan (unicellular eukaryotes, including  
304 fungi) OTUs. For bacterial OTUs, river samples had the highest species richness and  
305 phylogenetic diversity (FDR corrected  $p < 0.005$ ). Evenness in river samples was not significantly  
306 different from lagoon coastal waters in April and August. Among lagoon and coastal samples,  
307 richness was highest in June (FDR corrected  $p < 0.01$ , Fig. S1), phylogenetic diversity was lowest  
308 in August (FDR corrected  $p < 0.01$ ), and evenness was highest in August (FDR corrected  $p < 0.01$ )  
309 and lowest in June (FDR corrected  $p < 0.005$ ). There was no interannual variability in richness  
310 and evenness in April or June, but evenness was significantly greater in August 2012 and 2013  
311 than in 2011 (FDR corrected  $p < 0.05$ , Fig. S2). Bacterial richness and evenness were the same  
312 between sites within and outside of barrier islands except in August when evenness outside the  
313 barrier islands was lower (FDR corrected  $p = 0.0035$ , Fig. S3).

314 As with bacteria, eukaryotic species richness was greatest in rivers, but unlike bacteria the  
315 coastal eukaryotic communities had the lowest richness and phylogenetic diversity in June and  
316 the highest in April (Fig. S1). No significant differences in richness were observed among the

317 eukaryotic communities when grouped by month or location. There was also no interannual  
318 variability in eukaryotic richness, phylogenetic diversity, or evenness except in August 2011  
319 when richness and phylogenetic diversity values were significantly lower than later years (FDR  
320 adjusted  $p < 0.05$ , Fig. S2). Eukaryotic richness and evenness were the same between sites within  
321 and outside barrier islands in June, but richness was greater outside the islands in April (FDR  
322 adjusted  $p < 0.05$ , Fig. S3) and evenness was greater inside the islands in August (FDR adjusted  
323  $p \leq 0.021$ , Fig. S3).

324

#### 325 *Taxonomic composition*

326 River bacterial communities were dominated by Betaproteobacteria (22% of the community on  
327 average), Bacteroidetes (21%), Gammaproteobacteria (11%) and Alphaproteobacteria (11%)  
328 (Fig. 3A). Coastal bacterial communities in April and August were dominated by  
329 Gammaproteobacteria (36.3% and 29.6% respectively), Bacteroidetes (23.7% and 27.2%), and  
330 Alphaproteobacteria (17.4% in April and 23.4% in August), but differed in the abundant  
331 members of these groups. For example, in August, Gammaproteobacteria included many  
332 members of the oligotrophic marine clades SAR86, SAR92, OM60 and OM182 groups (43% of  
333 Gammaproteobacteria), whereas in April these taxa were less abundant (20% of  
334 Gammaproteobacteria) and the Gammaproteobacteria were dominated by other members of the  
335 orders Alteromonadales and Oceanospirillales (64% of Gammaproteobacteria, Fig. S4). April  
336 communities also included a large population of iron-oxidizing Zetaproteobacteria (4.6%; Fig.  
337 3A), and a diverse community of Deltaproteobacteria including the putative  
338 chemolithoautotrophic bacteria SAR324 (Sheik et al., 2014). June coastal bacterial communities  
339 were dominated by Bacteroidetes (32.6%), and Betaproteobacteria (25%), in part reflecting  
340 riverine influence, but many members of these groups differed from those in river samples (Fig.  
341 3A). For example, Betaproteobacteria in coastal waters were dominated by the marine genus  
342 *Polaromonas* (48% of Betaproteobacteria), while river samples were dominated by other  
343 Burkholderiales (64% of Betaproteobacteria, Fig. S5). Also, Bacteroidetes in June were  
344 dominated by members of the class Flavobacteriia (80% of Bacteroidetes), while this class made  
345 up only 49% the Bacteroidetes community in river samples (Fig. S6).

346 River protistan and fungal communities were dominated by Diatoms (20.7%), with  
347 substantial contributions from other Ochrophytes (14.7%; especially *Ochromonas* sp.  
348 CCMP1899), Nucleomyceta (13.7%), Rhizaria (12.5%) and Chlorophytes (11.1%; Fig. 3B). April  
349 eukaryotic communities were dominated by Ciliophora (27.8%) and Syndiniales (20.1%), with  
350 Dinophyceae (13.8%), non-Diatom Ochrophytes (10.6%) and marine stramenopiles (9.3%) also  
351 contributing to ice-covered eukaryotic populations (Fig. 3B). June eukaryotic communities were  
352 dominated by Diatoms (33.3%), Ciliophora (21.6%), Dinophyceae (10%) and Rhizaria (13.3%).  
353 River and lagoon eukaryotic communities in June were both dominated by Diatoms, but the  
354 dominant taxa differed (rivers: *Fragilaria* sp. (68%); lagoons: *Chaetoceros* (59%) and  
355 *Skeletonema* spp. (30%); Fig. S7). Eukaryotic communities transitioned from diatom-dominated  
356 during ice break-up in June to dinoflagellate-dominated in August (24.8%) when communities  
357 also included high proportions of Ciliophora (17.4%), Chlorophyta (13.1%) and non-Diatom  
358 Ochrophytes (10%, Fig. 3B). Across all seasons, Spirotrichaea was the dominant group of ciliates  
359 observed in coastal samples, with Heterotrichaea also abundant (5%) in April.  
360 *Gymnodiniphycidae* was the dominant dinoflagellate taxa (Fig. S8).

361

#### 362 *Beta diversity*

363 With respect to beta diversity, both bacterial and eukaryotic communities differed seasonally,  
364 and all coastal communities differed from river communities (Figs. 2B and 2C). We found that  
365 43% of the variance in bacterial communities and 27% of the variance in eukaryotic  
366 communities was accounted by seasonal coastal and river group differences (p-value=0.001,  
367 using PERMANOVA). Pairwise seasonal differences, as quantified using ANOSIM tests, were  
368 greater among eukaryotic communities (0.62–0.97 for eukaryotes and 0.4–0.96 for bacteria,  
369 p=0.001) with the exception of April-June comparisons, which had a higher ANOSIM R value  
370 for bacteria than for eukaryotes (0.93 vs. 0.88, p=0.001). In total, 1207 bacterial OTUs and 712  
371 eukaryotic OTUs were shared among all coastal microbial communities. Among coastal  
372 communities, June had the greatest number of unique bacterial OTUs (49.8%) but the fewest  
373 unique eukaryotic OTUs (38.9%). August had the most unique eukaryotic OTUs (55%). June  
374 coastal communities shared the greatest percentage of OTUs with river communities among all  
375 coastal water-river water comparisons (38.8% for bacteria and 50.9% for eukaryotes). August  
376 communities also shared a substantial percentage of their OTUs with river communities (34.1%  
377 for bacteria and 31.7% for eukaryotes), but April samples shared 20% or less of their OTUs with  
378 river communities.

379

#### 380 *Indicator species*

381 Indicator species analysis was used to determine which OTUs significantly contributed to  
382 differences among seasons. We focused on OTUs with indicator values greater than 0.7, p-  
383 values less than 0.001, and average relative abundance greater than 0.5% of the averaged  
384 community composition for the month for which the OTU was an indicator. In April, 23  
385 bacterial indicator taxa made up 36% of communities in these ice-covered waters (Fig. 4a).  
386 Many of these indicator taxa belonged to the Gammaproteobacteria order Oceanospirillales and  
387 the Bacteroidetes order Flavobacteriales. April indicator taxa also included members of the  
388 methanotrophic order Methylococcales, and several chemolithoautotrophic taxa including iron-  
389 oxidizing Zetaproteobacteria and sulfur-oxidizing SAR324. In June, 13 indicator taxa composed  
390 50% of communities in these highly productive, lower salinity waters (Fig. 4b). Most of these  
391 taxa belonged to the Bacteroidetes phylum, and to the Betaproteobacteria genus *Polaromonas*  
392 and methylotrophic order Methylophilales. June indicators also included Alphaproteobacteria  
393 related to *Loktanella* sp. In August, 22 indicator taxa made up 31% of the bacterial communities  
394 in these late summer, nutrient-poor waters (Fig. 4c). Many of these indicators belonged to the  
395 Alphaproteobacteria family Rhodobacteraceae, including *Phaeobacter* and *Octadecabacter* spp.  
396 August indicators also included Gammaproteobacteria from oligotrophic marine clades (OM60,  
397 OM182, SAR86 and SAR92).

398 As with the bacteria, a small number of eukaryotic indicator taxa made up a large fraction  
399 of the average April, June, and August communities (Fig. 4). In April, 13 eukaryotic indicator  
400 taxa from four phyla made up 31% of the April eukaryotic community (Fig. 4d) and included  
401 several OTUs closely related to the parasitic order Syndinales, and several marine stramenopiles  
402 (MAST) belonging to groups 1, 7, and 8. In June, a more diverse set of 17 indicator taxa made  
403 up 58% of the eukaryotic community (Fig. 4e). June indicators were dominated by several  
404 diatoms closely related to *Chaetoceros*, *Skeletonema* and *Melosira* sp., but also included a  
405 diverse community of taxa from the order Dinophyceae (dinoflagellates), phyla Ciliophora  
406 (ciliates), Chlorophyta (green algae), and Cercozoa. In August, an even broader array of  
407 indicators was observed, with 23 OTUs representing 32% of the eukaryotic community (Fig. 4f).  
408 August indicators were dominated by Chlorophyta, Dinophyceae, and Ochrophyta OTUs, but

409 included other taxa such as haptophytes, cryptophytes, and ciliates. While diatoms made up the  
410 bulk of the Ochrophyta indicators in June, this was not the case in August, when Ochrophyta  
411 indicators instead belonged to the Dictyochophyceae, Chrysophyceae, and Pelagophyceae.

412

413

#### 414 **Environmental drivers of coastal Beaufort Sea microbial communities**

415

416 Several methods were used to investigate relationships between physico-chemical parameters  
417 and microbial community composition. First, Procrustes analysis showed that both bacterial and  
418 eukaryotic community composition were significantly correlated with variation in Beaufort Sea  
419 lagoon environmental conditions ( $\text{Corr}_{\text{BAC}} = 0.7278$ ,  $\text{Corr}_{\text{EUK}} = 0.5923$ ,  $\text{sig} = 0.001$ ). Second,  
420 physico-chemical vectors that correlated significantly with bacterial and eukaryotic NMDS  
421 ordinations were overlain onto NMDS plots to determine the environmental gradient that  
422 correlated with the variations in community structure (Fig. S10). For the bacterial community,  
423 the first NMDS axis was negatively correlated with salinity and POC  $\delta^{13}\text{C}$  ( $r^2 < -0.7$ ) and  
424 positively correlated with SUVA<sub>254</sub>, POC, DOC, and Chl *a* suggesting that separation of June  
425 communities from August and April along this NMDS axis represents gradients in terrestrial  
426 input and productivity. The second NMDS axis was strongly correlated with temperature ( $r^2 < -$   
427 0.9) and negatively correlated with nitrate and ammonium ( $r^2 > 0.9$ , Fig. S10a), suggesting that  
428 separation of August from April communities is driven by seasonal changes in temperature and  
429 nutrients. Finally, redundancy analysis was used to quantify the amount of variation explained  
430 by these physico-chemical variables (Fig. S11). Approximately 70% of the variation in bacterial  
431 community composition could be explained by the Beaufort Sea environment.

432 For the eukaryotic community, the orientation of samples on the NMDS was rotated  
433 slightly relative to the bacterial NMDS, but the major trends were essentially the same. April  
434 and August communities were separated from June communities along gradients in terrestrial  
435 input and productivity (Fig. S10b). The C:N ratio of particulate organic matter (POM) and  
436 concentrations of DOC, nitrate, and ammonium were all strongly correlated this first NMDS axis  
437 ( $r^2 > 0.7$ ), suggesting that the August and April communities existed in waters with more  
438 degraded organic matter and lower nutrients than June communities. Like bacterial  
439 communities, April and August eukaryotic communities separated along a temperature and  
440 nutrient gradient, but productivity (e.g., Chl *a*) and organic matter source components (SUVA<sub>254</sub>,  
441 Chl *a*, Salinity and POC  $\delta^{13}\text{C}$ ) were also important correlates with the second NMDS axis for the  
442 eukaryotic ordination (Fig. S10b). Finally, redundancy analysis showed that approximately 55%  
443 of the variation in eukaryotic community composition could be explained by the Beaufort Sea  
444 environment (Fig. S11).

445 Correlations between high-abundance indicator taxa and measured physico-chemical  
446 variables reflected those of the whole communities (Fig. 5). April indicator taxa in ice-covered  
447 waters correlated with less productive and cold, nutrient-rich conditions (negative correlations  
448 POC, PN, Chl *a*, bacterial abundance; positive correlations with salinity and inorganic nutrients).  
449 This was particularly true for the eukaryotic MAST and Syndiniales OTUs, and several bacterial  
450 indicator taxa known to use diverse metabolic strategies for survival (e.g., Methylococcales,  
451 Zetaproteobacteria, and SAR324; Fig. 5). During ice-breakup, June indicator OTUs correlated  
452 with conditions representing riverine input (positive correlations with SUVA<sub>254</sub>, C:N, POC, PN,  
453 DOC, Dissolved Oxygen and Chl *a*; negative correlations with POC  $\delta^{13}\text{C}$  and PN  $\delta^{15}\text{N}$  and  
454 Salinity; Fig. 5). August indicators correlated with conditions representing post-bloom, nutrient-

455 deplete conditions (positive correlations with bacterial abundance and temperature; negative  
456 correlations with dissolved oxygen, nutrients, DOC, POC, and PN; Fig. 5).

457

## 458 **Microbial co-occurrence network properties**

459

460 *Network Structure*

461 Co-occurrence networks for the three seasons were strikingly different in size and topology  
462 (Table 2). The percentage of bacterial and eukaryotic OTUs retained in these networks after  
463 frequency filtering and subsequent co-occurrence analyses varied from 7 and 36 percent (Table  
464 S1), causing the networks to vary substantially in size. Among the taxa retained in these  
465 networks, significant combinations represented 1.4% to 14.9% of the possible combinations  
466 (Table S1), and average path length, or the number of nodes needed to link two nodes was short,  
467 ranging from 3.1 to 4.3 (Table 2). Network diameter, or the longest distance in a network, ranged  
468 from 10 edges (June) to 13 edges (August). Network density, a normalized measure for the  
469 average connectivity within a network, was the highest in June (0.057) and lowest in August  
470 (0.014). The average node degree, or the average number of connections for each node, was very  
471 high in June (111) compared to April (33) and August (9). Overall network complexity, as  
472 estimated by connectance (the fraction of all possible links that are realized in a network;  
473 Williams et al., 2002), was highest in June (0.0282) and lowest in August (0.0071) (Table 2).  
474 The number of connected components, or a set of nodes in the network graph for which there is  
475 always an interconnecting path (Corel et al., 2016), was the lowest in April (5) and highest in  
476 August (36, Table 2). If a network has only one connected component, all nodes can be linked to  
477 any other node in the network either directly or indirectly. The presence of more than one  
478 connected component indicates that some groups of nodes are segregated from the main network,  
479 not significantly correlated with any nodes in that graph.

480 Indicator taxa were most abundant in their corresponding seasonal networks, and river  
481 indicators were most abundant in the June network (Fig. S12). In all cases, these indicator taxa  
482 were outnumbered by non-indicator taxa, but in most cases indicator taxa had higher average  
483 node degrees than non-indicator taxa (Fig. S13), indicating that they were more highly connected  
484 within the networks. This was the case for seasonal indicators in the April and August networks,  
485 and for river indicator taxa in the June network underscoring the importance of river microbes in  
486 spring surface waters in these coastal lagoons.

487

## 488 *Network Composition*

489 Taxa that were abundant during each season were also abundant in corresponding seasonal  
490 networks. (Fig. S14). The April and August networks shared many of the same abundant taxa  
491 (Fig. S16) including bacterial taxa Rhodobacterales, Alteromonadales, Oceanospirillales, and  
492 Flavobacterales, and eukaryotic taxa Rhizaria, Diatomea, Ciliophora, Syndiniales, and  
493 Dinophyceae. The June network included some of the same abundant eukaryotic taxa with the  
494 addition of Chrysophyceae, but featured a different set of bacterial taxa including Legionellales  
495 and Actinobacteria (Fig. S16).

496 All three networks were dominated by positive edges (indicating co-presence), with far  
497 fewer negative edges (indicating mutual exclusion; Table 1). Also, organism-organism  
498 associations were far more abundant than those between organisms and environmental variables  
499 (Fig. S17). The June network was dominated by co-occurrences between prokaryotes (Fig. 8),

500 while April and August networks had a more even distribution of bacteria-bacteria (Bac-Bac),  
501 bacteria-eukaryote (Bac-Euk), and eukaryote-eukaryote (Euk-Euk) associations (Fig. S18).

502 We examined the positive and negative correlations among the 10 most abundant  
503 taxonomic groups within each network, which represented a total of 15 different groups (Fig. 6).  
504 In April, Euk-Euk edges were dominated by Syndiniales taxa, including marine alveolate  
505 (MALV) Groups I and II and *Amoebophrya*. These taxa correlated most frequently with  
506 themselves, with dinoflagellates including Gymnodiniphycidae and Peridiniphycidae, and with  
507 ciliates, including Oligotrichia and Choreotrichia (Fig. 6). Syndiniales also co-occurred with  
508 more bacterial taxa than other abundant eukaryotic taxa, and were positively correlated with  
509 Flavobacteriales and Deltaproteobacteria.

510 There were far fewer Euk-Euk and Bac-Euk edges than Bac-Bac edges in June, and the  
511 most abundant eukaryote in the June network, Chrysophyceae, was not the most abundant  
512 eukaryotic taxa in June samples (i.e., Diatomea). Chrysophyceae correlated mostly with  
513 themselves but also had significant correlations with Betaproteobacteria, Deltaproteobacteria,  
514 and Legionellales (Fig. 6). By comparison, Diatomea had far fewer correlations within the  
515 network. The June network was dominated by Bac-Bac edges involving Betaproteobacteria,  
516 *Legionellales*, and Rhizobiales, all of which are commonly associated with freshwater and  
517 brackish environments (Fig. 6). Deltaproteobacteria also had a high number of edges in June  
518 networks.

519 The August network featured many of the same taxonomic groups as the April network,  
520 but the connections among the nodes were different. Most Euk-Euk associations were positive  
521 correlations among Syndiniales and other dinoflagellates. By comparison, correlations involving  
522 ciliates were less frequent. Many Bac-Euk associations were negative, particularly those  
523 involving protist groups Syndiniales and Rhizaria and bacterial groups Alteromonadales,  
524 Flavobacteriales, Betaproteobacteria and Rhodobacterales (Fig. 6). In contrast, most Bac-Bac  
525 associations in the August network were positive.

526 The most connected taxa in the three networks were not always the most abundant taxa,  
527 suggesting that, in many cases, more abundant taxa may not require mutualistic interactions to  
528 thrive and can become abundant without the “help” of other microbial taxa, while the reverse  
529 may be true for the less abundant but highly-connected taxa (Fig. S15). In the April network, the  
530 highest node degrees were associated with relatively rare bacterial OTUs related to the  
531 gammaproteobacterium HTCC2188, Thiotrichales, and Gemmatimonadetes, and eukaryotic taxa  
532 *Developayella* and MAST-3 OTUs, a single *Goniomonas* OTU and a *Pirsonia* OTU (Fig. S19).  
533 Similarly, in the June network, taxa with the highest node degrees were relatively rare OTUs  
534 from the Enterobacteriales, WS3, and SR1 taxa; all with average node degrees >300 (Fig. S19).  
535 However, OTUs representing the abundant taxa Rhizobiales and Betaproteobacteria also had  
536 high average node degrees (>200). In the August network, many of the abundant taxa had high  
537 average node degrees, including Oceanospirillales and Alteromonadales (Fig. S19). Also, in  
538 August, several taxa with high average node degrees featured a large fraction of negative  
539 correlations including the bacteria Saprospirales, and eukaryotes MAST-9 and *Palpitomonas*  
540 (Fig. S19).

## 542 Discussion

543 Coastal waters along the North Slope of Alaska are important feeding and breeding grounds for  
544 many species of migratory birds (Johnson et al., 2007; Taylor et al., 2010) and fish, such as  
545 Arctic char and Arctic cod (Craig, 1984) that are critical to native subsistence fisheries (Dunton

546 et al., 2012). Maintenance of healthy lagoon and coastal ecosystems is crucial to sustaining these  
547 higher trophic levels. The base of food webs in these ecosystems is occupied by several  
548 interacting and species-rich microbial communities that perform many important ecosystem  
549 services, including organic matter degradation, nutrient regeneration, and carbon fixation via  
550 photosynthesis. In coastal systems, these communities provide a critical pathway for the  
551 incorporation of terrestrial organic matter and nutrients into estuarine and marine food webs (e.g.  
552 Carlsson et al., 1993; McCallister et al., 2004), especially in the Arctic, where terrestrial inputs  
553 are high (Whitefield et al., 2015). In the Beaufort coastal lagoons, microbial communities must  
554 maintain ecosystem functions despite huge seasonal changes in environmental conditions. This  
555 study demonstrates that microbial communities in these lagoons respond to seasonal changes  
556 through annually repeating seasonal shifts in species composition of both prokaryotic and  
557 microbial eukaryotic communities.

558

#### 559 *Terrestrial subsidies*

560 Previous studies have shown that terrestrial inputs of organic matter help fuel food webs along  
561 the Alaska Beaufort Sea coast (Dunton et al., 2006, 2012; Harris et al., 2018), yet no studies to  
562 this point have characterized relationships between the microbial communities living within  
563 these coastal waters and the organic matter inputs to them. Characterized by relatively low  
564 concentrations of POC, PON, and pigments, especially Chl *a* (Connelly et al., 2015), April  
565 waters in these coastal lagoons had a low contribution of phototrophic microbial taxa. The  
566 suspended organic material present was highly processed, with high ratios of phaeopigments to  
567 Chl *a* and elevated saturated fatty acid proportions (Connelly et al., 2015), suggestive of a  
568 heterotroph-dominated system. Indeed we show that April communities were dominated by high  
569 proportions of small heterotrophs (e.g., MAST) and parasitic Syndiniales clades in eukaryotic  
570 communities (Fig. 2B). Furthermore, the refractory nature and low concentrations of organic  
571 matter favored relatively high proportions of chemoautotrophs in bacterial communities (Fig.  
572 2A, S4, S5). OTUs belonging to family Oceanospirillaceae, members of which have been  
573 implicated hydrocarbon degradation (Satomi and Fujii, 2014), were also in high relative  
574 abundance in April. Arctic peat contains hydrocarbons (Yunker et al., 1993) and aromatics that  
575 likely contribute to the DOM in these coastal waters, as observed further west in the coastal  
576 Chukchi Sea (Sipler et al., 2017). The ability to degrade what is commonly considered more  
577 refractory components of organic matter (Yunker et al., 2002) may give members of  
578 Oceanospirillaceae a competitive advantage at the end of winter, after all of the fresh  
579 phytoplankton-derived organic matter has been degraded.

580 By June, the peak of the spring freshet had passed and ice break-up was well underway.  
581 POM analyses pointed to a much more productive system characterized by carbon inputs from  
582 both terrestrial sources and autochthonous phytoplankton (Connelly et al. 2015). Eukaryotic  
583 microbial communities were dominated by diatoms, and bacterial communities by a mixture of  
584 freshwater bacteria and a distinct estuarine community that presumably grew to dominate these  
585 communities in each year of the study (Fig. 3B). Bacteroidetes, including Cyclobacteriaceae and  
586 *Flavobacterium* spp., and Betaproteobacteria, particularly *Polaromonas* sp. were abundant in the  
587 June surface waters of the lagoons. Cyclobacteriaceae and *Flavobacterium* sequences were found  
588 to be enriched in low-salinity waters of the Columbia River estuary in Oregon and generally  
589 showed tolerance to a wide range of salinities (Smith et al., 2017). *Polaromonas* is a euryhaline  
590 bacterial taxa that can survive across a wide range of salinities (Veillette et al., 2011).  
591 Interestingly, this taxa was observed to be enriched in sea ice brackish brines (salinity 2.4-9.6) in

592 the central Arctic Ocean but not in the surface seawater below the sea ice (salinity 33.3-34.9),  
593 which was thought to indicate that they were unable to survive the salinity shock during brine  
594 rejection (Fernández-Gómez et al., 2019). However, closer to the coast we observed that  
595 *Polaromonas* appears to survive this transit from sea ice into surface seawater; perhaps lower  
596 salinity surface waters resulting from river input coincident with sea ice melt provide a refuge for  
597 these taxa.

598 By the middle of the open-water period in August, POM was characterized by elevated  
599 proportions of terrestrial and dinoflagellate fatty acids relative to those of diatoms (Connelly et  
600 al., 2015), which was validated by a shift from a diatom-dominated community in June to a  
601 dinoflagellate-dominated community in August (Fig. 3B, discussed in detail below). Coincident  
602 with these changes in OM source and decreased inorganic nutrient concentrations, the bacterial  
603 community came to resemble a typical coastal ocean community, becoming enriched in bacterial  
604 clades commonly considered to be oligotrophic, including SAR86, SAR92, and OM182 (Fig. 4).  
605 Many of these clades were also present in April but in lower proportions. SAR92 and OM182  
606 belong to the oligotrophic marine Gammaproteobacteria (OMG), while SAR86 is more distantly  
607 related and possesses an even more streamlined genome (Spring et al., 2015). OM182 and  
608 SAR86 were observed to become more abundant in late summer and fall in brackish waters of  
609 the Baltic Sea (Hugerth et al., 2015), aligned with an oligotrophic lifestyle. SAR92 is common in  
610 coastal waters at high (Ghiglione et al., 2012) and lower latitudes (Teeling et al., 2012), often in  
611 association with or just following phytoplankton blooms. Since Chl *a* was lower in August than  
612 in June, it appears that SAR92 can also persist in coastal waters of the Beaufort Sea well after  
613 peak primary production. Altogether, these parallels between our study and Connelly et al.  
614 (2015), coupled with the high percentage (55-70%) of community variation explained by  
615 physico-chemical measurements, suggests strong linkages between organic matter source and  
616 microbial community composition, and are consistent with similar seasonal changes in POM  
617 pigments and phytoplankton communities observed further east near the Mackenzie River plume  
618 (Morata et al., 2008).

## 619 620 *Photosynthetic protists*

621 In much of the Arctic Ocean, diatoms are the most abundant primary producers in spring  
622 (Fig. 5), while smaller picoeukaryotes dominate the photoautotroph community the remainder of  
623 the year (Lovejoy et al., 2011; Marquardt et al., 2016). This also occurs in the Beaufort coastal  
624 lagoons in June despite significant river influence and lower salinity. *Chaetoceros* and  
625 *Thalassiosira*, two abundant taxa in June, are dominant diatoms in under-ice blooms on the  
626 Chukchi Shelf (Arrigo et al., 2012) and in pelagic spring blooms across the Arctic (Poulin et al.,  
627 2011), including in the Beaufort Sea (Balzano et al., 2012b). *Melosira* and *Navicula*, also  
628 abundant in June, are common sea-ice associated diatom taxa (Booth and Horner, 1997; Poulin et  
629 al., 2011) that are thought to seed pelagic phytoplankton communities in spring (Hardge et al.,  
630 2017; Michel et al., 1993). In the Beaufort coastal lagoons *Melosira* was only abundant in June,  
631 suggestive of a sea-ice source, but *Navicula* was present in all seasons demonstrating that, while  
632 sea-ice may be a source for *Navicula*, members of this genus persist in the water column and  
633 contribute to the pelagic phytoplankton community (Hardge et al., 2017). Other notable primary  
634 producers in spring included the chlorophytes *Carteria*, *Chlamydomonas*, and chrysophyte  
635 *Ochromonas* which are commonly considered to be freshwater and snow genera, but their  
636 presence has been reported in Arctic coastal waters influenced by the Mackenzie River (Balzano  
637 et al., 2012a) and in sea ice and melt ponds elsewhere in the Arctic (Kiliias et al., 2014; Silkin et

638 al., 2003). Given that members of these genera appear to survive across a wide range of  
639 salinities, these euryhaline phototrophs may become increasingly important in coastal Arctic  
640 waters, and across the Arctic as a whole, with the forecasted freshening of the Arctic Ocean  
641 (McPhee et al., 2009; Morison et al., 2012).

642 As spring progressed into summer the composition of the primary producers shifted from  
643 large cells (diatoms) to smaller picophytoplankton, predominately prasinophytes *Micromonas*  
644 and *Bathycoccus*. *Micromonas* was dominant in 2011 (average 11% vs. 0.9% for *Bathycoccus*)  
645 when summertime waters were relatively cold (7.9°C) and salty (27.5 PSU). *Bathycoccus* was  
646 dominant in 2012 and 2013 (4.7% and 6.5% vs. 0.6% and 0.5% for *Micromonas*) when waters  
647 were warmer and fresher (9-11.2°C, 19.6-22.1 PSU). *Micromonas* is commonly thought to be the  
648 most abundant Arctic prasinophyte (Terrado et al., 2013), but *Bathycoccus* was more abundant  
649 on the river-influenced Mackenzie Shelf (Monier et al., 2015) and during polar sunset and polar  
650 night in the Amundsen Gulf Region (Joli et al., 2017), possibly due to differences in low-light  
651 survival strategies. In both cases, light, grazing, and nutrients were hypothesized to drive this  
652 taxonomic shift. Both *Micromonas* and *Bathycoccus* have been shown to be capable of  
653 osmotrophy (Hernández-Ruiz et al., 2018), but *Bathycoccus* appears to have a stronger  
654 preference for amino acids as a carbon source relative to bicarbonate, suggesting that  
655 *Bathycoccus* is particularly adapted to organic matter utilization. Low-light adaptation and the  
656 ability to consume organic matter may explain the success of *Bathycoccus* in 2012 and 2013,  
657 when river input and organic matter concentrations were higher.

658 Under the ice in April, photoautotrophs were much less abundant, and consisted mainly  
659 of the prasinophytes discussed above, stramenopiles related to Bolidophyceae (2.7%) and  
660 dictyochophyte Pedinellales (3.4%), which was also abundant in August (4.1%). Bolidophyceae  
661 and Pedinellales have been observed elsewhere in the Beaufort Sea (Balzano et al., 2012a;  
662 Terrado et al., 2013), under the ice in the Central Arctic Ocean (Pedinellales only; Hardge et al.,  
663 2017), and in Canadian High Arctic sea ice (Piwoz et al., 2013). 17% of the bolidophyte cells  
664 investigated from sea ice were found to have at least one bacterium in their food vacuole (Piwoz  
665 et al., 2013) and thus their presence under ice may be sustained through heterotrophy rather than  
666 photosynthesis.

#### 667 *Chemolithoautotrophs and methylotrophs*

668 Ice-covered waters were dominated by bacterial taxa known to thrive in low organic  
669 matter conditions, such as chemolithoautotrophs including Zetaproteobacteria (4.6%),  
670 Deltaproteobacteria clade SAR324 (1.3%), and methylotrophs including Methylococcales (2%)  
671 (Fig. 3). Zetaproteobacteria (4.6%) are mat-forming Fe(II) oxidizers that are closely related to  
672 the chemotrophic iron-oxidizing genus *Mariprofundus* (Singer et al. 2011). Their presence in  
673 April waters was consistent with the orange tint observed on several April sample filters, but was  
674 surprising given that this is, to our knowledge, the first evidence of this microbial taxa in coastal  
675 Arctic waters. Zetaproteobacteria have been observed in iron-rich hydrothermal vents of the  
676 Loihi Seamount (McAllister et al., 2011), and coastal waters in Maine, USA (McBeth et al.,  
677 2011). Our study extends their distribution to include the coastal Arctic Ocean. These lagoons  
678 receive large pulses of iron during the spring snow melt (Rember and Trefry 2004), and iron  
679 concentration in arctic freshwaters increases through spring and summer (Pokrovsky et al. 2016)  
680 and may be enhanced by permafrost thaw (Barker et al. 2014).

681 SAR324 (1.3%) have genes for sulfur and alkane oxidation and have the capacity to  
682 degrade short-chain fatty acids, among other metabolic strategies (Sheik et al. 2014).

684 Interestingly, Connelly et al. (2015) observed the highest proportional abundance of short-chain  
685 fatty acids in April waters compared to June or August. SAR324 were also found to be  
686 proportionally more abundant in surface waters under-ice than in open waters off Point Barrow  
687 (Sipler et al. 2017) and were shown to be important in nitrogen cycling in the winter (Connelly et  
688 al. 2014). Chemoautotrophic production under ice may help sustain biological communities  
689 during the long winter, as it is thought to in other continually ice-covered systems (Boyd et al.,  
690 2014; Vick-Majors et al., 2016).

691 Methylococcales are exclusively methylotrophs and type I methanotrophs (Kato et al.  
692 2012, Quaiser et al. 2014) that have been observed to thrive in association with iron-oxidizing  
693 microbial mats in freshwater systems (Quaiser et al. 2014). Our data suggest that iron-oxidizing  
694 and methane-oxidizing bacteria may also live in close association in iron-rich, coastal marine  
695 waters. Methane is present in shallow sediments throughout the Beaufort Sea shelf (Coffin et al.  
696 2013), and dissolved methane is highly concentrated in Beaufort Sea water (Lorenson et al  
697 2016), particularly in shallow waters. This methane is mainly generated by microbial  
698 degradation of organic matter (Lorenson et al. 2016), but may also arise from permafrost-  
699 associated methane gas hydrates (Shakhova et al. 2016), which are present throughout the  
700 Beaufort shelf region (Riedel et al. 2016). We did not measure methane concentrations in our  
701 water samples, but wintertime under-ice methane concentrations to the west of our sample region  
702 were 3-28 times greater than in summer (Kvenvolden et al. 1993). While both of the iron- and  
703 methane-oxidizing taxa in our samples are aerobic, they prefer to live at oxic-anoxic interfaces to  
704 allow for the presence of both oxygen and reduced electron donors, which may have been  
705 available given the presence of low oxygen levels in some lagoons in April (Connelly et al.  
706 2015). Overall, the presence of these bacterial functional groups suggests that iron, methane,  
707 nitrogen, and sulfur cycling become relatively important under the ice in these coastal lagoons as  
708 more labile organic matter is progressively depleted through the long Arctic winter.

709  
710 *Parasites*

711 Heterotrophic protists play an important part in marine food webs as grazers of  
712 phytoplankton and bacterioplankton, and as food for zooplankton. In the Central Arctic Ocean,  
713 their biomass can rival or exceed that of phototrophic protists (Sherr et al., 1997). Heterotrophic  
714 and parasitic protists were relatively abundant in the Beaufort coastal lagoons in all seasons, but  
715 were particularly dominant in April when sea ice and snow attenuated light penetration into  
716 surface waters, limiting the abundance of photosynthetic protists (Fig 3). Thus, heterotrophy and  
717 parasitism likely dominated the protistan lifestyle in April waters. This is corroborated by the  
718 presence of abundant sequences related to ciliates, heterotrophic dinoflagellates, parasitic  
719 Syndiniales, and MAST taxa in the under-ice community (Fig. 3). Heterotrophic protists were  
720 relatively less abundant in spring, but became dominant again later in summer, following the  
721 spring bloom and depletion of macronutrients (Table 1).

722 Syndiniales, including the MALVs, are a globally-distributed parasitic group within the  
723 Alveolates (de Vargas et al., 2015; Guillou et al., 2008), that constitute a substantial component  
724 of the global marine interactome (Lima-Mendez et al., 2015), and are generally considered to  
725 have a broad host range from other protists to metazoans (Guillou et al., 2008). We observed  
726 clear seasonality in Syndiniales, especially Groups I and II, with the greatest relative abundance  
727 under ice in April (20%), and lower relative abundance in June (4%) and August (6.3%).  
728 Syndiniales followed a similar abundance pattern in Franklin Bay further east in the Beaufort Sea  
729 (Terrado et al., 2009), in a high arctic Fjord (Marquardt et al., 2016), and in Antarctic waters

730 (Cleary and Durbin, 2016). Oxygen may influence the distribution of these two groups in the  
731 water column, with Group I preferring low oxygen waters or sediments and Group II preferring  
732 oxygenated waters (Guillou et al., 2008), although both groups were abundant in suboxic and  
733 anoxic fjord waters in British Columbia (Torres-Beltrán et al., 2018). Low dissolved oxygen  
734 was measured in some of the lagoons under the ice (Connelly et al., 2015), yet Group II were the  
735 most abundant Syndiniales in this season, which further suggests that oxygen is not the only  
736 driver of their distribution and that other factors, such as host availability and host stress under  
737 winter conditions (Cleary and Durbin, 2016) control the abundance and diversity of Syndiniales.

738

### 739 *Grazers*

740 Heterotrophic flagellates like marine stramenopiles are ubiquitous in the global ocean (de  
741 Vargas et al., 2015; Lovejoy et al., 2006) and, as bacterivores, represent important links in  
742 marine microbial food webs, transferring carbon from bacteria to higher trophic levels like  
743 zooplankton (Monier et al., 2013; Worden et al., 2015). More abundant in the lagoons during less  
744 productive months, MAST clades MAST-1 and MAST-6 had the highest relative abundances in  
745 our dataset with MAST-1A and MAST-1C most abundant in April (6% of 18S rRNA genes).  
746 These clades were also found to be abundant in near-ice or under-ice stations along a transect  
747 from the Labrador Sea west to the Beaufort Sea (Thaler and Lovejoy, 2013). In August, MAST-6  
748 was the most abundant MAST clade (2.2%). This clade has rarely been reported in the Arctic,  
749 but that is likely due to the fact that it is missed by the PCR primer set commonly used to assess  
750 protist diversity in Arctic waters (e.g. Thaler and Lovejoy, 2015). Using CARD-FISH, MAST-6  
751 was found in first year sea ice in the Canadian Arctic Archipelago, with 20% of the cells  
752 containing at least one bacterium in their food vacuoles, suggesting that MAST-6, like MAST-1,  
753 are bacterivorous (Piwosz et al., 2013). In the Baltic Sea, MAST-6 cells were found to have both  
754 phytoplankton and bacteria in their food vacuoles suggesting that they are both algivorous and  
755 bacterivorous (Piwosz and Pernthaler, 2010). This clade of marine stramenopiles has been  
756 observed to prefer sediments across several coastal stations around Europe (Logares et al., 2012),  
757 however our observations show that they are also important in pelagic systems in the Arctic.

758 Dinoflagellates had the highest relative abundance in August (24%), followed by April  
759 (14%) and June (10%), however, like with MAST, the dominant taxa varied by season. While  
760 both April and August were dominated by the *Gyrodinium* sp., *Gymnodinium* sp. was also  
761 abundant in August. While difficult to identify microscopically (Kubiszyn and Wiktor, 2016;  
762 Lovejoy, 2014), these two genera of naked heterotrophic dinoflagellates are abundant in 18S  
763 rRNA gene surveys of Arctic waters (Comeau et al., 2011; Marquardt et al., 2016). The  
764 dinoflagellate population in June was dominated by *Pelagodinium* sp. (7.6%), a member of the  
765 *Suessiaceae*. *Pelagodinium* is thought to be a symbiont of Foraminifera (Siano et al., 2010), but  
766 forams were a very small fraction of the protist communities, especially in June (<0.001%). The  
767 highest abundance of *Foraminifera* was observed in April (0.1%), but still was small compared  
768 to the relative abundance *Pelagodinium* sp. in June. Given these observations, it is possible that  
769 we detected this symbiont during the free-living stage of its life cycle or that it is also a symbiont  
770 of other taxa abundant in June.

771 While typically less abundant than dinoflagellates in the Arctic, ciliates represent another  
772 important group of grazers in marine systems (e.g. Sherr et al., 1997). In line with  
773 microscopically-obtained abundance estimates, dinoflagellate 18S rRNA gene sequences were  
774 always at least twice as abundant as ciliates regardless of season in a high-Arctic fjord  
775 (Marquardt et al., 2016). We observed more seasonality in the ratios of these two groups of

776 protists, with ciliate sequences twice as abundant as dinoflagellate sequences in April and June,  
777 but less abundant in August (17%, compared to 24% dinoflagellates). This suggests that ciliates  
778 may play a more important role in coastal lagoon food webs than in other Arctic systems.

779 Oligotrich ciliates were the most abundant group of ciliates across all seasons, including  
780 *Strombidium* and *Laboea* (the later only in August; 1.4%). OTUs classified as *Strombidium* were  
781 two times more abundant in June and August than April, while all months had a large percentage  
782 of reads that could not be classified beyond *Oligotrichia*, similar to other studies of ciliates in  
783 polar waters (Onda et al., 2017). *Strombidium* was found to be abundant in surface waters  
784 elsewhere in the Arctic, especially in the spring and summer, perhaps in part due to a  
785 mixotrophic lifestyle (Stoecker et al., 2017). *Strombidium* and *Laboea* have been observed to  
786 temporarily retain and gain energy from the chloroplasts from ingested diatoms or other  
787 phototrophic prey (Dolan and Pérez, 2000). This could provide an energetic advantage over  
788 ciliates that rely solely on phagotrophy. April had higher relative abundances of ciliates  
789 belonging to the Mesodiniidae (3.1%) and Oligohymenophorea (specifically Scuticociliatia;  
790 2.5%). Oligohymenophorea are strictly bacterivorous (Vaqué et al., 2008), but some  
791 Mesodiniidae species are mixotrophic, bordering autotrophic, with a preferred diet of  
792 cryptomonads as a source for harvested chloroplasts (McManus and Santoferrara, 2012).  
793 Cryptomonads were most abundant in April and August, in line with the distribution of  
794 Mesodiniidae OTUs. Mixotrophy was found to be the primary metabolism of ciliates in the  
795 oligotrophic waters of Fram Strait (Seuthe et al., 2011). The dominance of several potentially  
796 mixotrophic groups of ciliates in this study suggests that mixotrophy is also important in the  
797 coastal lagoons of the Beaufort Sea and could contribute to the overall productivity of these  
798 waters.

799

#### 800 *Community connectivity and microbial food web*

801 We used co-occurrence network analysis to investigate prokaryotic and eukaryotic  
802 community connectedness in each season using data from multiple years. We were unable to find  
803 similar seasonal networks for comparison in marine systems because most marine networks have  
804 been grouped by depth (Lima-Mendez et al., 2015; Milici et al., 2016) or were generated for  
805 entire time-series datasets without seasonal breakdown (e.g. Chow et al., 2013). Still, our  
806 network sizes and clustering coefficients (Table 2) were within the range of these marine co-  
807 occurrence networks.

808 In one of the only aquatic microbial time series studies that performed seasonal network  
809 analysis it was observed that network complexity of lake microbial communities was the greatest  
810 in spring, compared to summer or autumn (Kara et al., 2013). Similarly, we found that the June  
811 network was the largest, most connected and most complex, having the highest clustering  
812 coefficient, highest connectance and the lowest average path length, while the August network  
813 was the least complex and the under-ice network in April was intermediate. Kara et al. (2013)  
814 also noted that spring and autumn samples had the lowest and highest diversity, respectively,  
815 resulting in a negative relationship between network complexity and diversity. We did not  
816 observe this same relationship in the lagoons, possibly due to the contribution of freshwater  
817 bacteria and protists to the marine system and the formation of a diverse brackish microbial  
818 community in June. Given the same seasonal trends in network complexity between the lake  
819 study and our study, but differences in diversity-network complexity relationships, it is possible  
820 that seasonal trends in aquatic microbial network characteristics may be independent of the

821 number of taxa present and driven more by ecosystem productivity, with food web complexity  
822 being highest during periods high production.

823 River indicator taxa had the highest average node degree in June networks (Fig. S16) and  
824 common freshwater and brackish bacterial taxa accounted for the bulk of the significant  
825 correlations in the June networks (e.g. *Legionellales*, *Betaproteobacteria*, *Deltaproteobacteria*,  
826 and *Rhizobiales*, Fig. 6). Whether these taxa were actively interacting or just happen to be  
827 passively co-existing is impossible to determine from this analysis, but it is important to note that  
828 river-impacted, nearshore systems may follow different diversity and connectivity patterns than  
829 lake or open ocean systems because mixing of freshwater and marine communities may elevate  
830 microbial diversity and form more complex microbial networks. The prevalence of freshwater  
831 and brackish microbial nodes in the spring network underscores the importance of these taxa in  
832 the coastal Arctic ecosystem during the spring freshet. Interestingly, two bacterial candidate  
833 phyla with small genomes, including WS3 and SR1 (Farag et al., 2017; Kantor et al., 2013),  
834 represented network “hubs” in June, with average node degrees  $>300$ . Microbes with streamlined  
835 genomes have also been observed to be network hubs in other studies of freshwater and marine  
836 systems (Milici et al., 2016; Peura et al., 2015), relying on interactions with other taxa in order to  
837 obtain metabolites that they cannot synthesize themselves.

838 Protists represented a small fraction of the nodes in the June networks, possibly due to the  
839 higher relative abundance of photoautotrophic protists during ice break-up. Most of the  
840 significant protistan relationships in June were between protists and bacteria rather than with  
841 other protists and were dominated by Chrysophytes (which can be mixotrophic; Beisser et al.,  
842 2017), diatoms, and heterotrophic groups of Rhizaria (Nakamura and Suzuki, 2015). These  
843 protists could be obtaining a necessary metabolite produced by co-located bacteria or, if  
844 heterotrophic or mixotrophic, could be grazing on bacteria, which can be enhanced during  
845 phytoplankton blooms (Hyun and Kim, 2003). Still it is important to note that the total number of  
846 significant protist-bacteria edges (11,256) in June exceeded those in April or August, but was far  
847 smaller than the number of Bac-Bac edges (94,983) and thus the relative contribution was less  
848 than in other months.

849 The April network was the next largest and contained the largest number (and  
850 percentage) of eukaryote nodes and Euk-Euk edges, especially among nodes belonging to the  
851 Syndiniales, other dinoflagellates, and ciliates (Fig. 6A, Fig. S19). These relationships are in line  
852 with the known hosts for this group of parasites (Guillou et al., 2008; Torres-Beltrán et al., 2018)  
853 and supports our hypothesis that parasitism was an important component of the under-ice food  
854 web. Extreme winter conditions in polar systems may increase parasitism due to environmental  
855 stress (e.g. low light, low *in situ* production). Syndiniales were also the most abundant group in  
856 co-occurrence networks generated as part of the Tara Oceans project from all regions sampled  
857 except for the Southern Ocean (the Arctic Ocean was not sampled as part of Tara Oceans; Lima-  
858 Mendez et al., 2015). As was observed at lower latitudes, these parasitic OTUs were most  
859 commonly correlated with other Syndiniales OTUs and with Dinophyceae OTUs. Syndiniales  
860 also correlated with several radiolarians, consistent with direct observations of similar  
861 associations through single-cell sequencing of radiolarians from a Norwegian fjord (Bråte et al.,  
862 2012), and with correlations between these protist groups under the ice north of Svalbard  
863 (Meshram et al., 2017). But unlike at lower latitudes (Lima-Mendez et al., 2015), correlations  
864 between Syndiniales and Ciliophora OTUs were common under the ice in the April. It is not  
865 possible to determine if this means that parasitism of ciliates is more prevalent in Arctic waters

866 than at lower latitudes, but these observations suggest that correlations between putatively  
867 parasitic OTUs and presumed hosts under sea ice warrant continued investigation.

868 The August microbial community was less connected and more fragmented than other  
869 seasons, with a higher number of connected components, highest average path length (number of  
870 nodes needed to link individual nodes), and the lowest connectance (fraction of all possible links  
871 that are realized). A similar pattern was found for a Wisconsin lake in which the autumn network  
872 had the smallest network size and highest path length (Kara et al., 2013). The breakdown of  
873 microbial networks between June and August may be driven by physical processes such as  
874 increased mixing and reduced water column stratification, which was weaker in August than in  
875 June (Harris et al., 2017). Another possible explanation is that the August food web is not as  
876 reliant on fast energy transfer from large, fast-growing phytoplankton but rather on a slower  
877 energy transfer characteristic of a more detrital food web, the latter of which is often  
878 characterized by longer path lengths and generally weaker links (Rooney and McCann, 2012).

879 The August network featured the greatest percentage of negative relationships between  
880 nodes, suggesting more antagonistic relationships in the microbial food web in the summer than  
881 the spring (Fig. 6). This is supported by our observation of high relative abundance of  
882 heterotrophic protist sequences in August. Furthermore, the concentration of phaeopigments was  
883 the highest in August (Connelly et al., 2015) which also supports high grazing on and microbial  
884 remineralization of phytoplankton-derived POM. If microbial populations were more focused on  
885 degrading or grazing on phytodetritus in August this could result in fewer significant correlations  
886 among taxa and also longer chains within the food web as compared to other seasons. Bacterial  
887 networks associated with POM tended to be smaller than free-living networks in the Atlantic  
888 Ocean (Milici et al., 2016). Indeed common particle-associated bacteria (Flavobacteriales,  
889 Alteromonadales, and Rhodobacterales) made up a large component of our August networks  
890 (e.g. Buchan et al., 2014). Syndiniales, Dinophyceae, and ciliates were also abundant in the  
891 August network with a much more even distribution than in April, highlighting that both grazers  
892 and parasites were integral components of the August food web. The most connected protists  
893 belonged to the heterotrophic flagellate *Palpitomonas* (Yabuki et al., 2010) and the bacterivorous  
894 MAST-9, with a high percentage of significant negative correlations suggestive of an important  
895 predatory role.

### 896 *Conclusions*

897 We observed strong seasonal changes in the composition and connectivity of bacterial and  
898 protistan communities in nearshore waters of the eastern Alaskan Beaufort Sea (Fig. 2, Fig. 3,  
899 Fig. 7). Environmental conditions beneath sea ice favored parasitism and chemoautotrophy,  
900 including the surprising finding of Zetaproteobacteria. The presence of an increased relative  
901 abundance of chemoautotrophs suggests that iron, methane, nitrogen and sulfur cycling are  
902 important under the ice during a time when the food web is often considered to be less  
903 productive. In the spring we observed the formation of a complex and highly-connected,  
904 brackish microbial community highlighting the importance and influence of terrestrial inputs into  
905 coastal marine ecosystems. Given the freshening of the Arctic Ocean, these microbes may  
906 become increasingly important in Arctic marine food webs in years to come. Nutrient depletion  
907 over the course of the summer favored a shift from a diatom-dominated food web to one  
908 characterized by an increased relative abundance of heterotrophic and mixotrophic protists,  
909 especially dinoflagellates, as well as picophototrophs *Micromonas* and *Bathycoccus* and other  
910 small phytoflagellates. Bacterial communities became increasingly enriched in common marine

912 oligotrophic clades typically considered to have lower carbon demands and an increased ability  
913 to consume more recalcitrant organic matter. This shift to a more detrital food web in the late  
914 summer yielded a smaller and less connected network with longer paths between organisms than  
915 in April or June.

916 The Arctic is currently experiencing a number of physical changes that can have far-  
917 reaching effects on Arctic Ocean food webs. Surface air temperatures are warming at twice the  
918 rate of the rest of the globe, sea ice age and thickness continues to decline, and summer sea  
919 surface temperatures continue to show a warming trend year after year (Osborne et al., 2018).  
920 These changes are no doubt amplified in shallow, coastal systems such as our study system.  
921 These warmer temperatures also result in changes in precipitation and runoff patterns. We now  
922 have a baseline understanding of microbial communities in this region from which to predict  
923 community responses to a changing Arctic Ocean; one characterized by unique brackish  
924 communities with diatom blooms in the spring followed by long periods of nutrient poor  
925 conditions in shallow waters inhabited by small grazers, picophototrophs and oligotrophic  
926 bacterial clades. Continued long-term observations in this region are necessary to validate these  
927 predictions and assess their effects on higher trophic levels.

## 929 Acknowledgements

930 We thank R. Thompson, S. Linn, S. Smith, C. Harris, T. Dunton, and J. Dunton for their help  
931 with field sampling. We especially acknowledge the field and microbial sample collection efforts  
932 and intellectual contribution of T. L. Connelly. We thank L. Fine and M. Stuart for help with  
933 DNA extractions, and K. Meyer and K. Watkins-Brandt for help with flow cytometry. We also  
934 thank the US Fish and Wildlife Service, especially D. Payer, CH2M Hill Polar Services (CPS)  
935 and the Kaktovik Inuviat Corporation for their support. This project was funded by NSF Polar  
936 Programs awards 1023465, 1023582, and 1656026.

## 937 References

938 Alonso-Sáez, L., Sánchez, O., Gasol, J. M., Balagué, V., and Pedrós-Alio, C. (2008). Winter-to-  
939 summer changes in the composition and single-cell activity of near-surface Arctic  
940 prokaryotes. *Environ. Microbiol.* 10, 2444–2454. doi:10.1111/j.1462-2920.2008.01674.x.  
941 Anderson, M. J. (2017). “Permutational Multivariate Analysis of Variance (PERMANOVA),” in  
942 *Wiley StatsRef: Statistics Reference Online* (Chichester, UK: John Wiley & Sons, Ltd), 1–  
943 15. doi:10.1002/9781118445112.stat07841.  
944 Ardyna, M., Babin, M., Gosselin, M., Devred, E., Rainville, L., and Tremblay, J.-É. (2014).  
945 Recent Arctic Ocean sea ice loss triggers novel fall phytoplankton blooms. *Geophys. Res.*  
946 *Lett.* 41, 6207–6212. doi:10.1002/2014GL061047.  
947 Aronesty, E. (2011). ea-utils: Command-line tools for processing biological sequencing data.  
948 <http://code.google.com/p/ea-utils> (Durham, NC).  
949 Arrigo, K. R., Perovich, D. K., Pickart, R. S., Brown, Z. W., Van Dijken, G. L., Lowry, K. E., et  
950 al. (2012). Massive phytoplankton blooms under arctic sea ice. *Science (80-. ).* 336, 1408.  
951 doi:10.1126/science.1215065.  
952 Arrigo, K. R., and van Dijken, G. L. (2015). Continued increases in Arctic Ocean primary  
953 production. *Prog. Oceanogr.* 136, 60–70. doi:10.1016/j.pocean.2015.05.002.  
954 Azam, F., and Malfatti, F. (2007). Microbial structuring of marine ecosystems. *Nat. Rev.*  
955 *Microbiol.* 5, 782–791. doi:10.1038/nrmicro1747.  
956 Balzano, S., Gourvil, P., Siano, R., Chanoine, M., Marie, D., Lessard, S., et al. (2012a). Diversity

958 of cultured photosynthetic flagellates in the northeast Pacific and Arctic Oceans in summer.  
959 *Biogeosciences* 9, 4553–4571. doi:10.5194/bg-9-4553-2012.

960 Balzano, S., Marie, D., Gourvil, P., and Vaulot, D. (2012b). Composition of the summer  
961 photosynthetic pico and nanoplankton communities in the Beaufort Sea assessed by T-  
962 RFLP and sequences of the 18S rRNA gene from flow cytometry sorted samples. *ISME J.*  
963 6, 1480–1498. doi:10.1038/ismej.2011.213.

964 Beisser, D., Graupner, N., Bock, C., Wodniok, S., Grossmann, L., Vos, M., et al. (2017).  
965 Comprehensive transcriptome analysis provides new insights into nutritional strategies and  
966 phylogenetic relationships of chrysophytes. *PeerJ* 5, e2832. doi:10.7717/peerj.2832.

967 Bell, L., Bluhm, B., and Iken, K. (2016). Influence of terrestrial organic matter in marine food  
968 webs of the Beaufort Sea shelf and slope. *Mar. Ecol. Prog. Ser.* doi:10.3354/meps11725.

969 Benjamini, Y., and Hochberg, Y. (1995). Controlling the False Discovery Rate: A Practical and  
970 Powerful Approach to Multiple. Available at:  
971 <https://www.jstor.org/stable/pdf/2346101.pdf?refreqid=excelsior%3Adcf58cf3af7d68b55fd095e11763fd3> [Accessed November 11, 2018].

972 Booth, B. C., and Horner, R. A. (1997). Microalgae on the Arctic ocean section, 1994: Species  
973 abundance and biomass. *Deep. Res. Part II Top. Stud. Oceanogr.* 44, 1607–1622.  
974 doi:10.1016/S0967-0645(97)00057-X.

975 Boyd, E. S., Hamilton, T. L., Havig, J. R., Skidmore, M. L., and Shock, E. L. (2014).  
976 Chemolithotrophic primary production in a subglacial ecosystem. *Appl. Environ. Microbiol.*  
977 80, 6146–53. doi:10.1128/AEM.01956-14.

978 Bråte, J., Krabberød, A. K., Dolven, J. K., Ose, R. F., Kristensen, T., Bjørklund, K. R., et al.  
979 (2012). Radiolaria Associated with Large Diversity of Marine Alveolates. *Protist* 163, 767–  
980 777. doi:10.1016/J.PROTIS.2012.04.004.

981 Brown, S., Bart, J., Lanctot, R. B., Johnson, J. A., Kendall, S., Payer, D., et al. (2006). Shorebird  
982 Abundance and Distribution of the Coastal Plain of the Arctic National Wildlife Refuge.  
983 *Condor* 109, 1–14. Available at: <http://www.bioone.org/doi/pdf/10.1650/0010-5422%282007%29109%5B1%3ASAADOT%5D2.0.CO%3B2> [Accessed November 30, 984 2017].

985 Bunse, C., and Pinhassi, J. (2017). Special Series: Microbial Communities Marine  
986 Bacterioplankton Seasonal Succession Dynamics Role of Bacteria in Marine  
987 Biogeochemical Cycling. *Trends Microbiol.* 25, 494–505. doi:10.1016/j.tim.2016.12.013.

988 Caporaso, J. G., Kuczynski, J., Stombaugh, J., Bittinger, K., Bushman, F. D., Costello, E. K., et  
989 al. (2010). QIIME allows analysis of high-throughput community sequencing data. *Nat. Methods* 7, 335–336. doi:10.1038/nmeth.f.303.

990 Caporaso, J. G., Lauber, C. L., Walters, W. A., Berg-Lyons, D., Lozupone, C. A., Turnbaugh, P.  
991 J., et al. (2011). Global patterns of 16S rRNA diversity at a depth of millions of sequences  
992 per sample. *Proc. Natl. Acad. Sci.* 108, 4516–4522. doi:10.1073/pnas.1000080107.

993 Carlsson, P., Segatto, A. Z., and Graneli, E. (1993). Nitrogen bound to humic matter of terrestrial  
994 origin—a nitrogen pool for coastal phytoplankton? Available at: <https://www.int-res.com/articles/meps/97/m097p105.pdf> [Accessed May 14, 2019].

995 Chao, A. (1984). Nonparametric Estimation of the Number of Classes in a Population on JSTOR.  
996 *Scand. J. Stat.* 11, 265–270. Available at:  
997 [https://www.jstor.org/stable/4615964?seq=1#metadata\\_info\\_tab\\_contents](https://www.jstor.org/stable/4615964?seq=1#metadata_info_tab_contents) [Accessed  
998 September 12, 2019].

999 Chow, C.-E. T., Sachdeva, R., Cram, J. A., Steele, J. A., Needham, D. M., Patel, A., et al.  
1000

1004 (2013). Temporal variability and coherence of euphotic zone bacterial communities over a  
1005 decade in the Southern California Bight. *ISME J.* 7, 2259–2273.  
1006 doi:10.1038/ismej.2013.122.

1007 Clarke, K. R. (1993). Non-parametric multivariate analyses of changes in community structure.  
1008 *Austral Ecol.* 18, 117–143. doi:10.1111/j.1442-9993.1993.tb00438.x.

1009 Cleary, A. C., and Durbin, E. G. (2016). Unexpected prevalence of parasite 18S rDNA sequences  
1010 in winter among Antarctic marine protists. *J. Plankton Res.* 38, 401–417.  
1011 doi:10.1093/plankt/fbw005.

1012 Comeau, A. M., Li, W. K. W., Tremblay, J. É., Carmack, E. C., and Lovejoy, C. (2011). Arctic  
1013 ocean microbial community structure before and after the 2007 record sea ice minimum.  
1014 *PLoS One* 6. doi:10.1371/journal.pone.0027492.

1015 Connelly, T., McClelland, J., Crump, B., Kellogg, C., and Dunton, K. (2015). Seasonal changes  
1016 in quantity and composition of suspended particulate organic matter in lagoons of the  
1017 Alaskan Beaufort Sea. *Mar. Ecol. Prog. Ser.* 527, 31–45. doi:10.3354/meps11207.

1018 Corel, E., Lopez, P., Méheust, R., and Bapteste, E. (2016). Network-Thinking: Graphs to  
1019 Analyze Microbial Complexity and Evolution. *Trends Microbiol.* 24, 224–237.  
1020 doi:10.1016/J.TIM.2015.12.003.

1021 Craig, P. C. (1984). Fish use of coastal waters of the Alaska Beaufort Sea: a review. *Trans. Am.*  
1022 *Fish. Soc.* 113, 265–282. doi:10.1577/1548-8659(1984)113<265:FUOCWO>2.0.CO;2.

1023 Cram, J. A., Chow, C.-E. T., Sachdeva, R., Needham, D. M., Parada, A. E., Steele, J. A., et al.  
1024 (2015). Seasonal and interannual variability of the marine bacterioplankton community  
1025 throughout the water column over ten years. *ISME J.* 9, 563–580.  
1026 doi:10.1038/ismej.2014.153.

1027 de Vargas, C., Audic, S., Henry, N., Decelle, J., Mahé, F., Logares, R., et al. (2015). Ocean  
1028 plankton. Eukaryotic plankton diversity in the sunlit ocean. *Science* 348, 1261605.  
1029 doi:10.1126/science.1261605.

1030 Dolan, J. R., and Pérez, M. T. (2000). Costs, benefits and characteristics of mixotrophy in  
1031 marine oligotrichs. *Freshw. Biol.* 45, 227–238. doi:10.1046/j.1365-2427.2000.00659.x.

1032 Dufrêne, M., and Legendre, P. (1997). Species assemblages and indicator species: The need for a  
1033 flexible asymmetrical approach. *Ecol. Monogr.* 67, 345–366. doi:10.1890/0012-  
1034 9615(1997)067[0345:SAAIST]2.0.CO;2.

1035 Dunton, K. H., Schonberg, S. V., and Cooper, L. W. (2012). Food Web Structure of the Alaskan  
1036 Nearshore Shelf and Estuarine Lagoons of the Beaufort Sea. *Estuaries and Coasts* 35, 416–  
1037 435. doi:10.1007/s12237-012-9475-1.

1038 Dunton, K. H., Weingartner, T., and Carmack, E. C. (2006). The nearshore western Beaufort Sea  
1039 ecosystem: Circulation and importance of terrestrial carbon in arctic coastal food webs.  
1040 *Prog. Oceanogr.* 71, 362–378. doi:10.1016/j.pocean.2006.09.011.

1041 Edgar, R. C. (2013). UPARSE: highly accurate OTU sequences from microbial amplicon reads.  
1042 *Nat. Methods* 10, 996–998. doi:10.1038/nmeth.2604.

1043 Faith, D. P. (1992). Conservation evaluation and phylogenetic diversity. *Biol. Conserv.* 61, 1–10.

1044 Falkowski, P. G., Fenchel, T., and Delong, E. F. (2008). The microbial engines that drive Earth's  
1045 biogeochemical cycles. *Science* 320, 1034–9. doi:10.1126/science.1153213.

1046 Farag, I. F., Youssef, N. H., and Elshahed, M. S. (2017). Global Distribution Patterns and  
1047 Pangenomic Diversity of the Candidate Phylum "Latescibacteria" (WS3). *Appl.*  
1048 *Environ. Microbiol.* 83, e00521-17. doi:10.1128/AEM.00521-17.

1049 Faust, K., Sathirapongsasuti, J. F., Izard, J., Segata, N., Gevers, D., Raes, J., et al. (2012).

1050 Microbial Co-occurrence Relationships in the Human Microbiome. *PLoS Comput. Biol.* 8,  
1051 e1002606. doi:10.1371/journal.pcbi.1002606.

1052 Fernández-Gómez, B., Díez, B., Polz, M. F., Arroyo, J. I., Alfaro, F. D., Marchandon, G., et al.  
1053 (2019). Bacterial community structure in a sympagic habitat expanding with global  
1054 warming: brackish ice brine at 85–90 °N. *ISME J.* 13, 316–333. doi:10.1038/s41396-018-  
1055 0268-9.

1056 Ferrera, I., Sebastian, M., Acinas, S. G., and Gasol, J. M. (2015). Prokaryotic functional gene  
1057 diversity in the sunlit ocean: Stumbling in the dark. Elsevier Current Trends  
1058 doi:10.1016/j.mib.2015.03.007.

1059 Fuhrman, J. A., Cram, J. A., and Needham, D. M. (2015). Marine microbial community  
1060 dynamics and their ecological interpretation. *Nat. Rev. Microbiol.* 13, 133–146.  
1061 doi:10.1038/nrmicro3417.

1062 Garneau, M.-È., Roy, S., Lovejoy, C., Gratton, Y., and Vincent, W. F. (2008). Seasonal  
1063 dynamics of bacterial biomass and production in a coastal arctic ecosystem: Franklin Bay,  
1064 western Canadian Arctic. *J. Geophys. Res.* 113, C07S91. doi:10.1029/2007JC004281.

1065 Ghiglione, J.-F., Galand, P. E., Pommier, T., Pedros-Alio, C., Maas, E. W., Bakker, K., et al.  
1066 (2012). Pole-to-pole biogeography of surface and deep marine bacterial communities. *Proc.  
1067 Natl. Acad. Sci. U. S. A.* 109, 17633–17638. doi:10.1073/pnas.1208160109.

1068 Gilbert, J. A., Steele, J. A., Caporaso, J. G., Steinbrück, L., Reeder, J., Temperton, B., et al.  
1069 (2012). Defining seasonal marine microbial community dynamics. *ISME J.* 6, 298–308.  
1070 doi:10.1038/ismej.2011.107.

1071 Gu, Z., Gu, L., Eils, R., Schlesner, M., and Brors, B. (2014). circlize implements and enhances  
1072 circular visualization in R. *Bioinformatics* 30, 2811–2812.  
1073 doi:10.1093/bioinformatics/btu393.

1074 Guidi, L., Chaffron, S., Bittner, L., Eveillard, D., Larhlimi, A., Roux, S., et al. (2016). Plankton  
1075 networks driving carbon export in the oligotrophic ocean. *Nature* 532, 465–470.  
1076 doi:10.1038/nature16942.

1077 Guillou, L., Viprey, M., Chambouvet, A., Welsh, R. M., Kirkham, A. R., Massana, R., et al.  
1078 (2008). Widespread occurrence and genetic diversity of marine parasitoids belonging to  
1079 Syndiniales (Alveolata). doi:10.1111/j.1462-2920.2008.01731.x.

1080 Hardge, K., Peek, I., Neuhaus, S., Lange, B. A., Stock, A., Stoeck, T., et al. (2017). The  
1081 importance of sea ice for exchange of habitat-specific protist communities in the Central  
1082 Arctic Ocean. *J. Mar. Syst.* 165, 124–138. doi:10.1016/J.JMARSYS.2016.10.004.

1083 Harris, C. M., McClelland, J. W., Connelly, T. L., Crump, B. C., and Dunton, K. H. (2017).  
1084 Salinity and Temperature Regimes in Eastern Alaskan Beaufort Sea Lagoons in Relation to  
1085 Source Water Contributions. *Estuaries and Coasts* 40, 50–62. doi:10.1007/s12237-016-  
1086 0123-z.

1087 Harris, C. M., McTigue, N. D., McClelland, J. W., and Dunton, K. H. (2018). Do high Arctic  
1088 coastal food webs rely on a terrestrial carbon subsidy? *Food Webs* 15, e00081.  
1089 doi:10.1016/j.fooweb.2018.e00081.

1090 Hernández-Ruiz, M., Prieto, A., Barber-Lluch, E., and Teira, E. (2018). Amino acid utilization  
1091 by eukaryotic picophytoplankton in a coastal upwelling system. *Mar. Ecol. Prog. Ser.* 588,  
1092 43–57. doi:10.3354/meps12435.

1093 Holmes, R. M., McClelland, J. W., Peterson, B. J., Tank, S. E., Bulygina, E., Eglinton, T. I., et  
1094 al. (2012). Seasonal and Annual Fluxes of Nutrients and Organic Matter from Large Rivers  
1095 to the Arctic Ocean and Surrounding Seas. *Estuaries and Coasts* 35, 369–382.

doi:10.1007/s12237-011-9386-6.

Hugerth, L. W., Larsson, J., Alneberg, J., Lindh, M. V., Legrand, C., Pinhassi, J., et al. (2015). Metagenome-assembled genomes uncover a global brackish microbiome. *Genome Biol.* 16, 279. doi:10.1186/s13059-015-0834-7.

Hyun, J., and Kim, K. (2003). Bacterial abundance and production during the unique spring phytoplankton bloom in the central Yellow Sea. *Mar. Ecol. Prog. Ser.* 252, 77–88. doi:10.3354/meps252077.

Johnson, J. A., Lanctot, R. B., Andres, B. A., Bart, J. R., Brown, S. C., Kendall, S. J., et al. (2007). Predicting breeding shorebird distributions on the Arctic Coastal Plain of Alaska. *Arctic* 60, 277–293. doi:<http://dx.doi.org/10.1890/ES12-00292.1>.

Joli, N., Monier, A., Logares, R., and Lovejoy, C. (2017). Seasonal patterns in Arctic prasinophytes and inferred ecology of *Bathycoccus* unveiled in an Arctic winter metagenome. *ISME J.* 117, 1372–1385. doi:10.1038/ismej.2017.7.

Kantor, R. S., Wrighton, K. C., Handley, K. M., Sharon, I., Hug, L. A., Castelle, C. J., et al. (2013). Small genomes and sparse metabolisms of sediment-associated bacteria from four candidate phyla. *MBio* 4, e00708-13. doi:10.1128/mBio.00708-13.

Kara, E. L., Hanson, P. C., Hu, Y. H., Winslow, L., and McMahon, K. D. (2013). A decade of seasonal dynamics and co-occurrences within freshwater bacterioplankton communities from eutrophic Lake Mendota, WI, USA. *ISME J.* 7, 680–684. doi:10.1038/ismej.2012.118.

Kilias, E. S., Peek, I., and Metfies, K. (2014). Insight into protist diversity in Arctic sea ice and melt-pond aggregate obtained by pyrosequencing View supplementary material. doi:10.3402/polar.v33.23466.

Kubiszyn, A. M., and Wiktor, J. M. (2016). The *Gymnodinium* and *Gyrodinium* (Dinoflagellata: Gymnodiniaceae) of the West Spitsbergen waters (1999–2010): biodiversity and morphological description of unidentified species. *Polar Biol.* 39, 1739–1747. doi:10.1007/s00300-015-1764-2.

Li, W. K. W., McLaughlin, F. A., Lovejoy, C., and Carmack, E. C. (2009). Smallest algae thrive as the Arctic Ocean freshens. *Science* 326, 539. doi:10.1126/science.1179798.

Lima-Mendez, G., Faust, K., Henry, N., Decelle, J., Colin, S., Carcillo, F., et al. (2015). Determinants of community structure in the global plankton interactome. *Science* (80-. ). 348. doi:10.1126/science.1262073.

Logares, R., Audic, S., Santini, S., Pernice, M. C., De Vargas, C., and Massana, R. (2012). Diversity patterns and activity of uncultured marine heterotrophic flagellates unveiled with pyrosequencing. *ISME J.* 6, 1823–1833. doi:10.1038/ismej.2012.36.

Lovejoy, C. (2014). Changing Views of Arctic Protists (Marine Microbial Eukaryotes) in a Changing Arctic. *Acta Protozool.* 53, 91–100. doi:doi:10.4467/16890027AP.14.009.1446.

Lovejoy, C., Galand, P. E., and Kirchman, D. L. (2011). Picoplankton diversity in the Arctic Ocean and surrounding seas. *Mar. Biodivers.* 41, 5–12. doi:10.1007/s12526-010-0062-z.

Lovejoy, C., Massana, R., and Pedrós-Alió, C. (2006). Diversity and distribution of marine microbial eukaryotes in the Arctic Ocean and adjacent seas. *Appl. Environ. Microbiol.* 72, 3085–95. doi:10.1128/AEM.72.5.3085-3095.2006.

Marchese, C., Albouy, C., Tremblay, J.-É., Dumont, D., D'Ortenzio, F., Vissault, S., et al. (2017). Changes in phytoplankton bloom phenology over the North Water (NOW) polynya: a response to changing environmental conditions. *Polar Biol.* 40, 1721–1737. doi:10.1007/s00300-017-2095-2.

Marquardt, M., Vader, A., Stübner, E. I., Reigstad, M., and Gabrielsen, T. M. (2016). Strong

1142 Seasonality of Marine Microbial Eukaryotes in a High-Arctic Fjord (Isfjorden, in West  
1143 Spitsbergen, Norway). *Appl. Environ. Microbiol.* 82, 1868–80. doi:10.1128/AEM.03208-  
1144 15.

1145 McAllister, S. M., Davis, R. E., McBeth, J. M., Tebo, B. M., Emerson, D., and Moyer, C. L.  
1146 (2011). Biodiversity and emerging biogeography of the neutrophilic iron-oxidizing  
1147 Zetaproteobacteria. *Appl. Environ. Microbiol.* 77, 5445–57. doi:10.1128/AEM.00533-11.

1148 McBeth, J. M., Little, B. J., Ray, R. I., Farrar, K. M., and Emerson, D. (2011). Neutrophilic iron-  
1149 oxidizing “Zetaproteobacteria” and mild steel corrosion in nearshore marine environments.  
1150 *Appl. Environ. Microbiol.* 77, 1405–1412. doi:10.1128/AEM.02095-10.

1151 McCallister, S. L., Bauer, J. E., Cherrier, J. E., and Ducklow, H. W. (2004). Assessing sources  
1152 and ages of organic matter supporting river and estuarine bacterial production: A multiple  
1153 isotope (D14C, d13C, and d15N) approach. *Limnol. Oceanogr.* 49, 1687–1702.  
1154 doi:10.4319/lo.2004.49.5.1687.

1155 McClelland, J. W., Déry, S. J., Peterson, B. J., Holmes, R. M., and Wood, E. F. (2006). A pan-  
1156 arctic evaluation of changes in river discharge during the latter half of the 20th century.  
1157 *Geophys. Res. Lett.* 33, L06715. doi:10.1029/2006GL025753.

1158 McClelland, J. W., Townsend-Small, A., Holmes, R. M., Pan, F., Stieglitz, M., Khosh, M., et al.  
1159 (2014). River export of nutrients and organic matter from the North Slope of Alaska to the  
1160 Beaufort Sea. *Water Resour. Res.* 50, 1823–1839. doi:10.1002/2013WR014722.

1161 McManus, G. B., and Santoferrara, L. F. (2012). “Tintinnids in Microzooplankton  
1162 Communities,” in *The Biology and Ecology of Tintinnid Ciliates* (Chichester, UK: John  
1163 Wiley & Sons, Ltd), 198–213. doi:10.1002/9781118358092.ch9.

1164 McMurdie, P. J., and Holmes, S. (2014). Waste Not, Want Not: Why Rarefying Microbiome  
1165 Data Is Inadmissible. *PLoS Comput. Biol.* 10, e1003531. doi:10.1371/journal.pcbi.1003531.

1166 McPhee, M. G., Proshutinsky, A., Morison, J. H., Steele, M., and Alkire, M. B. (2009). Rapid  
1167 change in freshwater content of the Arctic Ocean. *Geophys. Res. Lett.* 36, L10602.  
1168 doi:10.1029/2009GL037525.

1169 Meshram, A. R., Vader, A., Kristiansen, S., and Gabrielsen, T. M. (2017). Microbial Eukaryotes  
1170 in an Arctic Under-Ice Spring Bloom North of Svalbard. *Front. Microbiol.* 8, 1099.  
1171 doi:10.3389/fmicb.2017.01099.

1172 Meyer, K. A., O’Neil, J. M., and Hitchcock, G. L. (2014). Microbial production along the West  
1173 Florida Shelf: Responses of bacteria and viruses to the presence and phase of *Karenia brevis*  
1174 blooms. *Harmful Algae* 38, 110–118. doi:10.1016/J.HAL.2014.04.015.

1175 Michel, C., Legendre, L., Therriault, J.-C., Demers, S., and Vandevalde, T. (1993). Springtime  
1176 coupling between ice algal and phytoplankton assemblages in southeastern Hudson Bay,  
1177 Canadian Arctic. Springer-Verlag Available at:  
1178 <https://link.springer.com/content/pdf/10.1007%2FBF00233135.pdf> [Accessed December  
1179 17, 2018].

1180 Milici, M., Deng, Z. L., Tomasch, J., Decelle, J., Wos-Oxley, M. L., Wang, H., et al. (2016). Co-  
1181 occurrence analysis of microbial taxa in the Atlantic ocean reveals high connectivity in the  
1182 free-living bacterioplankton. *Front. Microbiol.* 7. doi:10.3389/fmicb.2016.00649.

1183 Mohan, S. D., Connelly, T. L., Harris, C. M., Dunton, K. H., and McClelland, J. W. (2016).  
1184 Seasonal trophic linkages in Arctic marine invertebrates assessed via fatty acids and  
1185 compound-specific stable isotopes. *Ecosphere* 7. doi:10.1002/ecs2.1429.

1186 Monier, A., Comte, J., Babin, M., Forest, A., Matsuoka, A., and Lovejoy, C. (2015).  
1187 Oceanographic structure drives the assembly processes of microbial eukaryotic

1188        communities. *ISME J.* 9, 990–1002. doi:10.1038/ismej.2014.197.

1189        Monier, A., Terrado, R., Thaler, M., Comeau, A., Medrinal, E., and Lovejoy, C. (2013). Upper  
1190        Arctic Ocean water masses harbor distinct communities of heterotrophic flagellates.  
1191        *Biogeosciences* 10, 4273–4286. doi:10.5194/bg-10-4273-2013.

1192        Morata, N., Renaud, P., Brugel, S., Hobson, K., and Johnson, B. (2008). Spatial and seasonal  
1193        variations in the pelagic–benthic coupling of the southeastern Beaufort Sea revealed by  
1194        sedimentary biomarkers. *Mar. Ecol. Prog. Ser.* 371, 47–63. doi:10.3354/meps07677.

1195        Morison, J., Kwok, R., Peralta-Ferriz, C., Alkire, M., Rigor, I., Andersen, R., et al. (2012).  
1196        Changing Arctic Ocean freshwater pathways. *Nature* 481, 66–70. doi:10.1038/nature10705.

1197        Nakamura, Y., and Suzuki, N. (2015). “Phaeodaria: Diverse marine cercozoans of World-Wide  
1198        distribution,” in *Marine Protists: Diversity and Dynamics* (Tokyo: Springer Japan), 223–  
1199        249. doi:10.1007/978-4-431-55130-0\_9.

1200        Nolan, M., Churchwell, R., Adams, J., McClelland, J., Tape, K. D., Kendall, S., et al. (2011).  
1201        Predicting the impact of glacier loss on fish, birds, floodplains, and estuaries in the Arctic  
1202        National Wildlife Refuge. in *Observing, Studying and Managing for Change. Proceedings  
1203        of the Fourth Interagency Conference on Research in the Watersheds: U.S. Geological  
1204        Survey Scientific Investigations Report*, eds. C. N. Medley, G. Patterson, and M. J. Parker,  
1205        49–54.

1206        Oksanen, J., Blanchet, F. G., Friendly, M., Kindt, R., Legendre, P., McGlinn, D., et al. (2019).  
1207        vegan: Community Ecology Package. *R Packag. version 2.5-4*. Available at: <https://cran.r-project.org/package=vegan>.

1208        Onda, D. F. L., Medrinal, E., Comeau, A. M., Thaler, M., Babin, M., and Lovejoy, C. (2017).  
1209        Seasonal and Interannual Changes in Ciliate and Dinoflagellate Species Assemblages in the  
1210        Arctic Ocean (Amundsen Gulf, Beaufort Sea, Canada). *Front. Mar. Sci.* 4, 16.  
1211        doi:10.3389/fmars.2017.00016.

1212        Osborne, E., Richter-Menge, J., and Jeffries, M. (2018). Arctic Report Card 2018. Available at:  
1213        <https://www.arctic.noaa.gov/Report-Card>.

1214        Peres-Neto, P. R., and Jackson, D. A. (2001). How well do multivariate data sets match? The  
1215        advantages of a Procrustean superimposition approach over the Mantel test. *Oecologia* 129,  
1216        169–178. doi:10.1007/s004420100720.

1217        Peura, S., Bertilsson, S., Jones, R. I., and Eiler, A. (2015). Resistant Microbial Cooccurrence  
1218        Patterns Inferred by Network Topology. *Appl. Environ. Microbiol.* 81, 2090–2097.  
1219        doi:10.1128/aem.03660-14.

1220        Piwosz, K., and Pernthaler, J. (2010). Seasonal population dynamics and trophic role of  
1221        planktonic nanoflagellates in coastal surface waters of the Southern Baltic Sea. *Environ.  
1222        Microbiol.* 12, 364–377. doi:10.1111/j.1462-2920.2009.02074.x.

1223        Piwosz, K., Wiktor, J. M., Niemi, A., Tatarek, A., and Michel, C. (2013). Mesoscale distribution  
1224        and functional diversity of picoeukaryotes in the first-year sea ice of the Canadian Arctic.  
1225        *ISME J.* 7, 1461–1471. doi:10.1038/ismej.2013.39.

1226        Poulin, M., Daugbjerg, N., Gradinger, R., Ilyash, L., Ratkova, T., and von Quillfeldt, C. (2011).  
1227        The pan-Arctic biodiversity of marine pelagic and sea-ice unicellular eukaryotes: A first-  
1228        attempt assessment. *Mar. Biodivers.* 41, 13–28. doi:10.1007/s12526-010-0058-8.

1229        Quast, C., Pruesse, E., Yilmaz, P., Gerken, J., Schweer, T., Yarza, P., et al. (2013). The SILVA  
1230        ribosomal RNA gene database project: Improved data processing and web-based tools.  
1231        *Nucleic Acids Res.* 41, D590–D596. doi:10.1093/nar/gks1219.

1232        Rooney, N., and McCann, K. S. (2012). Integrating food web diversity, structure and stability.

1233

1234        *Trends Ecol. Evol.* 27, 40–46. doi:10.1016/J.TREE.2011.09.001.

1235        Satomi, M., and Fujii, T. (2014). The family oceanospirillaceae. *The Prokaryotes: Gammaproteobacteria* 9783642389, 491–527. doi:10.1007/978-3-642-38922-1\_286.

1236        Schreiner, K. M., Bianchi, T. S., Eglinton, T. I., Allison, M. A., and Hanna, A. J. M. (2013). Sources of terrigenous inputs to surface sediments of the Colville River Delta and Simpson's Lagoon, Beaufort Sea, Alaska. *J. Geophys. Res. Biogeosciences* 118, 808–824. doi:10.1002/jgrg.20065.

1237        Serreze, M. C., and Barry, R. G. (2011). Processes and impacts of Arctic amplification: A research synthesis. *Glob. Planet. Change* 77, 85–96. doi:10.1016/j.gloplacha.2011.03.004.

1238        Seuthe, L., Töpper, B., Reigstad, M., Thyrhaug, R., and Vaquer-Sunyer, R. (2011). Microbial communities and processes in ice-covered Arctic waters of the northwestern Fram Strait (75 to 80°N) during the vernal pre-bloom phase. *Aquat. Microb. Ecol.* 64, 253–266. doi:10.3354/ame01525.

1239        Sheik, C. S., Jain, S., and Dick, G. J. (2014). Metabolic flexibility of enigmatic SAR324 revealed through metagenomics and metatranscriptomics. *Environ. Microbiol.* 16, 304–317. doi:10.1111/1462-2920.12165.

1240        Sherr, E. B., Sherr, B. F., and Fessenden, L. (1997). Heterotrophic protists in the Central Arctic Ocean. *Deep Sea Res. Part II Top. Stud. Oceanogr.* 44, 1665–1682. doi:10.1016/S0967-0645(97)00050-7.

1241        Siano, R., Montresor, M., Probert, I., Not, F., and de Vargas, C. (2010). *Pelagodinium* gen. nov. and *P. bēii* comb. nov., a Dinoflagellate Symbiont of Planktonic Foraminifera. *Protist* 161, 385–399. doi:10.1016/J.PROTIS.2010.01.002.

1242        Silkin, V. M., Chulkov, E. V., and Echenique, P. M. (2003). First-principles calculation of the electron inelastic mean free path in Be metal. *Phys. Rev. B - Condens. Matter Mater. Phys.* 68, 23466. doi:10.3402/polar.v33.23466.

1243        Sipler, R. E., Kellogg, C. T. E., Connelly, T. L., Roberts, Q. N., Yager, P. L., and Bronk, D. A. (2017). Microbial community response to terrestrially derived dissolved organic matter in the coastal Arctic. *Front. Microbiol.* 8. doi:10.3389/fmicb.2017.01018.

1244        Smith, B., and Wilson, J. B. (1996). A Consumer's Guide to Evenness Indices. *Oikos* 76, 70. doi:10.2307/3545749.

1245        Smith, M. W., Herfort, L., Fortunato, C. S., Crump, B. C., and Simon, H. M. (2017). Microbial players and processes involved in phytoplankton bloom utilization in the water column of a fast-flowing, river-dominated estuary. *Microbiologyopen* 6, e00467. doi:10.1002/mbo3.467.

1246        Smoot, M. E., Ono, K., Ruscheinski, J., Wang, P.-L., and Ideker, T. (2011). Cytoscape 2.8: new features for data integration and network visualization. *Bioinformatics* 27, 431–2. doi:10.1093/bioinformatics/btq675.

1247        Spring, S., Scheuner, C., Göker, M., and Klenk, H.-P. (2015). A taxonomic framework for emerging groups of ecologically important marine gammaproteobacteria based on the reconstruction of evolutionary relationships using genome-scale data. *Front. Microbiol.* 6, 281. doi:10.3389/fmicb.2015.00281.

1248        Stingl, U., Desiderio, R. A., Cho, J.-C., Vergin, K. L., and Giovannoni, S. J. (2007). The SAR92 clade: an abundant coastal clade of culturable marine bacteria possessing proteorhodopsin. *Appl. Environ. Microbiol.* 73, 2290–6. doi:10.1128/AEM.02559-06.

1249        Stoecker, D. K., Hansen, P. J., Caron, D. A., and Mitra, A. (2017). Mixotrophy in the Marine Plankton. *Ann. Rev. Mar. Sci.* 9, 311–335. doi:10.1146/annurev-marine-010816-060617.

1250        Stroeve, J. C., Serreze, M. C., Holland, M. M., Kay, J. E., Malanik, J., and Barrett, A. P. (2012).

1280 The Arctic's rapidly shrinking sea ice cover: a research synthesis. *Clim. Change* 110, 1005–  
1281 1027. doi:10.1007/s10584-011-0101-1.

1282 Taylor, A. R., Lanctot, R. B., Powell, A. N., Huettman, F., Nigro, D. A., and Kendall, S. J.  
1283 (2010). Distribution and community characteristics of staging shorebirds on the northern  
1284 coast of Alaska. *Arctic* 63, 451–467.

1285 Teeling, H., Fuchs, B. M., Becher, D., Klockow, C., Gardebrecht, A., Bennke, C. M., et al.  
1286 (2012). Substrate-Controlled Succession of Marine Bacterioplankton Populations Induced  
1287 by a Phytoplankton Bloom. *Science* (80-. ). 336, 608–611. doi:10.1126/science.1218344.

1288 Terrado, R., Scarella, K., Thaler, M., Vincent, W. F., and Lovejoy, C. (2013). Small  
1289 phytoplankton in Arctic seas: vulnerability to climate change. *Biodiversity* 14, 2–18.  
1290 doi:10.1080/14888386.2012.704839.

1291 Terrado, R., Vincent, W., and Lovejoy, C. (2009). Mesopelagic protists: diversity and succession  
1292 in a coastal Arctic ecosystem. *Aquat. Microb. Ecol.* 56, 25–39. doi:10.3354/ame01327.

1293 Thaler, M., and Lovejoy, C. (2013). Environmental selection of marine stramenopile clades in  
1294 the Arctic Ocean and coastal waters. *Polar Biol.* 37, 347–357. doi:10.1007/s00300-013-  
1295 1435-0.

1296 Thaler, M., and Lovejoy, C. (2015). Biogeography of heterotrophic flagellate populations  
1297 indicates the presence of generalist and specialist taxa in the Arctic Ocean. *Appl. Environ.*  
1298 *Microbiol.* 81, 2137–2148. doi:10.1128/AEM.02737-14.

1299 Timmermans, M.-L., and Ladd, C. (2018). Sea Surface Temperature. Available at:  
1300 <https://www.arctic.noaa.gov/Report-Card>.

1301 Torres-Beltrán, M., Sehein, T., Pachiadaki, M. G., Hallam, S. J., and Edgcomb, V. (2018).  
1302 Protistan parasites along oxygen gradients in a seasonally anoxic fjord: A network approach  
1303 to assessing potential host-parasite interactions. *Deep. Res. Part II Top. Stud. Oceanogr.*  
1304 doi:10.1016/j.dsr2.2017.12.026.

1305 Vaqué, D., Guadayol, Ò., Peters, F., Felipe, J., Angel-Ripoll, L., Terrado, R., et al. (2008).  
1306 Seasonal changes in planktonic bacterivory rates under the ice-covered coastal Arctic  
1307 Ocean. *Limnol. Oceanogr.* 53, 2427–2438. doi:10.4319/lo.2008.53.6.2427.

1308 Véillette, J., Lovejoy, C., Potvin, M., Harding, T., Jungblut, A. D., Antoniades, D., et al. (2011).  
1309 Milne Fiord epishelf lake: A coastal Arctic ecosystem vulnerable to climate change.  
1310 *Écoscience* 18, 304–316. doi:10.2980/18-3-3443.

1311 Vernet, M., Richardson, T. L., Metfies, K., Nöthig, E.-M., and Peeken, I. (2017). Models of  
1312 Plankton Community Changes during a Warm Water Anomaly in Arctic Waters Show  
1313 Altered Trophic Pathways with Minimal Changes in Carbon Export. *Front. Mar. Sci.* 4,  
1314 160. doi:10.3389/fmars.2017.00160.

1315 Vick-Majors, T. J., Mitchell, A. C., Achberger, A. M., Christner, B. C., Dore, J. E., Michaud, A.  
1316 B., et al. (2016). Physiological Ecology of Microorganisms in Subglacial Lake Whillans.  
1317 *Front. Microbiol.* 7, 1705. doi:10.3389/fmicb.2016.01705.

1318 von Biela, V. R., Zimmerman, C. E., Cohn, B. R., and Welker, J. M. (2013). Terrestrial and  
1319 marine trophic pathways support young-of-year growth in a nearshore Arctic fish. *Polar*  
1320 *Biol.* 36, 137–146. doi:10.1007/s00300-012-1244-x.

1321 Wassmann, P., Duarte, C. M., Agustí, S., and Sejr, M. K. (2011). Footprints of climate change in  
1322 the Arctic marine ecosystem. *Glob. Chang. Biol.* 17, 1235–1249. doi:10.1111/j.1365-  
1323 2486.2010.02311.x.

1324 Weiss, S., Van Treuren, W., Lozupone, C., Faust, K., Friedman, J., Deng, Y., et al. (2016).  
1325 Correlation detection strategies in microbial data sets vary widely in sensitivity and

1326 precision. *ISME J.* 10, 1669–1681. doi:10.1038/ismej.2015.235.

1327 Weitz, J. S., Stock, C. A., Wilhelm, S. W., Bourouiba, L., Coleman, M. L., Buchan, A., et al.

1328 (2015). A multitrophic model to quantify the effects of marine viruses on microbial food

1329 webs and ecosystem processes. *ISME J.* 9, 1352–1364. doi:10.1038/ismej.2014.220.

1330 Whitefield, J., Winsor, P., McClelland, J., and Menemenlis, D. (2015). A new river discharge

1331 and river temperature climatology data set for the pan-Arctic region. *Ocean Model.* 88, 1–

1332 15. doi:10.1016/j.ocemod.2014.12.012.

1333 Williams, R. J., Berlow, E. L., Dunne, J. A., Szló Barabá Si §, A.-L., Martinez, N. D., Williams,

1334 R. J., et al. (2002). Two degrees of separation in complex food webs. Available at:

1335 [www.pnas.org/cgi/doi/10.1073/pnas.192448799](http://www.pnas.org/cgi/doi/10.1073/pnas.192448799) [Accessed March 26, 2019].

1336 Worden, A. Z., Follows, M. J., Giovannoni, S. J., Wilken, S., Zimmerman, A. E., and Keeling, P.

1337 J. (2015). Rethinking the marine carbon cycle: Factoring in the multifarious lifestyles of

1338 microbes. *Science (80- ).* 347, 1257594–1257594. doi:10.1126/science.1257594.

1339 Yabuki, A., Inagaki, Y., and Ishida, K. (2010). Palpitomonas bilix gen. et sp. nov.: A Novel

1340 Deep-branching Heterotroph Possibly Related to Archaeplastida or Hacrobia. *Protist* 161,

1341 523–538. doi:10.1016/J.PROTIS.2010.03.001.

1342 Yilmaz, P., Parfrey, L. W., Yarza, P., Gerken, J., Pruesse, E., Quast, C., et al. (2014). The

1343 SILVA and “All-species Living Tree Project (LTP)” taxonomic frameworks. *Nucleic Acids*

1344 *Res.* 42, D643–D648. doi:10.1093/nar/gkt1209.

1345 Yunker, M. B., Backus, S. M., Graf Pannatier, E., Jeffries, D. S., and Macdonald, R. W. (2002).

1346 Sources and Significance of Alkane and PAH Hydrocarbons in Canadian Arctic Rivers.

1347 *Estuar. Coast. Shelf Sci.* 55, 1–31. doi:10.1006/ECSS.2001.0880.

1348 Yunker, M. B., Macdonald, R. W., Cretney, W. J., Fowler, B. R., and McLaughlin, F. A. (1993).

1349 Alkane, terpene and polycyclic aromatic hydrocarbon geochemistry of the Mackenzie River

1350 and Mackenzie shelf: Riverine contributions to Beaufort Sea coastal sediment. *Geochim.*

1351 *Cosmochim. Acta* 57, 3041–3061. doi:10.1016/0016-7037(93)90292-5.

1352

1353

1354 Table 1. Monthly average physical and chemical properties across all lagoons. Standard  
 1355 deviations are given in parentheses. BA = Bacterial abundance.

	<b>April</b> (n = 13)	<b>June</b> (n = 15)	<b>August</b> (n = 57)
<b>Salinity</b>	35.6 (4.4)	5.4 (9.9)	22.5 (6.8)
<b>Temperature (°C)</b>	-2.0 (0.3)	2.0 (1.5)	8.9 (2.9)
<b>DO (mg l<sup>-1</sup>)</b>	12.1 (2.1)	13.4 (1.0)	10.7 (1.3)
<b>Chl a (µg l<sup>-1</sup>)</b>	0.042 (0.03)	2.3 (3.8)	0.38 (0.4)
<b>pH</b>	7.5 (0.3)	7.9 (0.3)	7.9 (0.2)
<b>BA (x10<sup>8</sup> cells/L)</b>	4.0 (4.5)	6.6 (2.9)	8.7 (5.5)
<b>DOC (µmol)</b>	107.9 (23.2)	211.3 (57.2)	109.9 (37.7)
<b>DON (µmol)</b>	5.4 (6.6)	6.6 (2.9)	6.4 (2.0)
<b>DOC:DON</b>	15.6 (11.8)	45.4 (43.5)	18.5 (7.5)
<b>SUVA<sub>254</sub></b>	2.3 (1.1)	3.5 (0.5)	2.6 (1.0)
<b>S<sub>275-295</sub></b>	-0.014 (0.005)	-0.014 (0.001)	-0.014 (0.004)
<b>TDN (mg/l)</b>	0.18 (0.09)	0.13 (0.03)	0.10 (0.02)
<b>NO<sub>3</sub> (µmol)</b>	2.8 (2.0)	1.2 (1.6)	0.081 (0.3)
<b>NH<sub>4</sub> (µmol)</b>	4.9 (10.5)	1.4 (1.6)	0.3 (0.7)
<b>POC (µg l<sup>-1</sup>)</b>	106.6 (119.7)	538.4 (152.3)	216.4 (75.7)
<b>PN (µg l<sup>-1</sup>)</b>	17.9 (22.5)	74.4 (19.3)	36.6 (12.9)
<b>POC:PN</b>	6.7 (1.3)	7.3 (1.2)	6.0 (0.9)
<b>POC δ<sup>13</sup>C (‰)</b>	-26.7 (1.3)	-28.5 (1.4)	-26.8 (2.6)
<b>PN δ<sup>15</sup>N (‰)</b>	5.2 (2.4)	4.7 (2.3)	6.5 (1.7)
<b>H<sub>2</sub>O-δ<sup>18</sup>O</b>	-3.7 (0.5)	-15.3 (3.2)	-6.4 (3.0)

1356  
 1357  
 1358  
 1359  
 1360

1361

Table 2. Network Statistics, calculated in Cytoscape v. 3.6.1

Network Property	April	June	August
<b># Nodes (S)</b>	1272	1966	662
<b># Edges (L)</b>	21122	109143	3121
<b># Positive Edges</b>	18601	107836	2650
<b># Negative Edges</b>	2521	1936	471
<b>Link Density (L/S)</b>	16.61	55.52	4.71
<b>Connectance (L/S<sup>2</sup>)</b>	0.0131	0.0282	0.0071
<b>Ave. Degree</b>	33.2	111	9.4
<b>Network Diameter</b>	12	10	13
<b>Graph Density</b>	0.026	0.057	0.014
<b>Network Centralization</b>	0.146	0.222	0.104
<b>Connected Components</b>	5	6	35
<b>Clustering Coefficient</b>	0.363	0.441	0.385
<b>Average Path Length</b>	3.929	3.097	4.27

1362

1363

1364 Fig. 1. Map of the sampling region. Black circles indicate all locations from which samples were  
1365 collected. Site names in bold were sampled in all seasons, while those not bolded were sampled  
1366 only in August. The star indicates the location of the town of Kaktovik, Alaska.

1367

1368 Fig. 2. Principle components analysis (A) of environmental measurements, and multidimensional  
1369 scaling plots of microbial community betadiversity assessed with (B) Bacterial 16S rRNA gene,  
1370 and (C) Eukaryotic18S rRNA gene based on proportion of non-subsampled data.

1371

1372 Fig. 3. Boxplots of abundant (A) bacterial and (B) eukaryotic (protistan and fungal) groups for  
1373 each month sampled across all years sampled. River samples, though collected in August, were  
1374 averaged separately. The color of the lines next to taxa names indicates the month in which each  
1375 taxa or group of taxa was most abundant.

1376

1377 Fig. 4. Taxonomic affiliation of top Bacterial (A-C) and Eukaryotic (D-F) high abundance  
1378 indicator OTUs for each month. High abundance indicator OTUs are those OTUs that had an  
1379 indicator value of  $>0.7$ , a p-value  $<0.001$  and made up at least 0.5% of the community for the  
1380 month in which they were an indicator. The monthly average relative abundance of these  
1381 indicator OTUs is shown relative to proportion of non-indicator and low abundance ( $<0.5\%$ )  
1382 indicator taxa.

1383

1384 Fig. 5. Heatmap showing significant (FDR-corrected) spearman correlations between top  
1385 indicator OTUs and physico-chemical variables. Both the month and taxonomic affiliation of the  
1386 indicator OTU are indicated above the heatmap.

1387

1388 Fig. 6. Chord diagrams showing the positive and negative correlations among the top 15 taxa in  
1389 the monthly co-occurrence networks (April: A, B, June: C, D, and August: E, F). The inner circle  
1390 shows the breakdown of how the correlations within each month are distributed among these 15  
1391 taxa, with the outer circle showing the domains to which these taxa belong. The width of the bar  
1392 is proportional to the number of correlations (positive *and* negative) for each taxa with the other  
1393 14 taxa. The arcs drawn between bars (i.e. taxa) are proportional to the number of positive (left)  
1394 or negative (right) correlations between these two taxa. Arcs that remain within a bar denote  
1395 significant correlations among OTUs within that taxa.

1396

1397 Fig 7. Diagram depicting major seasonal microbial community changes in the Beaufort Lagoons  
1398 ecosystem, with arrows depicting hypothesized pathways for carbon flow from one group of  
1399 organisms to another. The size of the arrow indicates relative magnitude of this hypothesized  
1400 carbon flow, and the size of the text indicates relative size of carbon pool, based on the relative  
1401 abundance of microbial taxa each month.

Figure 1.TIF

Figure 1.

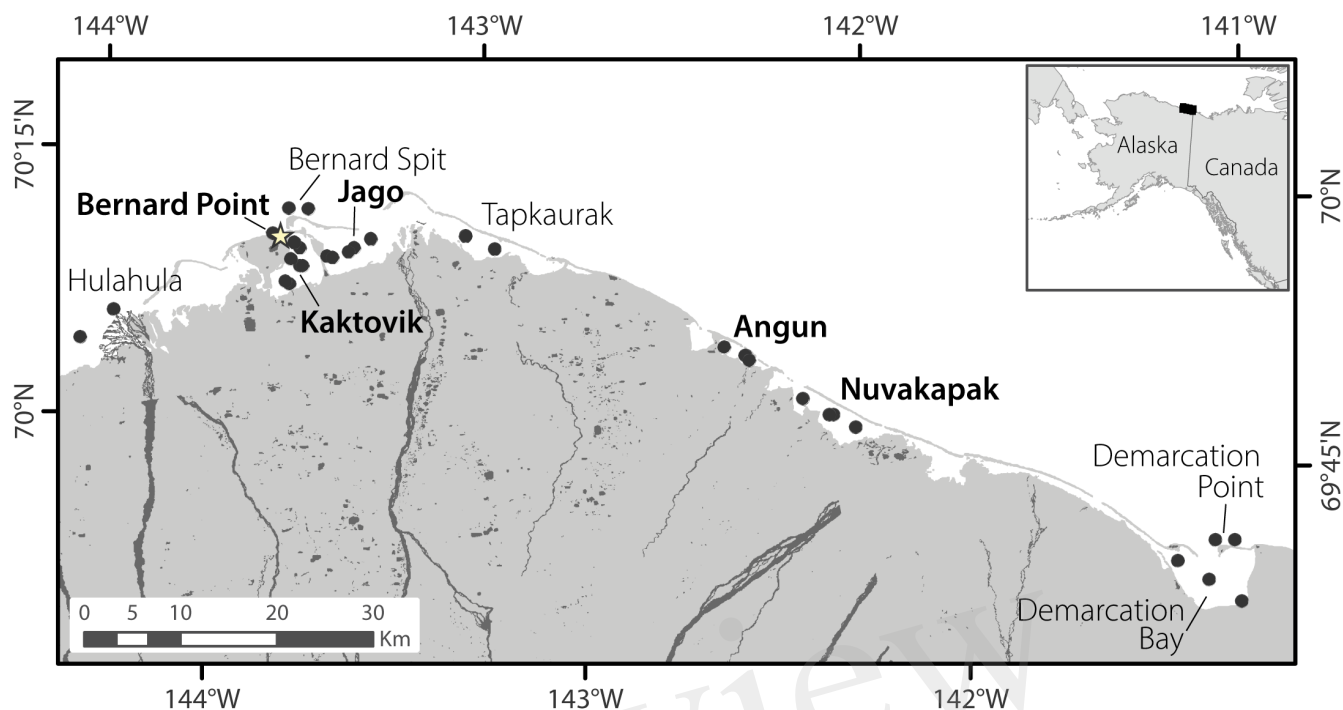


Figure 2.

Figure 2.TIF

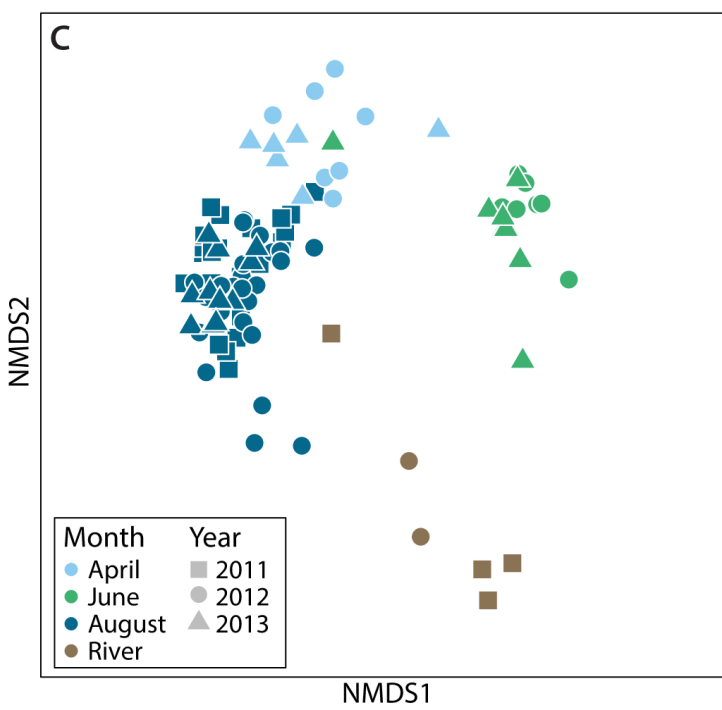
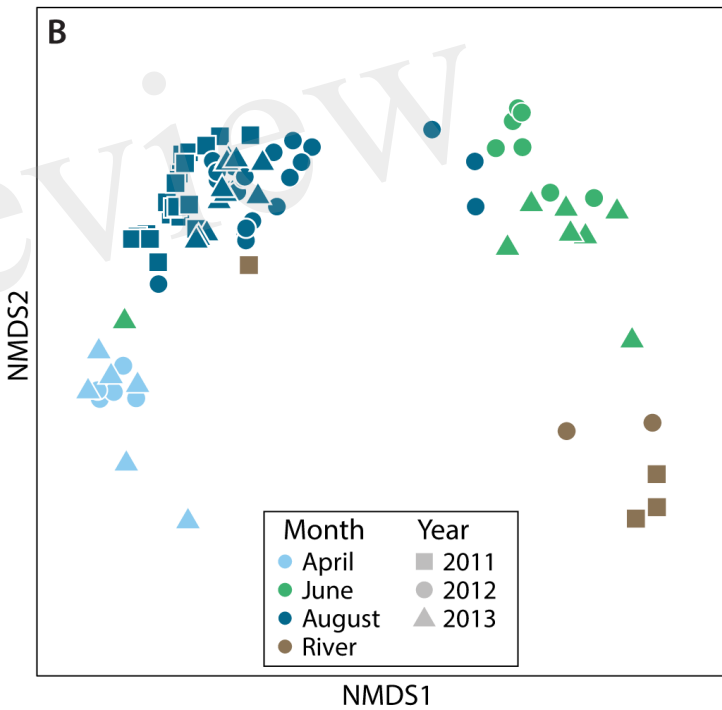
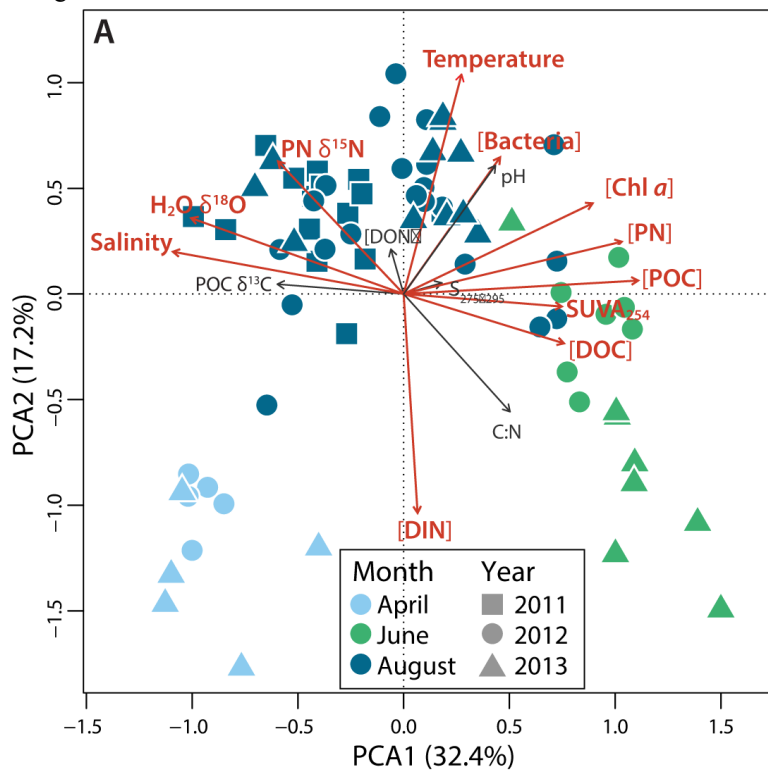


Figure 3.TIF

Figure 3.

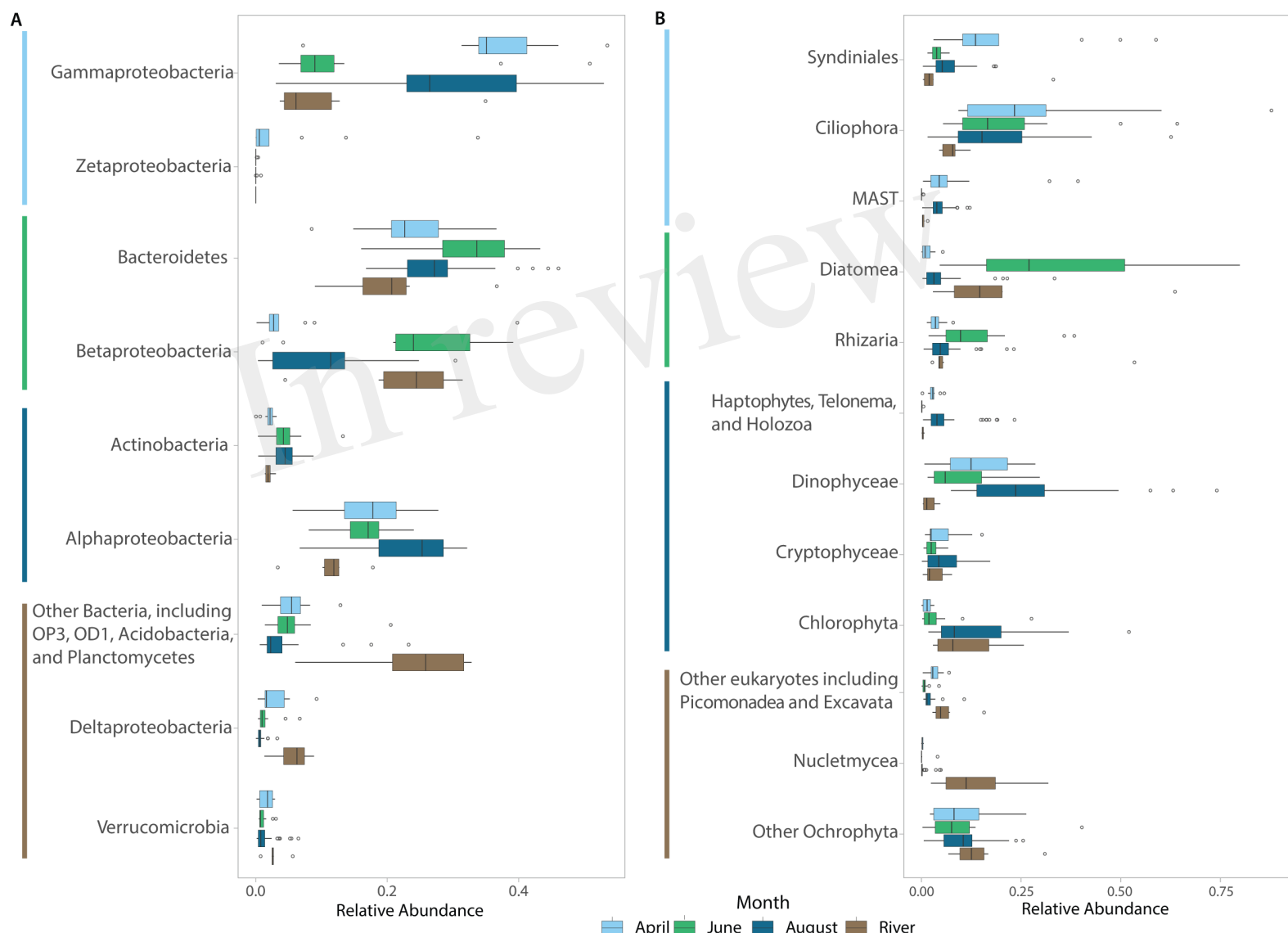


Figure 4.TIF

Figure 4.

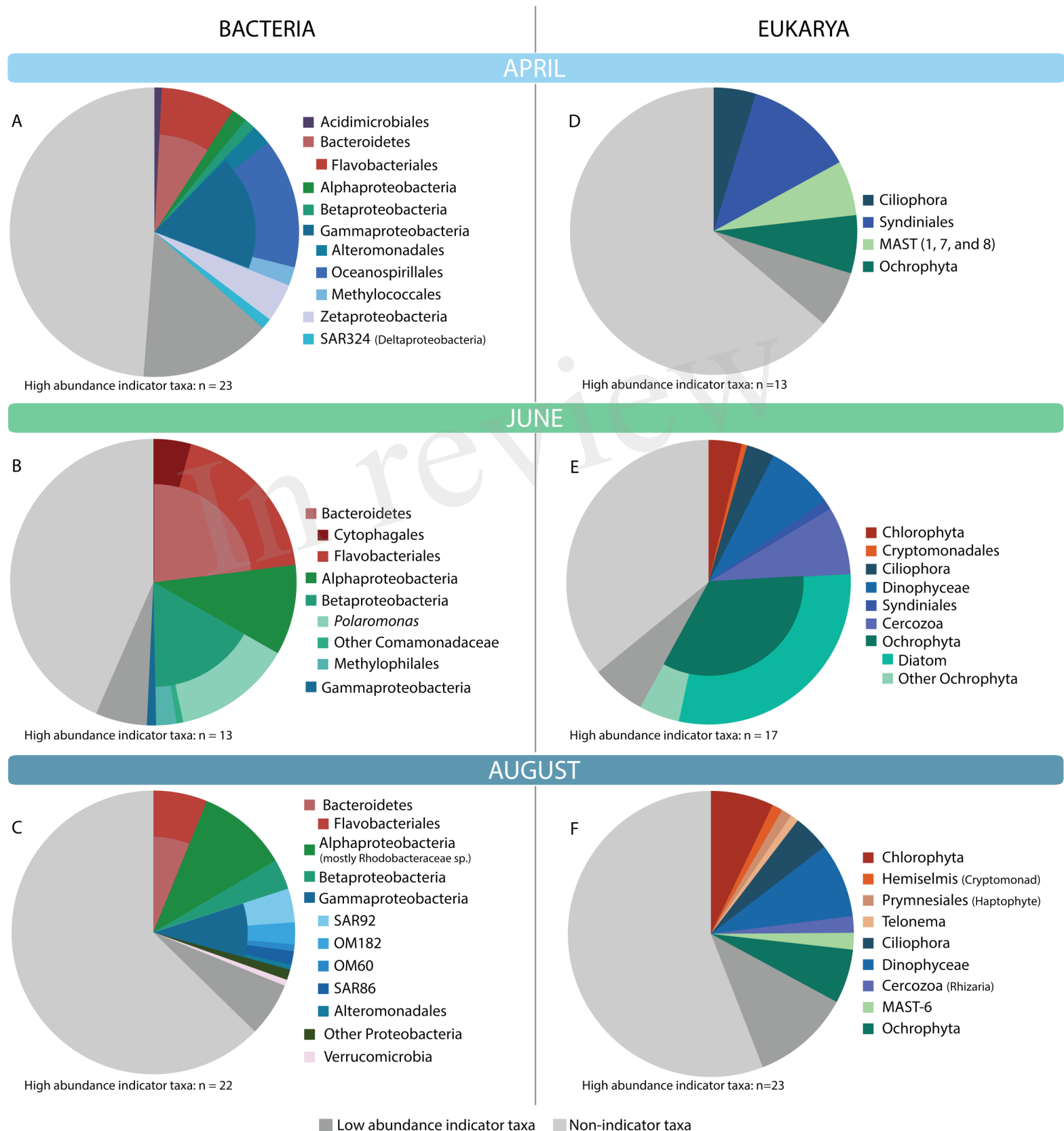


Figure 5.TIF

Figure 5.

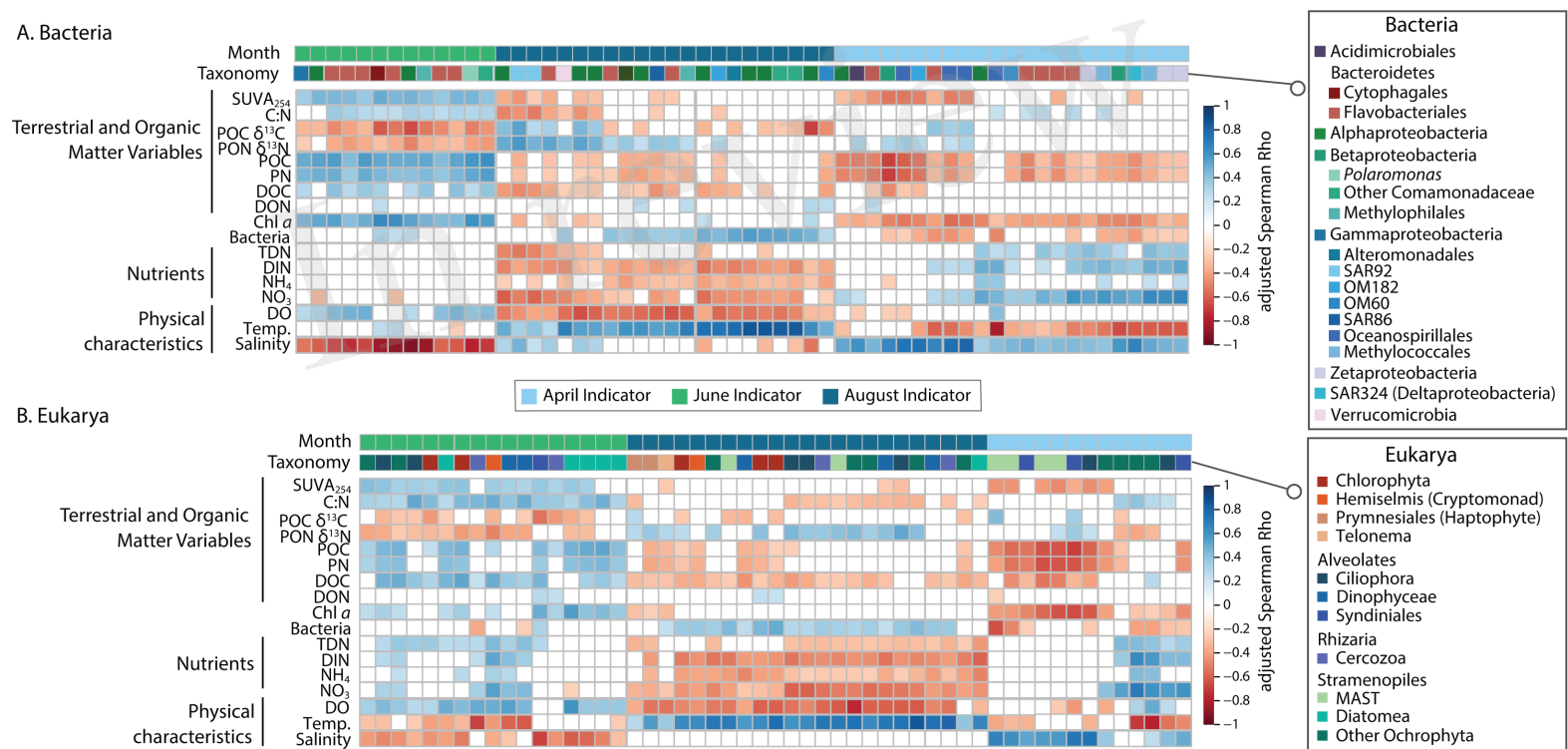


Figure 6.TIF

Figure 6.

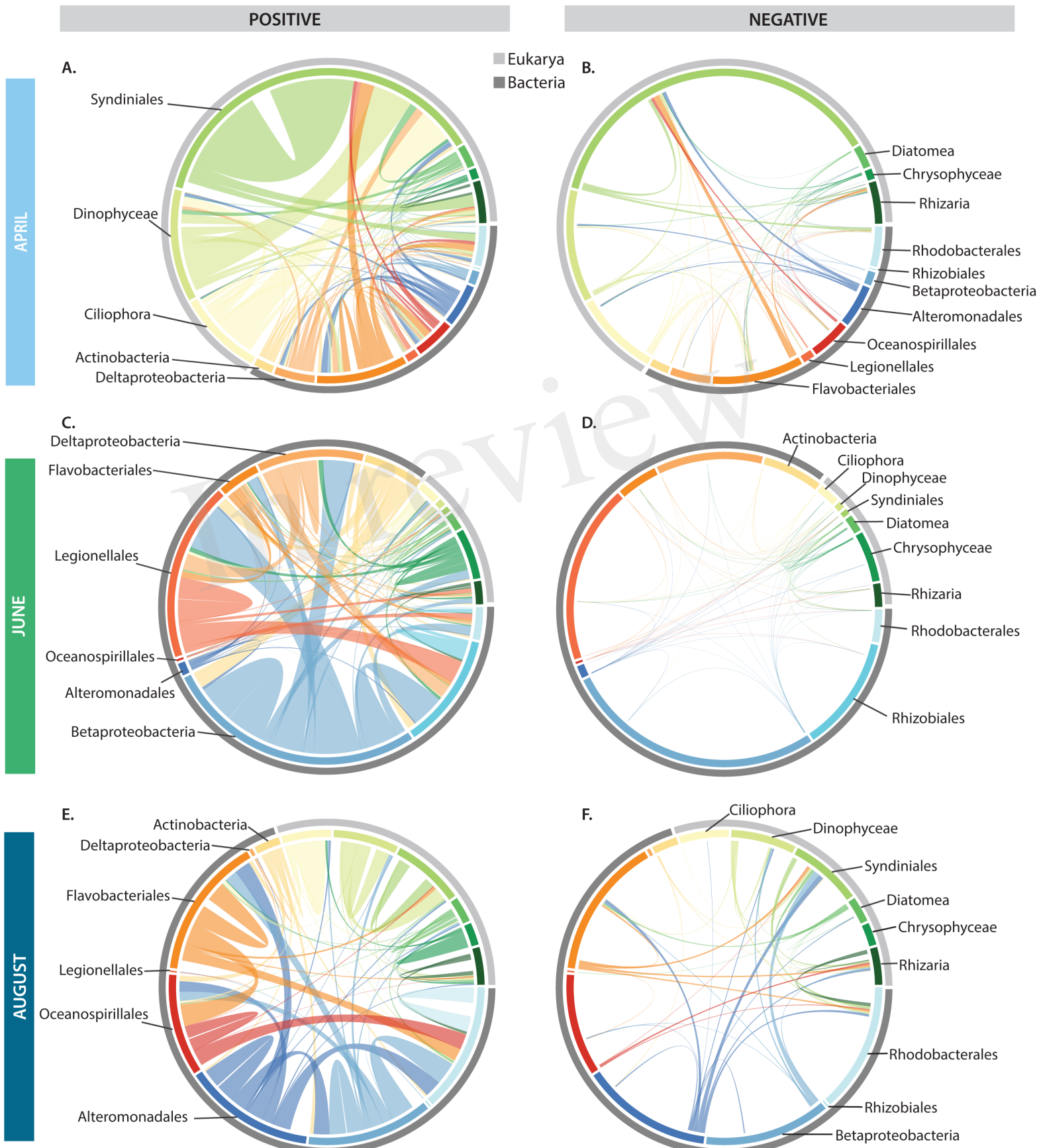
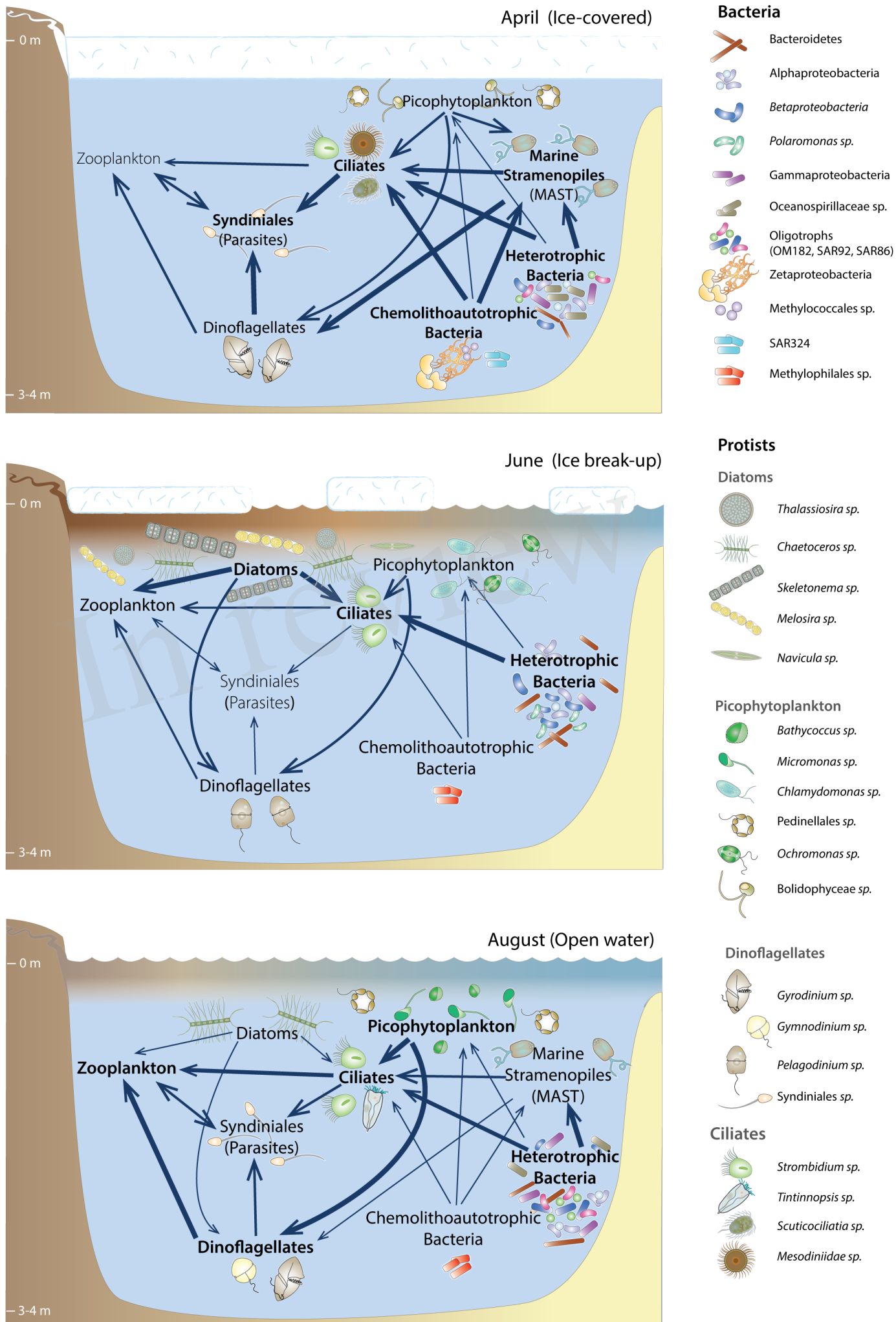


Figure 7.TIF

Figure 7.



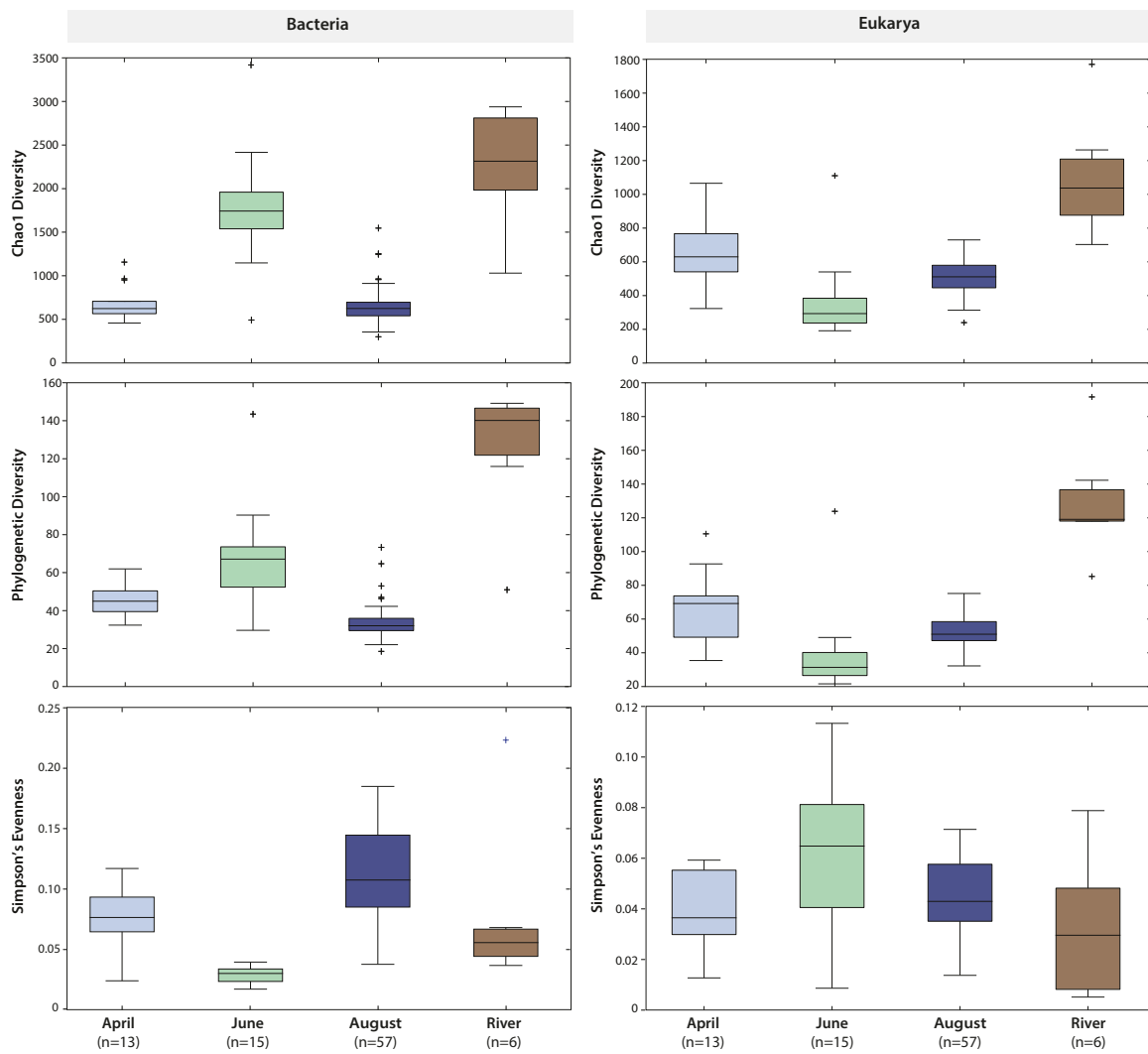


Fig. S1. Boxplots of the distribution of bacterial (left) and microbial eukaryotic (right) alpha diversity among months and the rivers sampled. Three different metrics were used: (top) Chao1 (middle) Phylogenetic Diversity and (bottom) Simpson's evenness. Chao1 and Phylogenetic diversity estimate the number of different taxa in a sample while Simpson's evenness is related to the distribution of reads across the OTUs in a sample.

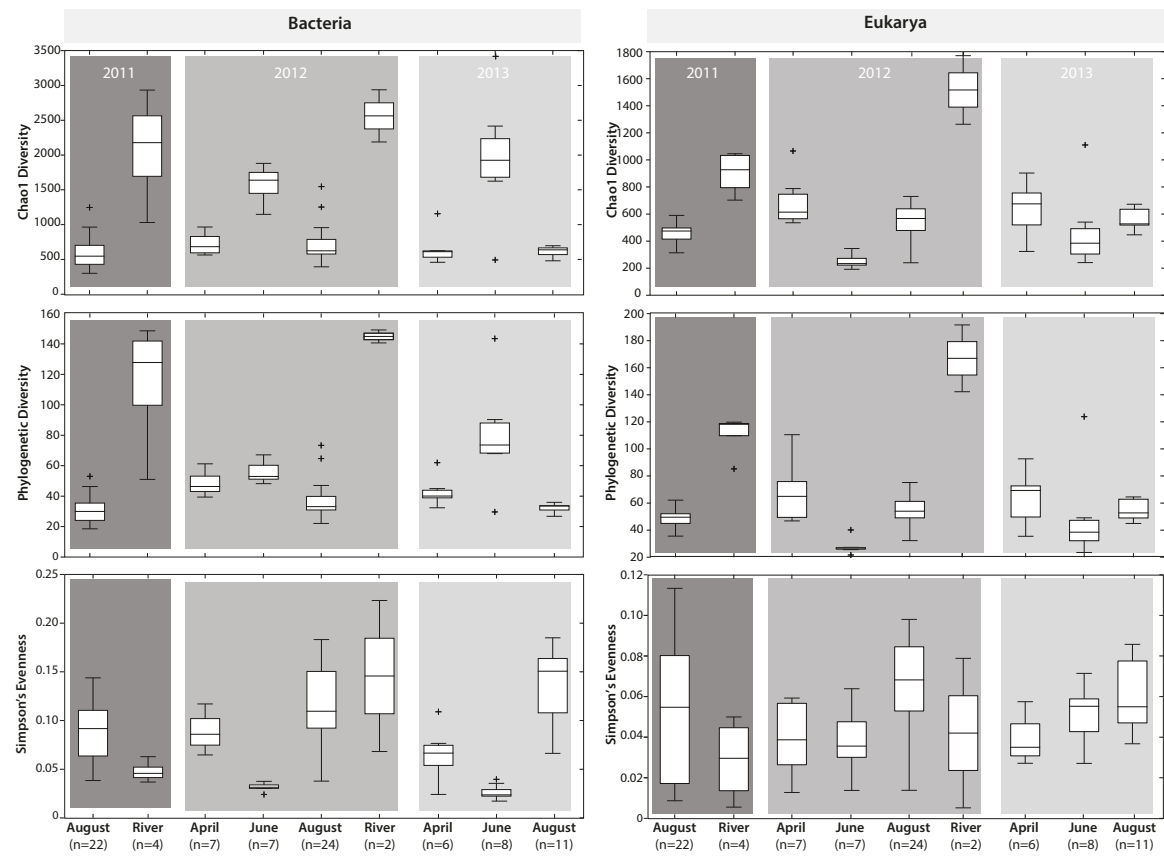


Fig. S2. Boxplots of bacterial (left) and microbial eukaryotic (right) alpha diversity, this time separated by year and month within each year to show interannual variability in diversity among months.

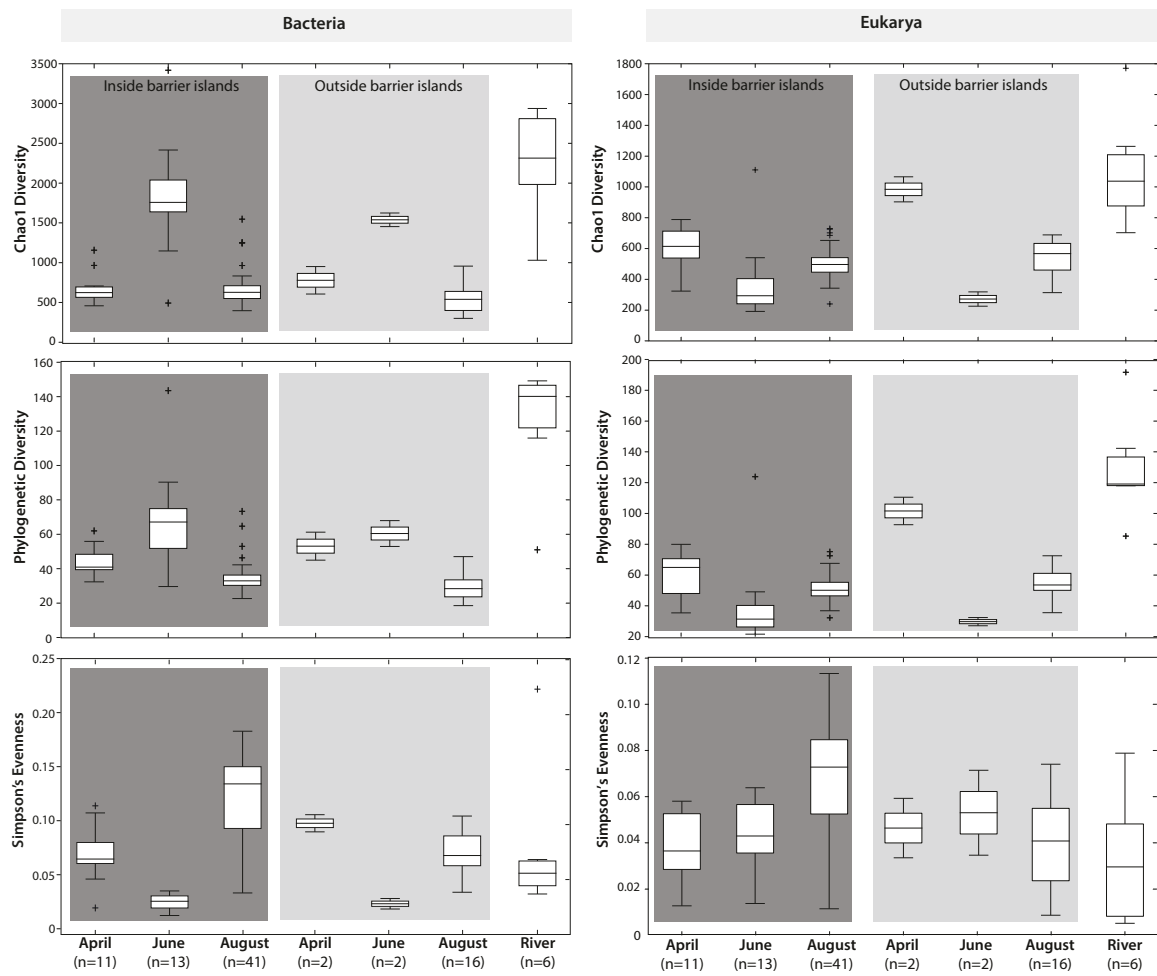


Fig. S3. Boxplots of bacterial (left) and microbial eukaryotic (right) alpha diversity, this time separated by whether the sites were located within or outside the barrier islands month. Within this grouping, samples were further grouped by month.

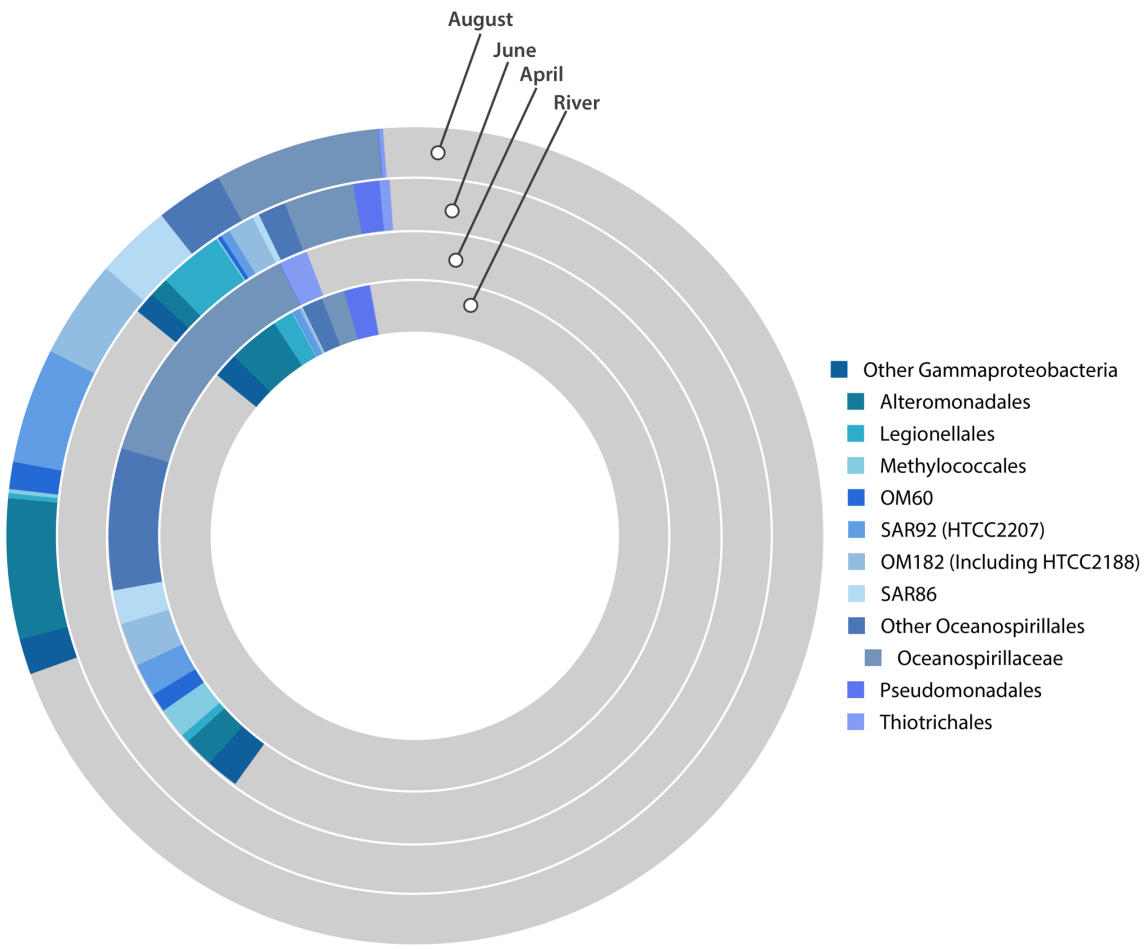


Fig. S4. Taxonomic breakdown of the proteobacterial class *Gammaproteobacteria*, averaged for each month across all years sampled.

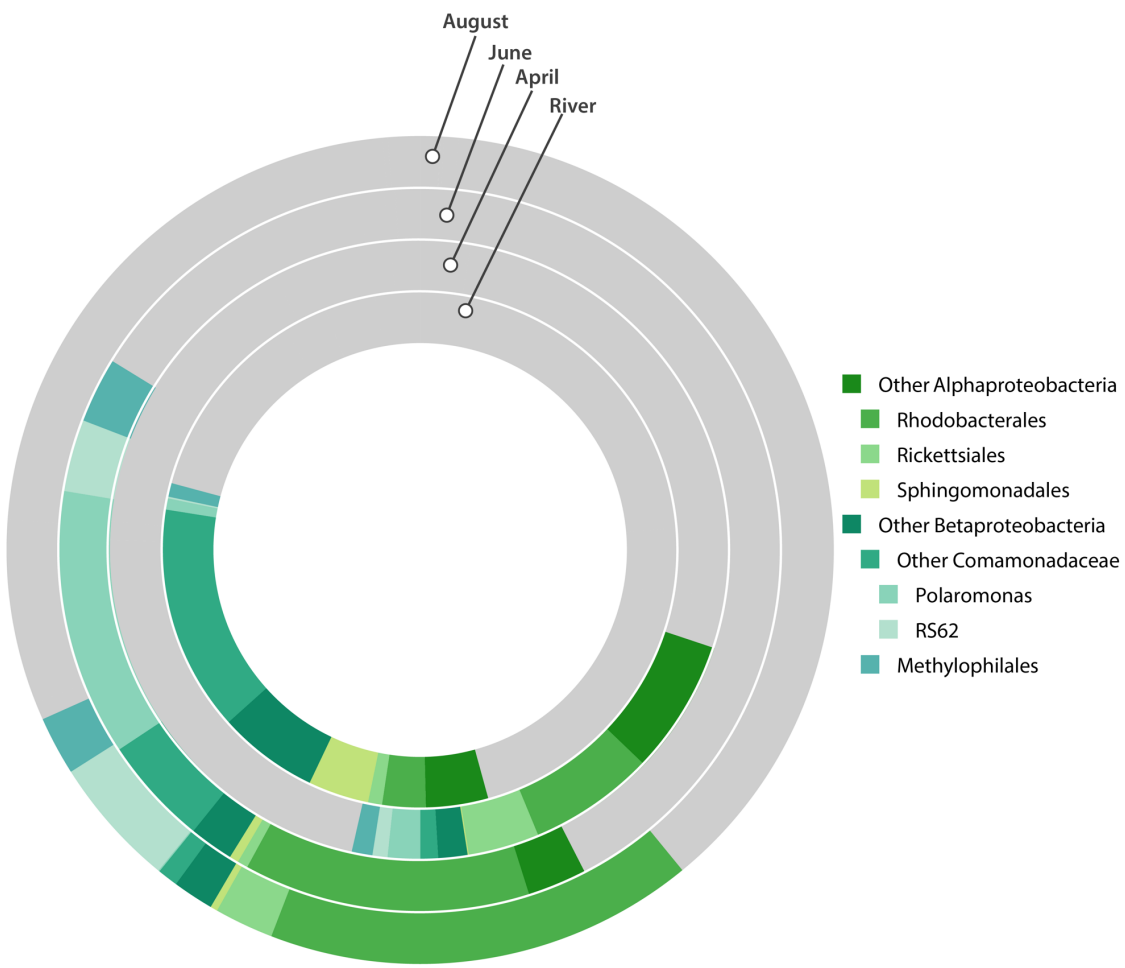


Fig. S5. Taxonomic breakdown of *Alphaproteobacteria* and *Betaproteobacteria* classes, averaged for each month across all years sampled.

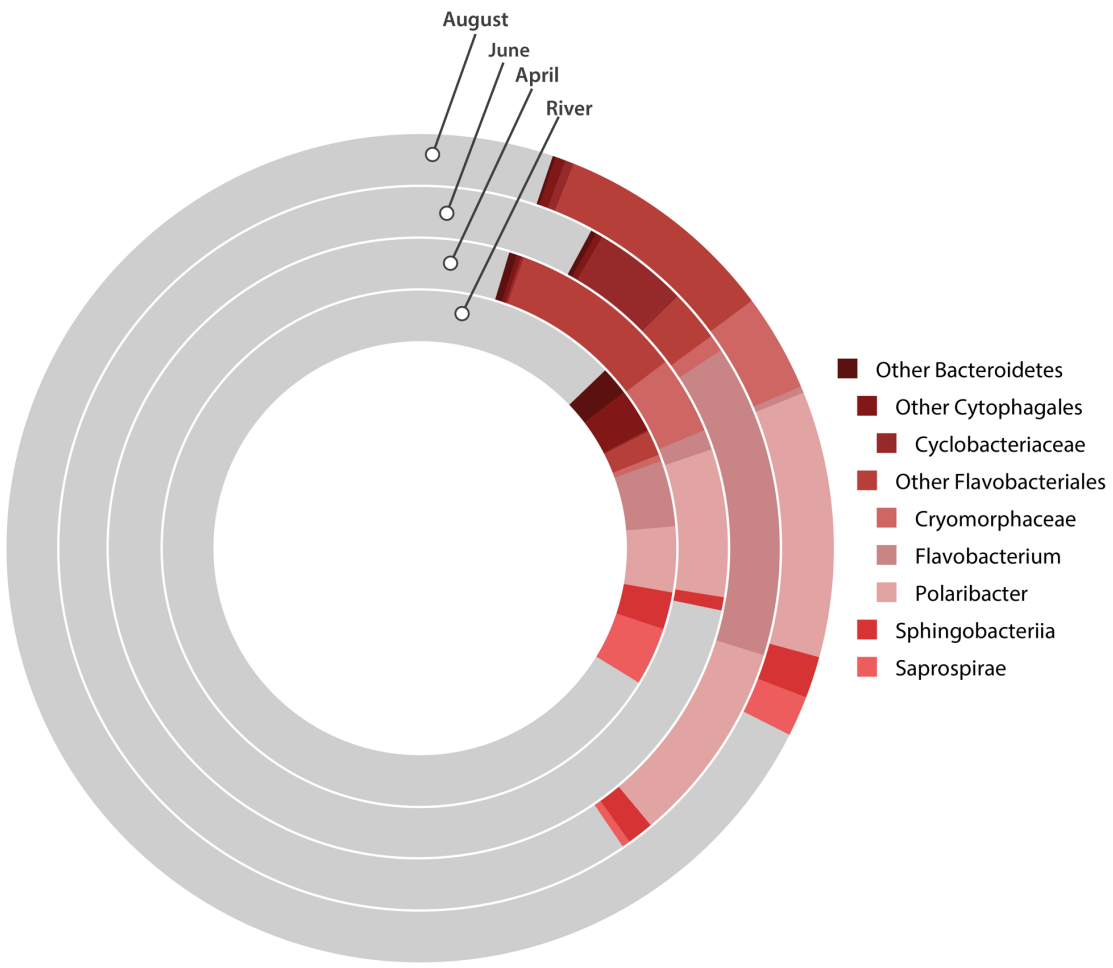


Fig. S6. Taxonomic breakdown of the *Bacteroidetes* phylum of the Bacteria, averaged for each month across all years sampled.

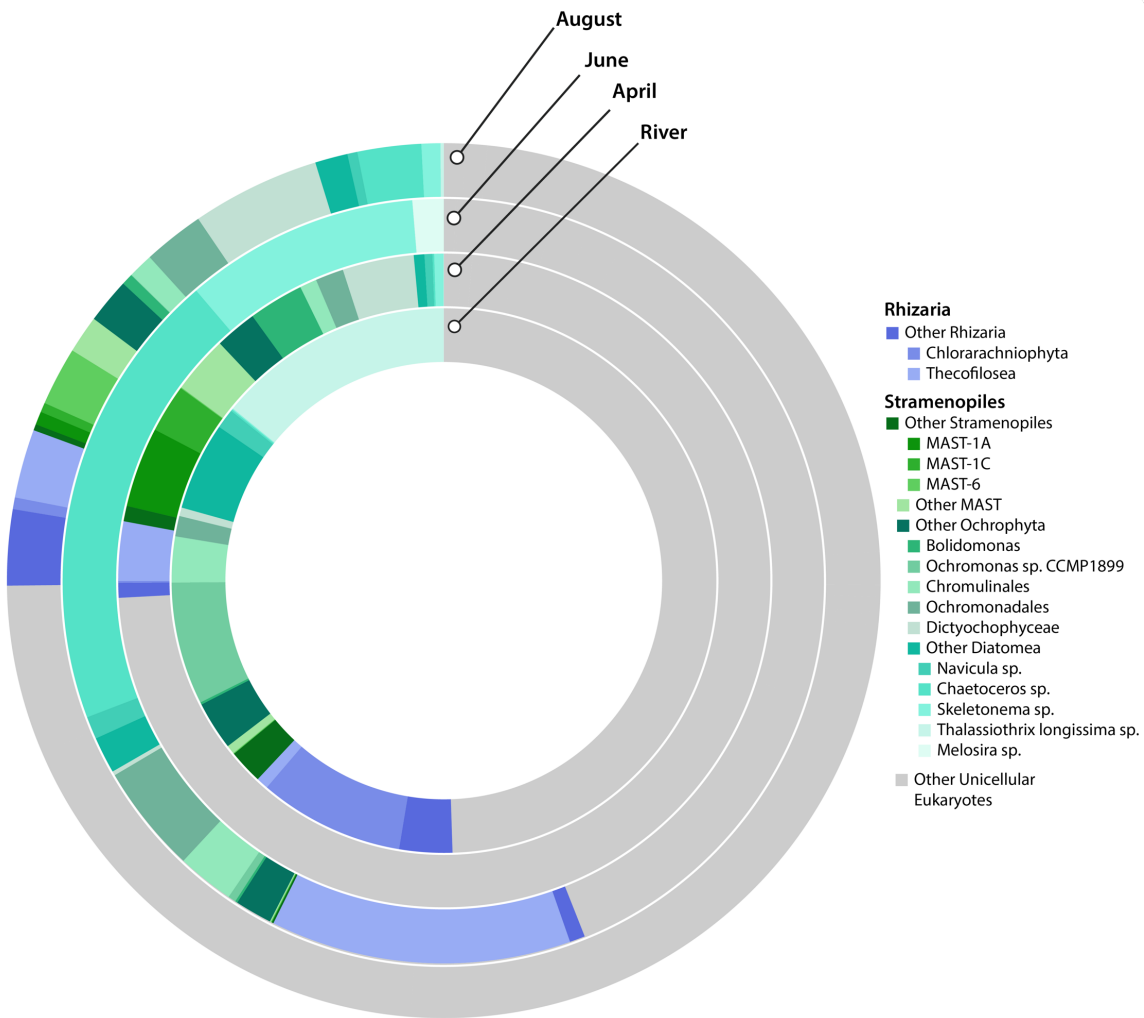


Fig. S7. Taxonomic breakdown of eukaryotic groups *Rhizaria* and *Stramenopiles*, averaged for each month across all years sampled.

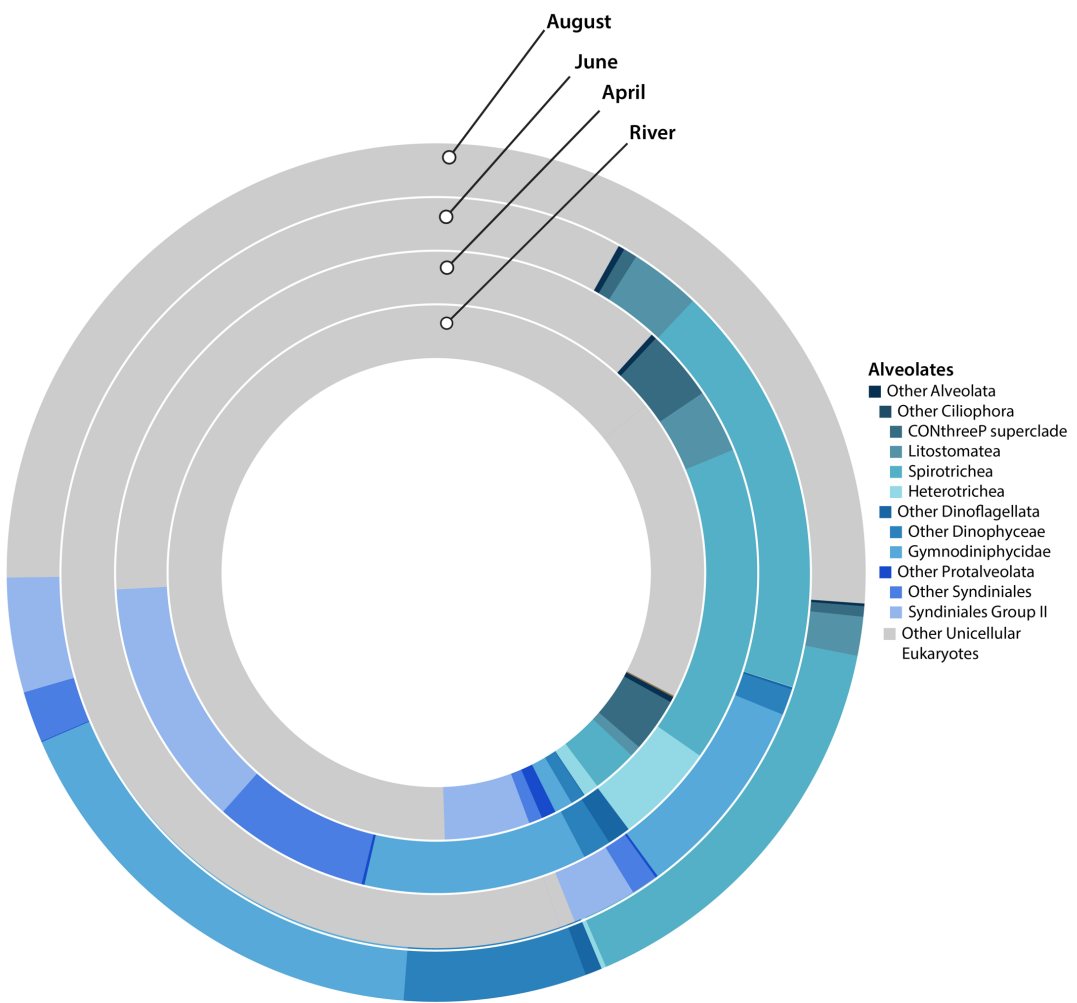


Fig. S8. Taxonomic breakdown of the eukaryotic group *Alveolata*, averaged for each month across all years sampled.

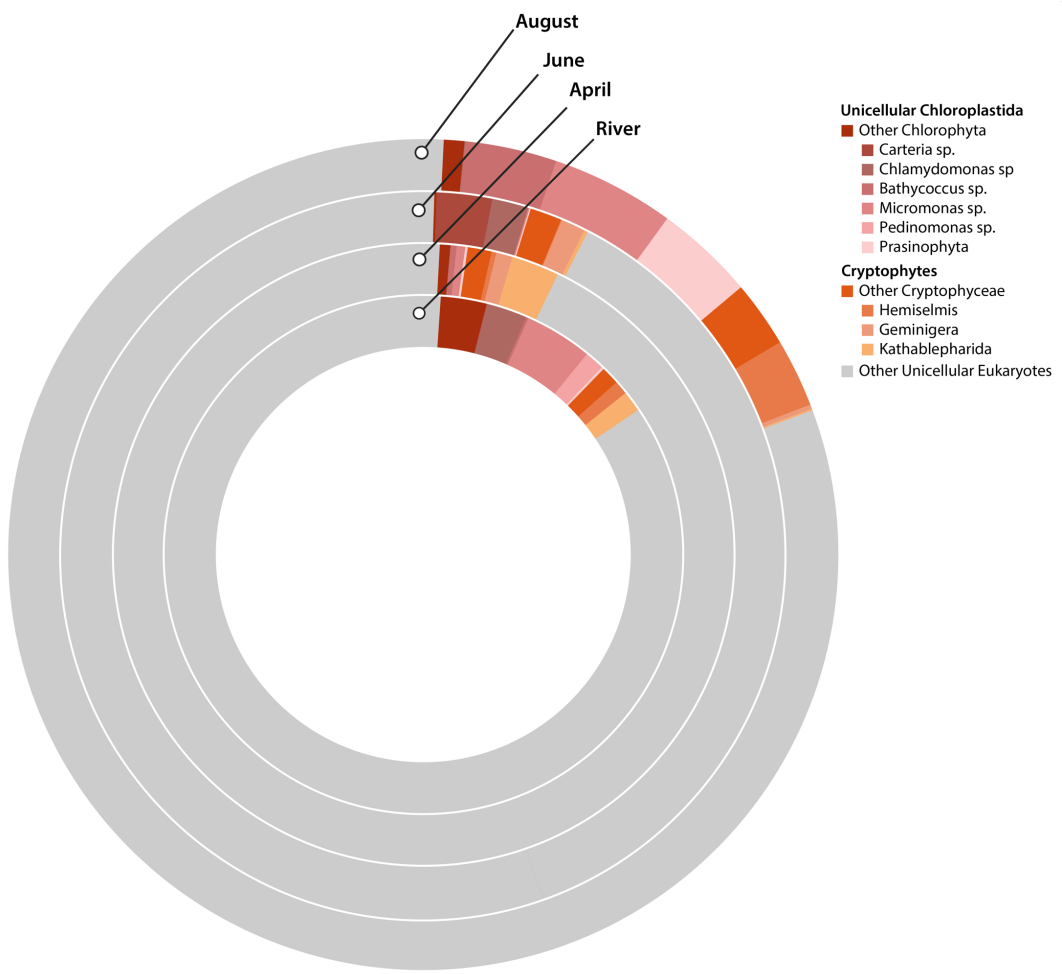


Fig. S9. Taxonomic breakdown of unicellular members of *Chloroplastida* and *Cryptophyta* averaged for each month across all years sampled.

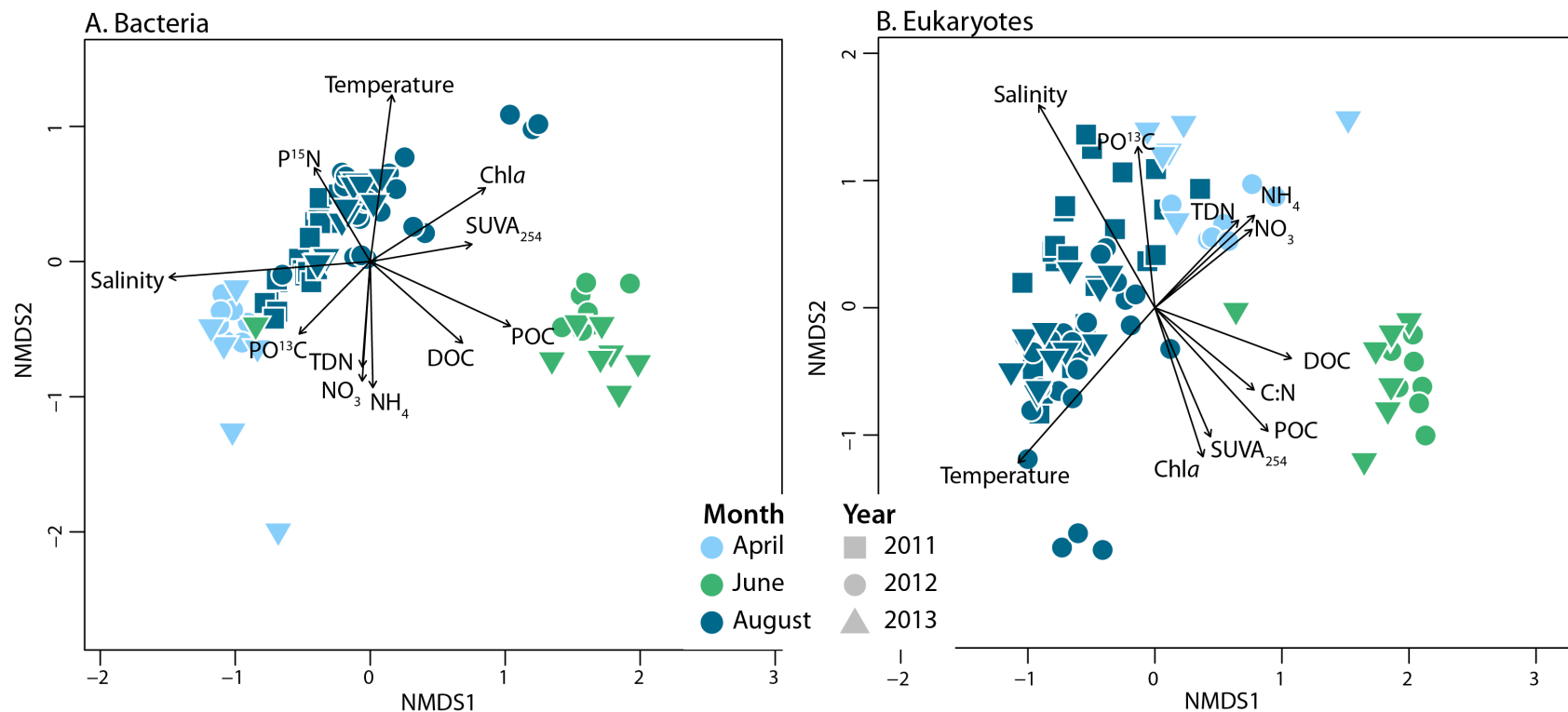


Fig S10. NMDS ordinations of coastal Beaufort Sea (A) bacterial and (B) eukaryotic communities (marine samples only) with vectors representing correlations between physico-chemical variables and each ordination. Only vectors for variables with correlations p-values of 0.001 or smaller are plotted.

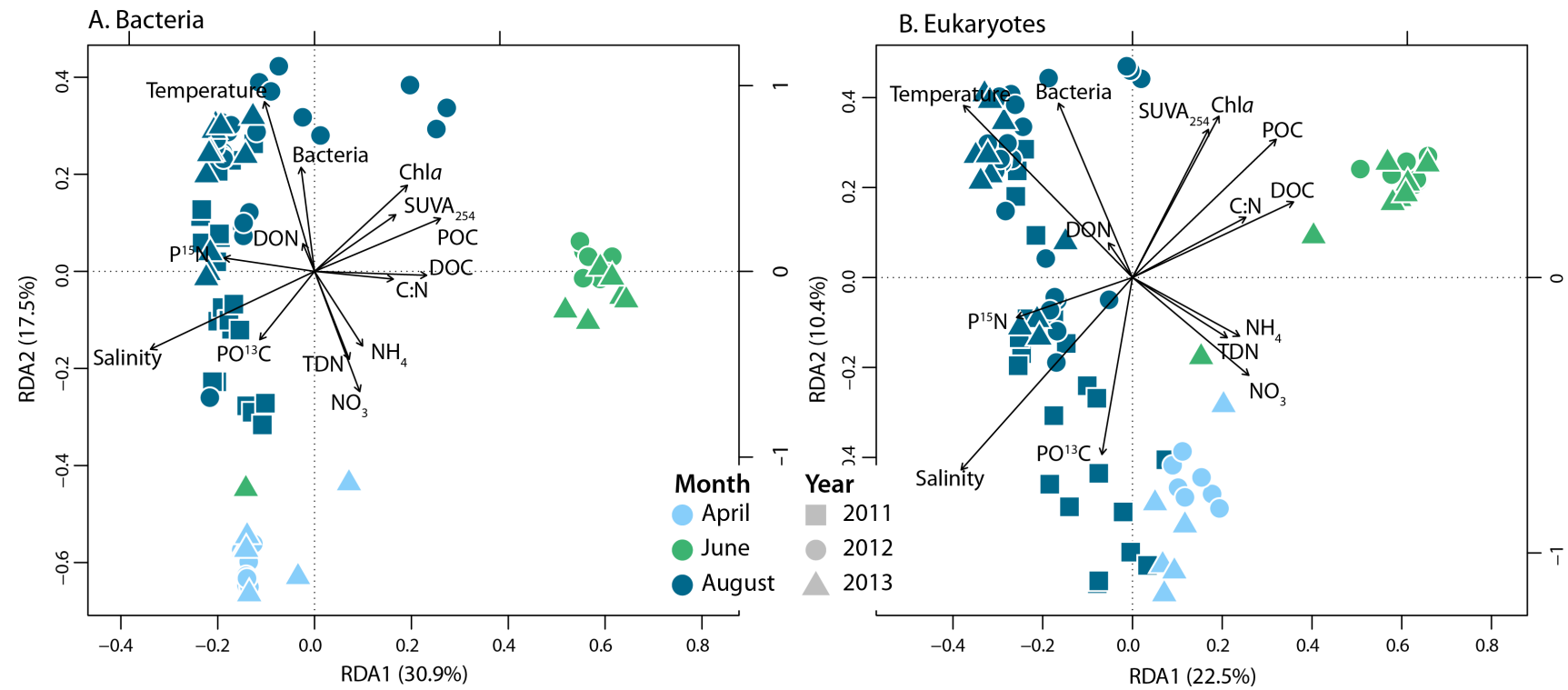


Fig. S11. Redundancy analysis biplots of (A) bacterial and (B) eukaryotic community-environment relationships.

Table S1. Summary of input and output OTUs and environmental variables in monthly co-occurrence networks. For the output OTUs, the percent of the input OTUs is also given in parentheses. The number of significant interactions (edges) as well as the total number of *possible* combinations of nodes is also given. Finally, we report the percent of significant interactions given the number of possible interactions for each network.

Month	Input			Output						
	Euk	Prok	Env	Euk	Prok	Env	Total Nodes	Significant Interactions	Possible Combinations	% Significant Interactions
<b>April</b>	1719	1893	20	628 (36.5)	628 (33.2)	16 (80)	1272	21122	808,356	2.6
<b>June</b>	1127	4874	20	196 (17.4)	1010 (20.7)	5 (25)	1211	109143	732,655	14.9
<b>August</b>	3183	5046	20	321 (10.1)	331 (6.6)	10 (50)	662	3121	218,791	1.4

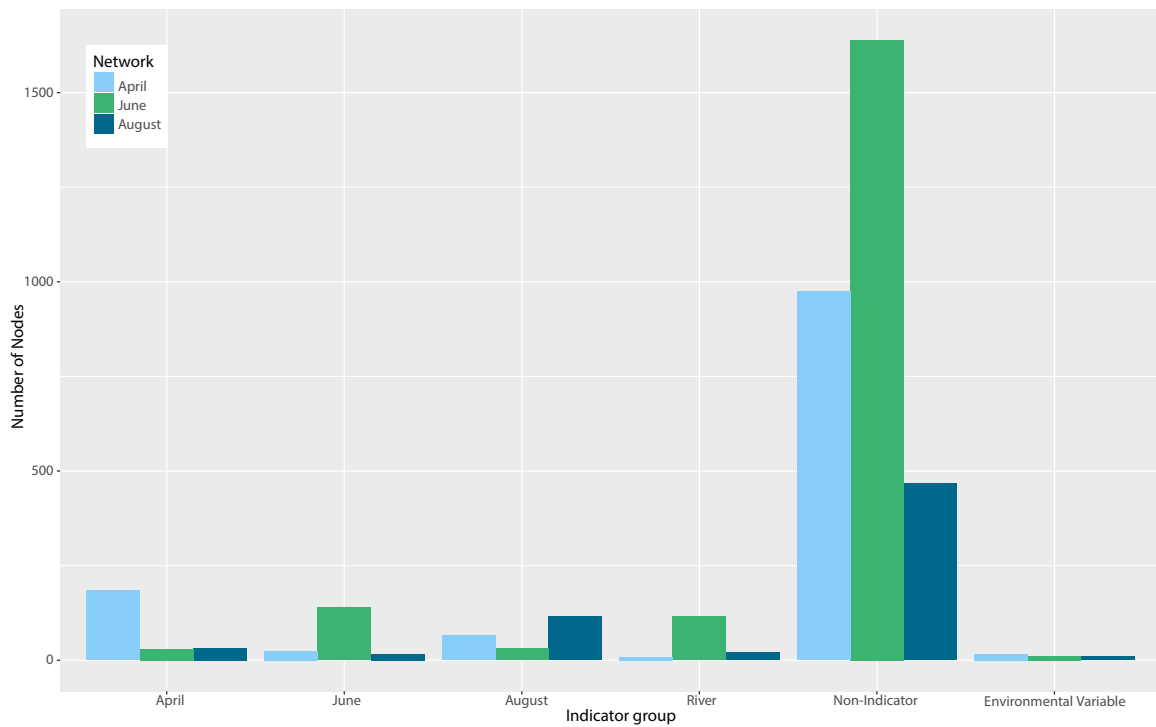


Fig. S12. Distribution of indicator taxa, non-indicator taxa, and environmental variables (x-axis) within each network (colored bars). For example, if you look at the number of April indicator taxa nodes (left-most set of bars), it is clear that the April network contains the most April indicator taxa but that some April indicator taxa are also present into June and August networks.

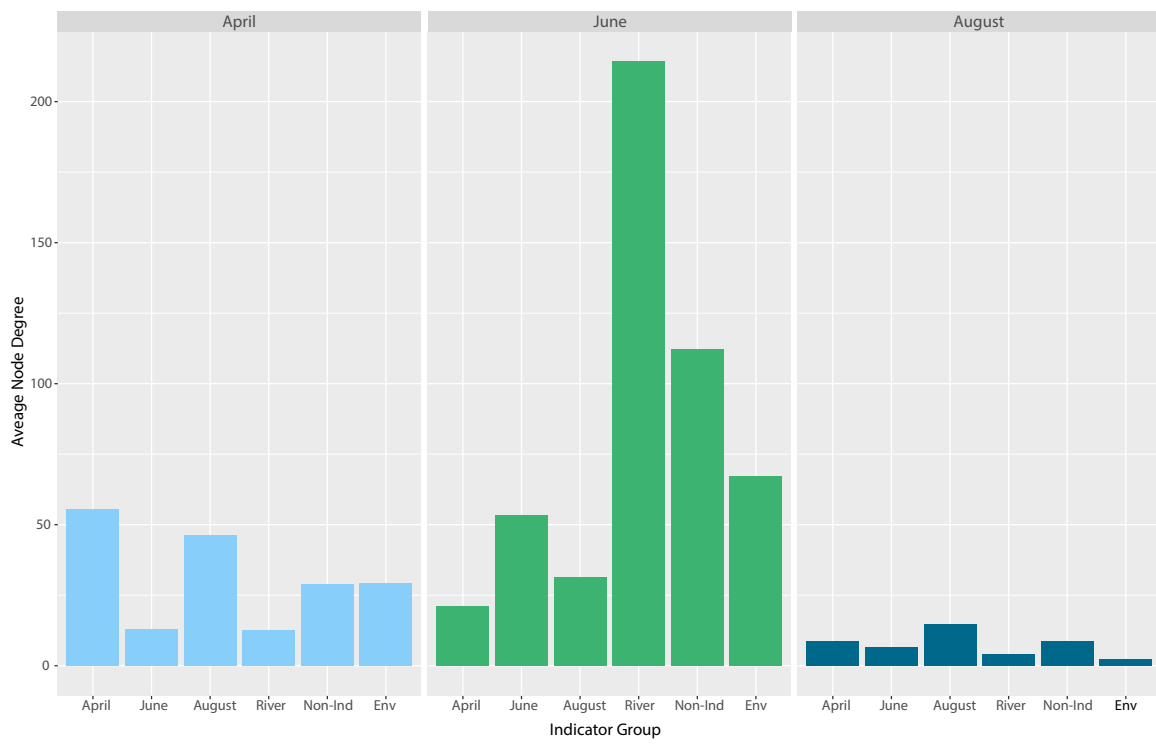


Fig. S13. Average node degree for indicator taxa, non-indicator taxa, and environmental variables within each network. OTUs with higher average node degrees are more connected within a network.

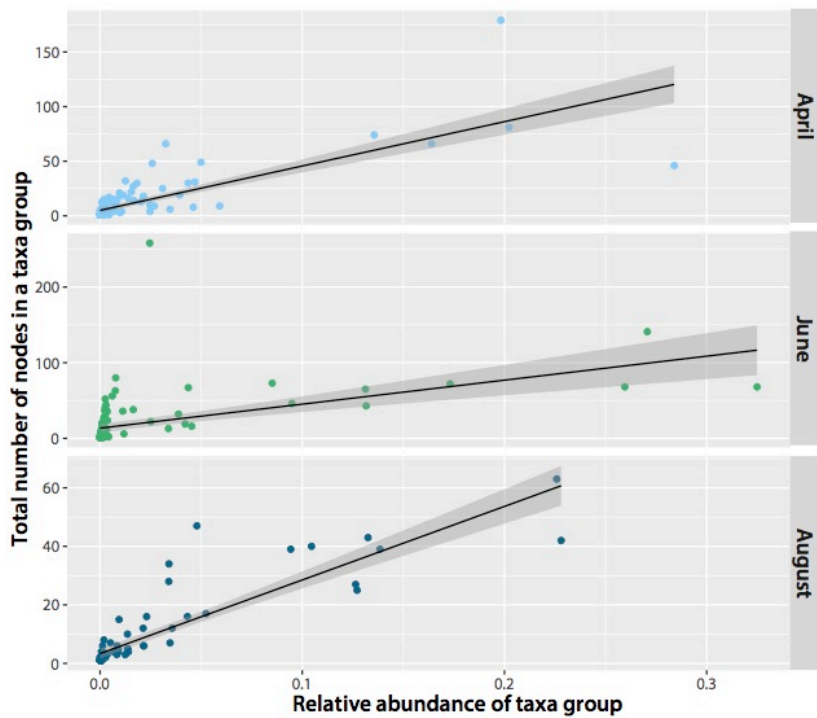


Fig. S14. Relationship between the total relative abundance of a taxonomic group in a month with the number of nodes assigned to that group for each network.

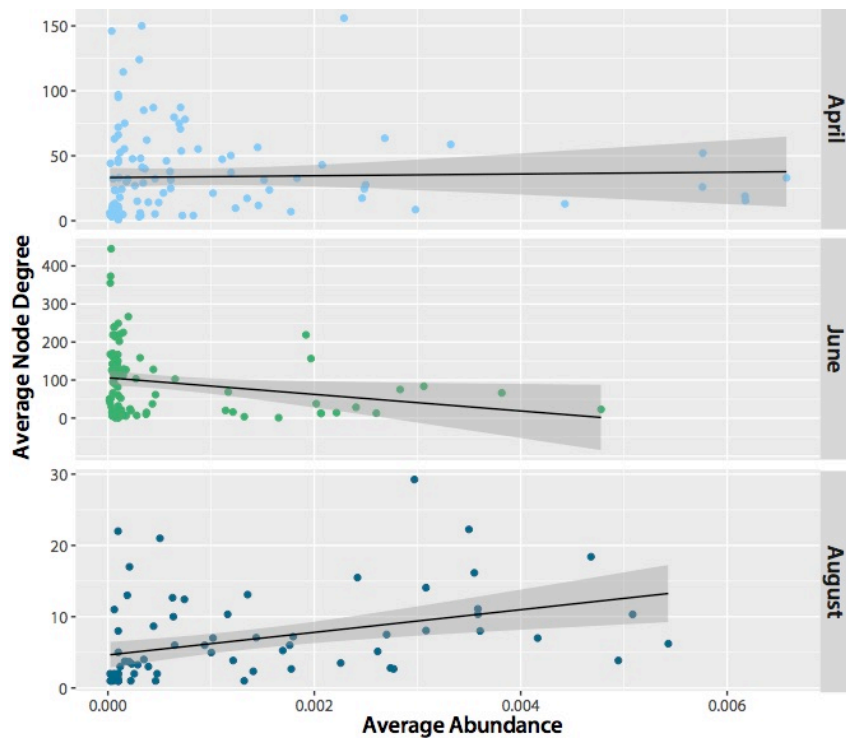


Fig. S15. Relationship between the average abundance of a taxa in that month and the average node degree of that taxa within a network.

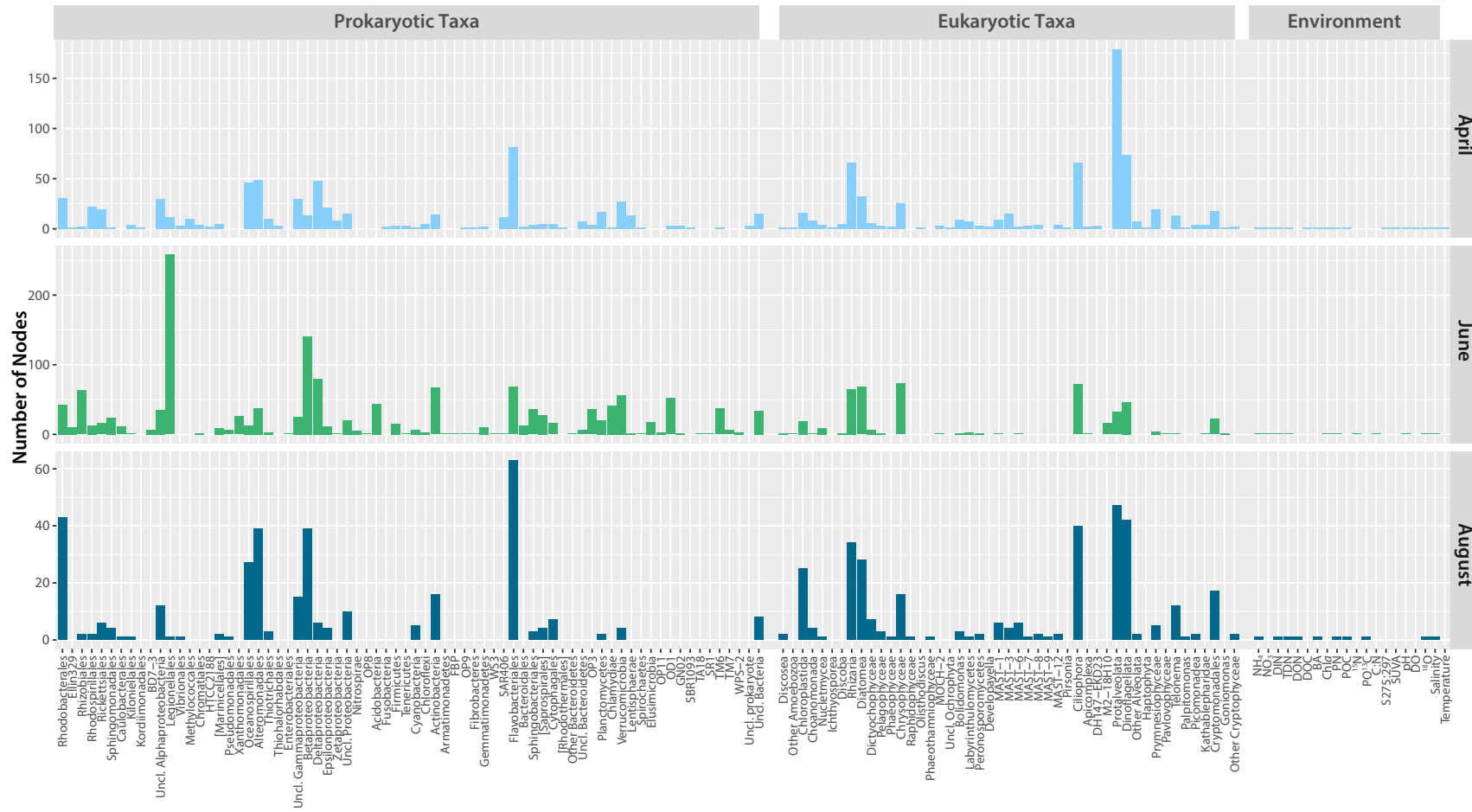


Fig. S16. Node distribution among major taxonomic groups for each network. Environmental variables can only occur a maximum of one time in a network and their inclusion in this figure simply shows whether or not a particular variable had significant relationships within a network. The number of edges associated with each environmental variable is shown in Fig. S21.

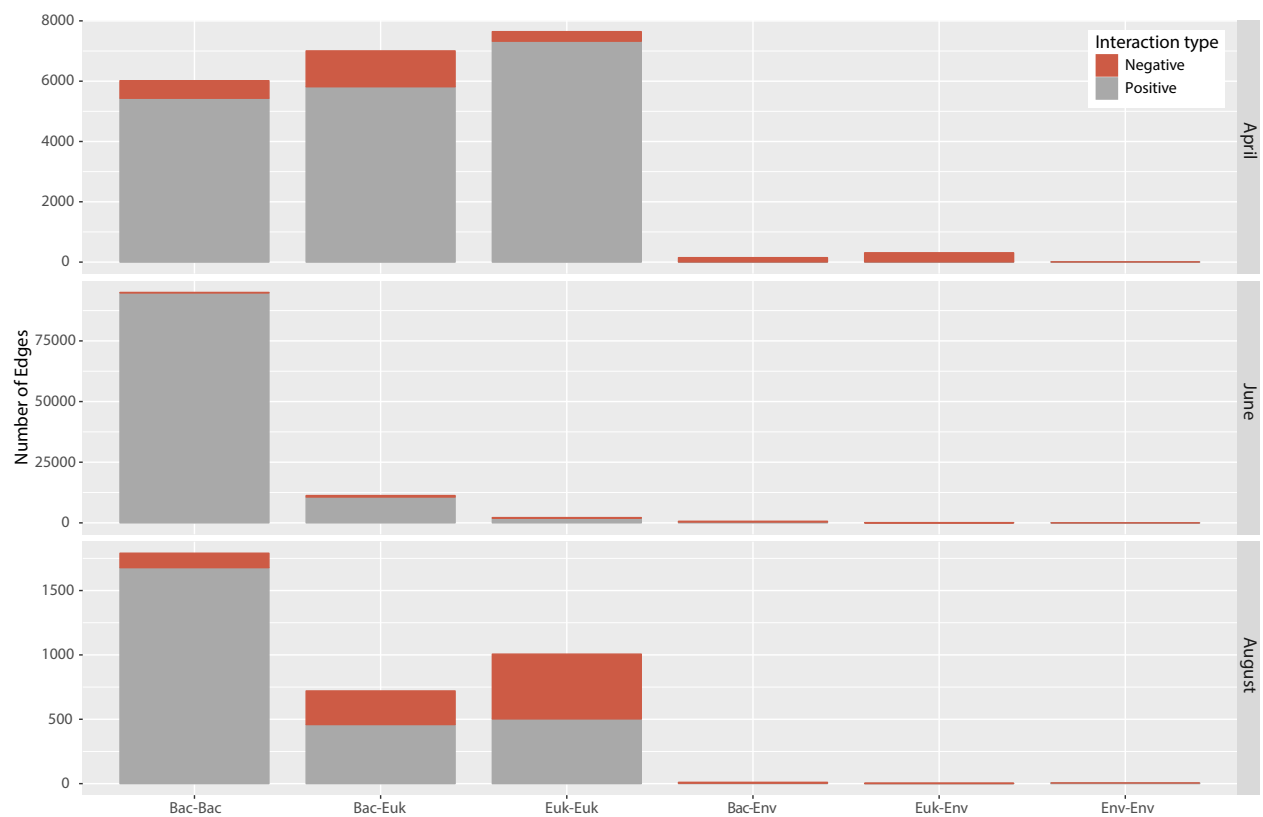


Fig. S17. Number of positive (co-occurrence) and negative (mutual exclusion) edges between bacteria (Bac), eukaryote (Euk), and environment nodes (Env) for each network.

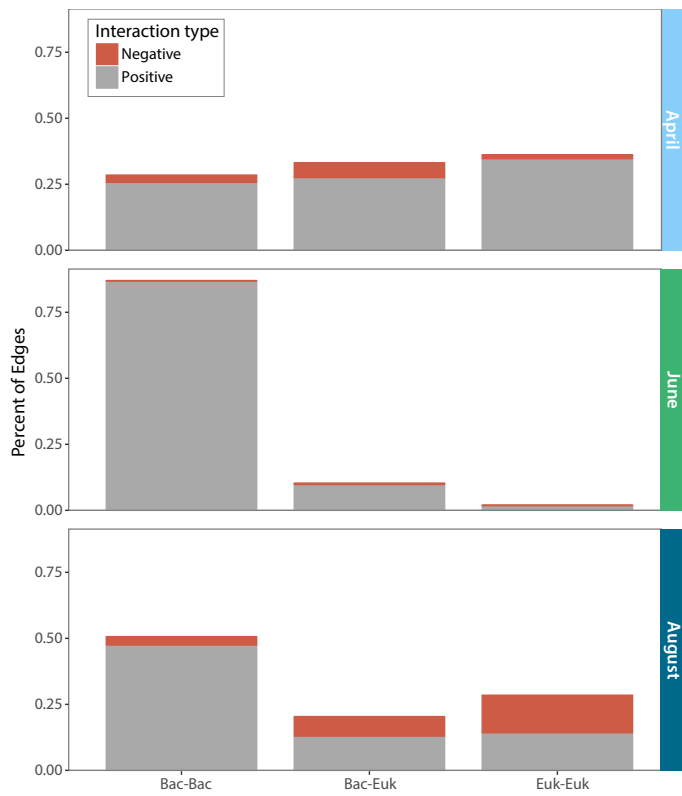


Fig. S18. Distribution of significant relationships between bacteria, bacteria and eukaryotes, and eukaryotes.

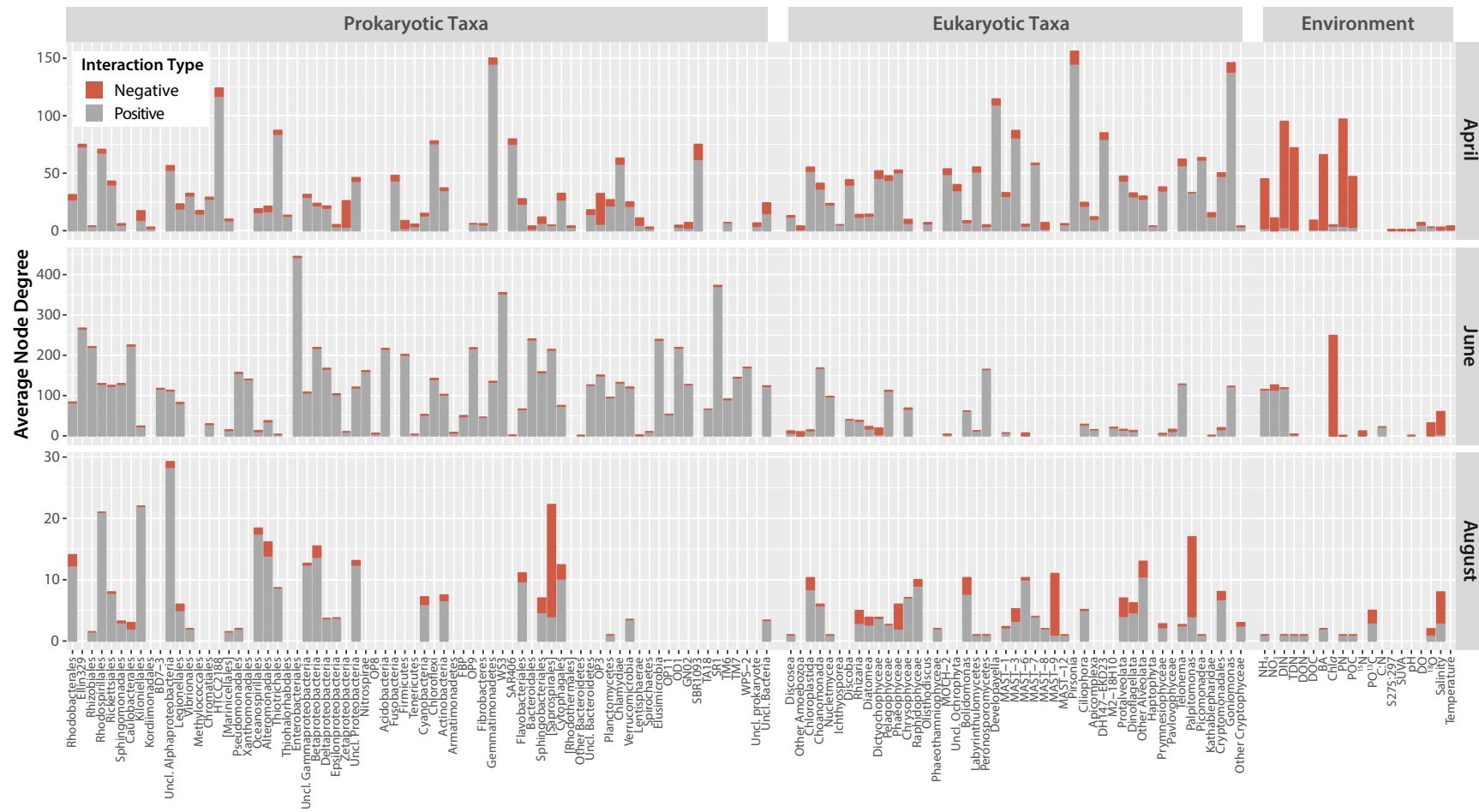


Fig. S19. Average node degree for each major microbial taxonomic group for each network. Bars are further broken down by the average relative amounts of negative (red) and positive (grey) edges for each taxa or environmental variable.